



UNIVERSITÀ DEGLI STUDI DI MILANO

Facoltà di Medicina e Chirurgia

Dottorato di ricerca in Scienze Fisiopatologiche, Neuropsicobiologiche ed  
Assistenziali del Ciclo della Vita



INFLUENCE OF IMPLANT NUMBER, IMPLANT LENGTH  
AND CROWN HEIGHT ON BONE STRESS DISTRIBUTION  
FOR THREE-UNIT BRIDGES IN THE POSTERIOR  
MANDIBLE: A 3D FINITE ELEMENT ANALYSIS.

**Coordinatore:** Chiar.mo Prof. Roberto Weinstein

**Tutor:** Chiar.mo Prof. Luca Francetti

Tesi di Dottorato di  
Nicolò Cavalli  
Matricola. N° R09967

Anno Accademico 2014 – 2015



# INDEX

---

Chapter 1 - INTRODUCTION	pag. 7
Chapter 2 - BIOMECHANICS	pag. 10
2.1 Basic biomechanical principles	pag. 10
2.2 Analysis of bone density	pag. 17
2.3 Bone adaptation to mechanical tension	pag. 21
2.4 Masticatory dynamic	pag. 24
2.5 Physiological and parafunctional masticatory forces	pag. 28
2.6 Implant failures and complications	pag. 32
Chapter 3 - FINITE ELEMENT ANALYSIS	pag. 36
3.1 Definition of Finite Element Analysis	pag. 36
3.2 Creating a model of living and non-living structures	pag. 37
3.3 Interfaces	pag. 40
3.4 Loading conditions and boundaries	pag. 41
3.5 Analysis of the stress	pag. 42
3.6 Other biomechanical studies in dentistry	pag. 43

Chapter 4 - SHORT IMPLANTS	pag. 47
4.1 Anatomic issues	pag. 47
4.2 Early mistrust and caution in using short implants	pag. 49
4.3 Implant surface	pag. 50
4.4 Biomechanical issues	pag. 51
4.5 Analysis of clinical success	pag. 52
4.6 Surgical protocol	pag. 53
4.7 Bone augmentation procedures	pag. 57
Chapter 5 - OBJECTIVES	pag. 59
Chapter 6 - METHODS AND MATERIALS	pag. 60
6.1 Development of finite element model	pag. 60
6.2 Experimental configurations	pag. 63
6.3 Data analysis	pag. 69
Chapter 7 - RESULTS	pag. 70
Chapter 8 - DISCUSSION	pag. 107
8.1 Effect of implant stress direction	pag. 107
8.2 Effect of implant length	pag. 108
8.3 Effect of implant crown height	pag. 109
8.4 Effect of implant number	pag. 110
8.5 Clinical relevance	pag. 110
8.6 Limits of the study	pag. 111

Chapter 9 - CONCLUSIONS

pag. 113

Chapter 10 REFERENCES

pag. 114

# Chapter 1

## INTRODUCTION

---

In the last forty years dental implants have been widely used for the rehabilitation of edentulous areas. (Adell et al. 1990; Jemt et al. 1993)

Patients rehabilitated with implant-supported fixed partial dentures in the posterior region of the maxilla or the mandible showed an improvement in the oral health-related quality-of-life if compared with those with removable partial dentures, particularly in elderly patients. (Petricevic et al. 2012; Furuyama et al. 2012)

Especially in the posterior region of jaws, reduced alveolar bone height due to post-extraction ridge resorption and maxillary sinus pneumatization represents a major limitation in the use of dental implants and increases the probability of an invasion with related possible damage to some anatomical structures, such as the inferior alveolar nerve and the maxillary sinus cavity and membrane. (Tawil & Younan 2003, das Neves et al. 2006; Pommer et al. 2011)

Many surgical bone augmentation techniques have been suggested. Although these approaches including onlay bone grafts have been proved effective in regaining bone volume, guided bone regeneration (GBR) (Merli et al. 2007;

Fontana et al. 2008), maxillary sinus elevation (Pjetursson et al. 2008; Del Fabbro et al. 2008; Del Fabbro et al. 2011; Katranji et al. 2008) and distraction osteogenesis (DO) (Chiapasco et al. 2004), they are hardly accepted by the patients because of the multiple complications and morbidity after surgery, the prolonged treatment duration and the high extra costs. (Pieri et al. 2012; Lai et al. 2012)

Short implants can be considered as an alternative treatment option. This strategy simplifies overall treatment and minimizes the incidence of complications associated with bone augmentation procedures. Biomechanical studies demonstrated that the crestal portion of the implant body is the most involved in load-bearing, whereas very little stress is transferred to the apical portion (Lum 1991). Moreover, some authors hypothesized that the increase of implant length from 7 to 10 mm can have a minor impact on its anchorage strength (Bernard et al. 2003). Therefore, implant length may not be a primary factor in distributing prosthetic loads to the bone-implant interface (Annibali et al. 2012).

However in the past years, short implants have been associated with lower survival rates (Lee et al. 2005, Romeo et al. 2010). There are several presumed reasons for the lower survival rate of short implants in the posterior maxilla or mandible. Firstly, most of those studies considered short implants with machined surface with longer implants with a comparable diameter. In that case an inferior bone to implant contact was demonstrated. Secondly, short implants are mostly placed in the posterior zone, where the quality of the alveolar bone is relatively poor, especially in the maxilla (type III or IV) (Lekholm & Zarb 1985).

Thirdly, often, a very oversized crown has to be made to reach occlusion, because of the extensive resorption in the posterior region, which causes a higher crown to implant ratio. Crown to implant ratios between 0.5 and 1 were proposed to prevent peri-implant bone stress, crestal bone loss and eventually implant failure (Haas et al. 1995, Rangert et al. 1997, Glantz & Nilner et al. 1998). However a recent systematic review on two studies on crown to implant ratios concluded that the ratio does not influence the peri-implant crestal bone loss (Blanes et al. 2009).

Recent studies evaluating short implants with rough surfaces could present a similar survival and success rate to conventional implants. However doubts about



biomechanical performances were risen (Sun et al. 2011; Telleman et al. 2011; Pommer et al. 2012; Annibali et al. 2012; Lai et al. 2012; Pieri et al. 2012).

Recently image-based approaches combined with Finite Element Analyses (FEA) have allowed effective stress–strain investigations in biological systems and in particular stress distribution in bone.

Dental implants can be virtually positioned within realistic models of human jaws reproduced from high definition CT image data with respect of the anatomical-physiological structures of bones. Worldwide, scientists have focused on this topic. (Frisardi 2012; Field 2010; Muhlberger 2009; Al Sukhun 2007).

Some authors considered the load transfer at the interface an important factor in determining the correct mechanical stimulation of the osteoblasts, which are assumed to be responsible for bone tissue regeneration and the consequent osseointegration of the implant (Frisardi et al. 2012; Bonnet et al. 2009; Park et al. 2010; Misch et al. 2005).

The aim of this finite element analysis will be the investigation of stresses transmitted to surrounding bone by restorations supported by different short implants combinations.

# Chapter 2

## BIOMECHANICS

---

Biomedical engineering, which applies engineering principles to living systems, has opened a new era in diagnosis, treatment planning and rehabilitation of patients. Biomechanics, a branch of this field, affects the response of biological tissues to the loads applied.

Its evolution is fundamental for what concerns the knowledge and success of many therapies of the stomatognathic system, including in particular the implant restoration. The advances in the design of prosthesis, implants and instruments were achieved thanks to the theory and practice of the mechanical design optimization. (National Institutes of Health Development 1988).

### **2.1 Basic principles of biomechanics**

The basic mechanical principles are the essentials requirements for the biomechanics description and understanding.

## **Forces and types of forces**

As force is meant a physical vector quantity which is expressed in the interaction between two or more bodies, this is classically described by Newton's second law [ $F = ma$ ] where  $m$  is the mass (SI units: kg) and  $a$  is the acceleration (SI units:  $m/s^2$ ). The unit of measurement of force is the N ( $kg * m / s^2$ ) in the SI, although in the dental implant literature is commonly expressed as kilograms of force, since the mass is the determinant factor on Earth where the gravitational constant is approximately the same.

Because forces are vector quantities they can be described according to intensity, duration, direction and multiplication factors. The longevity of an implant is not only influenced by the intensity and duration of a force but also by its direction. To understand his influence, the vector of the force is generally factorized into three components along the three main axes which are the mesial-distal, the buccal-lingual and the occlusal-apical (Figure 1).

The occlusion is usually managed in order to concentrate forces on the occlusal-apical axis because a load oriented along the other two axes is potentially dangerous for the longevity of the implants. The forces can be described as compression, tension or shear.

Compressive forces tend to push two masses towards each other, tensive ones are inclined to spread them apart and shearing forces cause the sliding of one mass on the other. In 1975 it was already shown that the cortical bone is more resistant to compression than to tensive or shearing forces (Reilly 1975). Furthermore cements, retaining screws, implant components and bone-implant interface are all able to adapt more to compressive forces than to tensive or shearing ones (Figure 2).

The shape and geometry of implants are structured in order to transfer the occlusal forces to maximize the compressive components at the bone-implant interface.

Figure 1 Axes of stress decomposition (Misch, Contemporary Implant dentistry 2002)

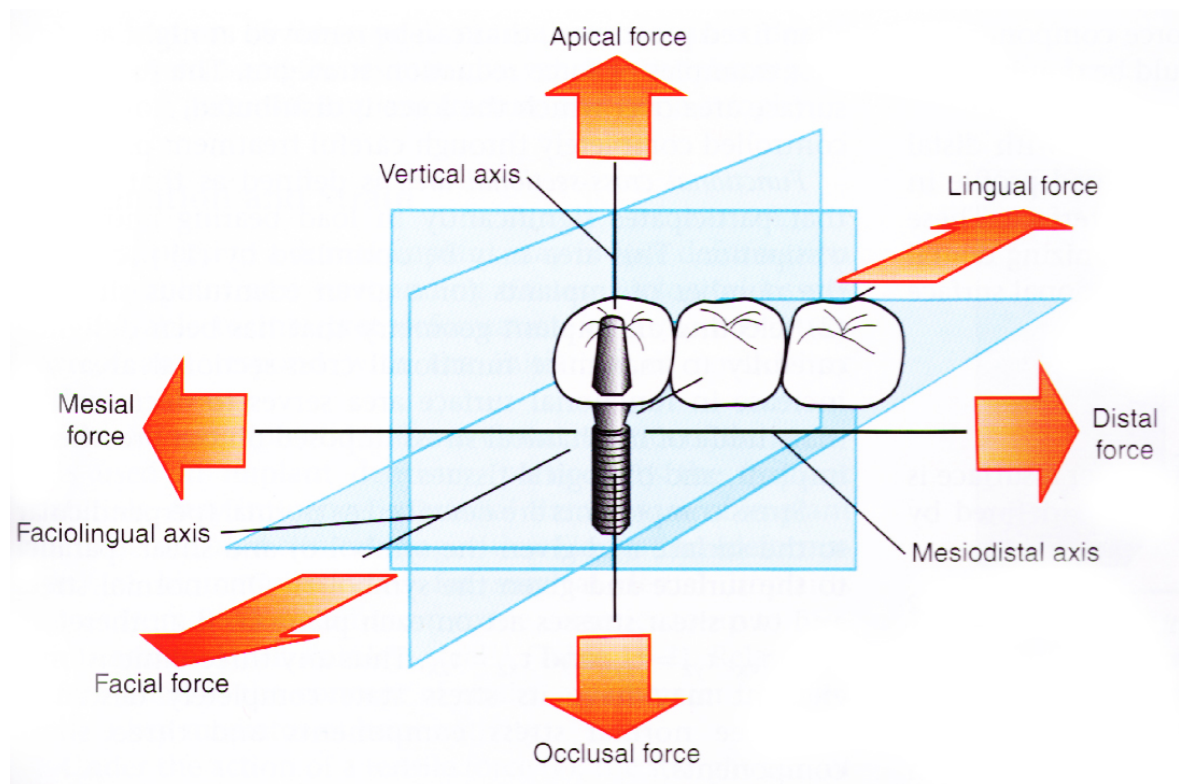
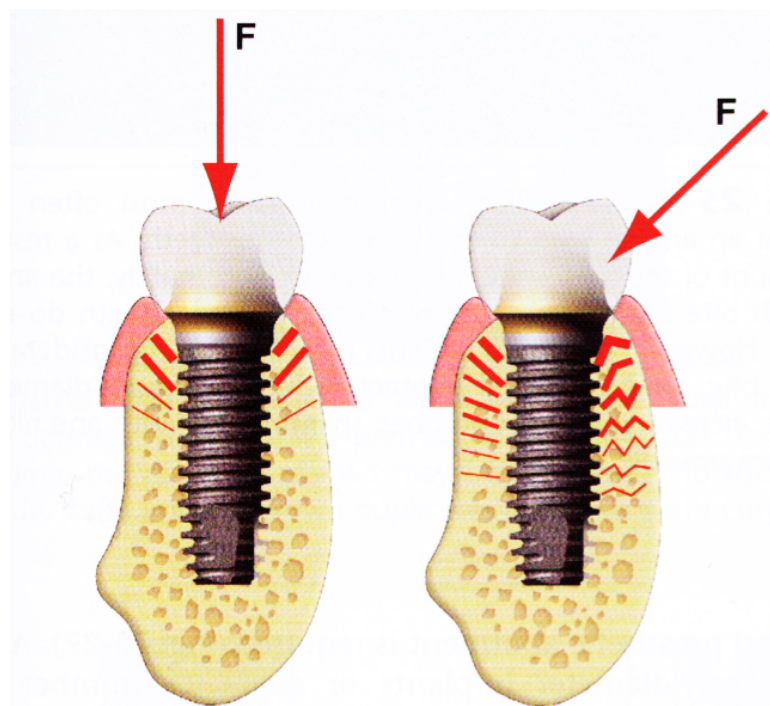


Figure 2 Comparison of stress between axial and non-axial forces (Misch 2002)



## Stress

The manner in which a force is distributed over an area is defined mechanical stress and it is specified by the following formula:  $[\sigma = F / A]$  where F is the force (N) and A is the area ( $\text{cm}^2$ ). The unit of measurement of mechanical stress is the Pa ( $= \text{N} / \text{m}^2$ ).

The intensity of the stress depends on two variables which are the magnitude of the force and the cross section area on which the force is distributed. The intensity of the force can be decreased by reducing some force intensifiers as length of the extensions, load-out-of-axis and height of the crowns.

The functional transversal area is defined as the surface that participates significantly to the bearing and dissipation of stress and it can be optimized by increasing the number of implants in the considered edentulous area and choosing an implant geometry designed to maximize the functional transversal area.

## Deformation and tension

The deformation of a body involves any change in the geometrical configuration of the body that, following the application of a stress, leads to a variation of its shape or dimensions. A straight bar, whose original length is  $l_0$ , under the action of a stress or a tension force stretches out up to a final length ( $l = l_0 + \Delta l$ ).

The linear deformation is therefore defined as elongation per unit of length, it does not have unit of measurement and is expressed by the formula  $\epsilon = (l-l_0) / l_0 = \Delta l / l_0$ . There is also a shear deformation that describes the modifications undergone at the right angle of a body in the presence of a stress of pure shear (Figure 3).

The deformation is highly dependent on the composition and mechanical capabilities of the material that undergoes the tensile stress.

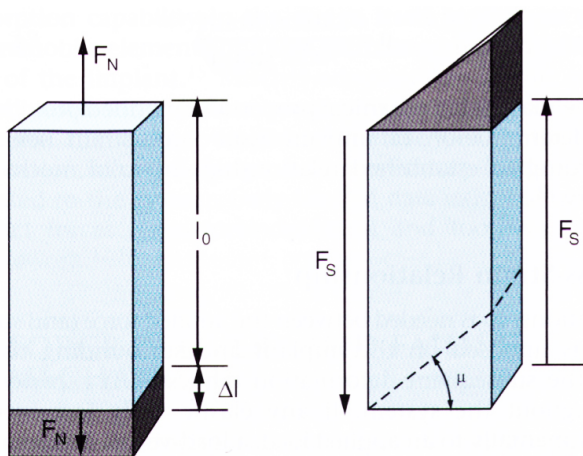
A classical stress-tension curve can be obtained by experimentally subjecting a body to a load, the inclination of the curve is the elasticity modulus E and its value indicates the stiffness of the studied material. Hooke's law describes the relationship between stress and tension in the simplest way  $[\sigma = E\epsilon]$  where  $\sigma$  is

the applied stress (Pa or kg / cm<sup>2</sup>), E is the elasticity modulus (Pa or kg / cm<sup>2</sup>) and  $\epsilon$  is the tension.

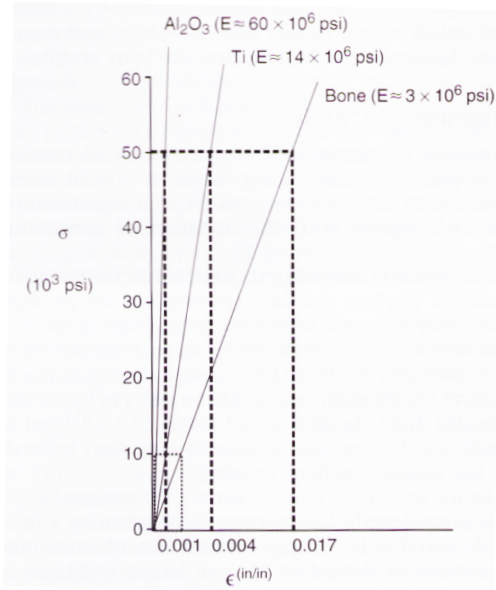
The closer the elasticity modulus of the system will resemble the one of the contiguous biological tissue, the lower will be the probability that a relative movement develops at the tissue-implant interface. As can be seen in the graph (Graph 1) the relative difference in stiffness between the bone and the titanium implant increases when the stress intensity grows, so the visco-elastic bone can stay in contact with the titanium implant in a more predictable way if the stress is low.

The cortical bone is approximately 5 times more flexible than the titanium and the denser a bone is the more rigid it will be, therefore the difference in stiffness between the bone and the titanium is lower for the bone type 1 compared to type 4 according to Albrekssonn and Zarb, analyzed in the previous chapter.

Figure 3. Shear and linear deformation (Misch 2002)



Graph 1. Difference in elasticity modulus of bone, Ti and Al<sub>2</sub>O<sub>3</sub> (Misch 2002)



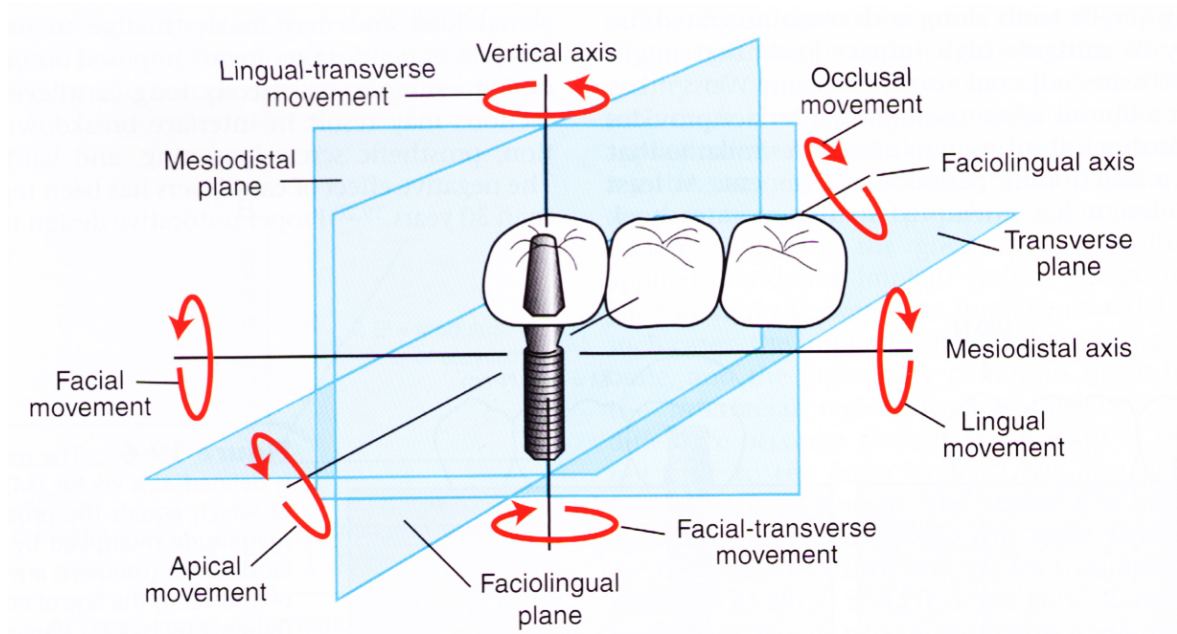
### Moment of loads and lever arms

The moment of a force is the tendency of a force to rotate an object and is defined as a vector whose intensity corresponds to the product of the intensity of the force multiplied by the perpendicular distance from the point of rotation examined at the line of the force action. This moment is also called *torque* or *torsional load* as it tends to produce rotation or bending at the applied point and it can have a destructive effect on an implant system if not correctly taken into account, as successively described.

In an implant system six different moments can develop, two for each axis of coordinate previously described (Figure 4), which can induce microrotations and concentrations of stress at the top of the crest at the implant-tissue level which can lead to crestal bone loss.

In implantology there are three clinical lever arms: the occlusal height, the length of the extension and the occlusal amplitude.

Figure 4. Moments of load in an implant system



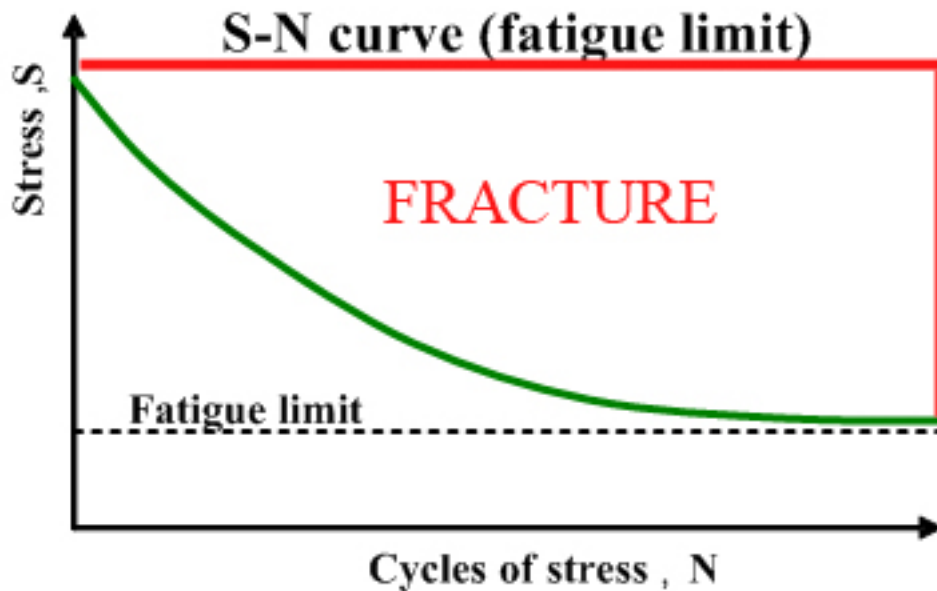
### Failure by fatigue

The failure by fatigue is characterized by dynamic conditions of load cycles. In dentistry it can be affected by the biomaterial, implant macrogeometry, force intensity and number of cycles.

The behavior of biomaterials is characterized by a fatigue curve S-N, a diagram of the stress applied to the number of load cycles (Graph 2). If an implant is subjected to particularly high stress few load cycles may be tolerated before fracture, while, if stress is below a certain limit, called *fatigue limit*, it can be subjected to an indefinite number of load cycles.



Graph 2. S-N Curve



## 2.2 Analysis of bone density

The bone is an organ able to change in relation to different factors, such as hormones, vitamins and mechanical influences. However the biomechanical parameters, such as the absence of load for an edentulous jaw, are predominant. (Roberts EW 1987, Klemetti E 1993, Mercier P 1981, Atwood DA 1971, Lavelle CLB 1993) The knowledge of this adaptability has been reported for the first time more than a century ago. In 1887, Meier described, from a quality point of view, the architecture of the trabecular bone in the femur. (Meier GH 1887)

In 1888, Kulmann noticed the similarity between the pattern of the trabecular bone in the femur and the trajectories of tension in the beams of the buildings. (Kulmann C 1888) Wolff, in 1892 elaborated these concepts further explaining: "Any change in the shape and function of the bone, or in the single function, is followed by some changes in the internal architecture and by changes equally defined in its external

conformation, in accordance with the mathematical laws "(Wolf J 1892) The edited function of the bone and the changes defined by the internal and external formations of vertebral skeleton, influenced by mechanical load, were reported by Murry. (Murry PDF 1936) Therefore the external architecture of the bone changes depending on the function and also the internal bone structure changes.

MacMillan (MacMillan HA 1926), Parfitt (Parfitt AM 1962) and later Spencer Atkinson with a systematic study of over 1,000 human skulls have observed the structural characteristics and changes in trabecular alveolar region of the jaw. For example, the maxilla and the mandible have different biomechanical functions (Figure 5). In fact, although equal and opposite functional loads are applied to both the first must absorb the full load while the second transfers it to the entire skull.

The mandible, as an independent structure, is designed as an absorption unit of the force. Therefore, when teeth are present, the cortical layer outside is more dense and thick and also the trabecular bone is thicker and denser, with trabeculae radially oriented (Figure 6). Its structure is similar to that of the diaphysis of a long bone and is loaded more in bending and torsion (Hylander WL 1979, 1981).

On the other hand, the jaw is a force distribution unit. Each tension on the upper jaw is transferred from the zygomatic arch and from palate far from the brain and orbits. (Figure 6) As can be seen in the representation the vertical components tend to be loaded in compression (negative stress) while the horizontal ones in tension (positive stress). (Atkinson, 1964) This is one of the more efficient structures to obtain the maximum resistance to compression with a minimum mass. Consequently, the upper jaw has a thin cortical lamina and a fine trabecular bone that supports the teeth. Being loaded primarily in compression, the jaw is structurally similar to the body of a vertebra.

These authors also observed that the bone density is greatest around the teeth (cribriform plate) and it is denser around the teeth at crest level, compared to that

around the apex. Orban showed a decrease in the trabecular bone pattern around a maxillary molar in the absence of the antagonist, compared to a tooth with occlusal contacts on the contralateral side (Orban B 1953).

Ulm et al. in 1999 and 2009 (Ulm 1999, 2009) presented studies that analyzed the bone quality and the amount of trabecular bone in the jaws at different levels, founding that in both cases the bone quality diminished by regions mesial to distal although It is significantly higher in the mandible than in the maxilla.

Not getting more mechanical stimuli, bone density decreases in the jaw after tooth loss. This decrease depends mainly on the time in which the region has remained edentulous and not loaded properly, on the initial density of the bone, on the bending and twisting of the lower jaw and on the parafunction, before and after the loss of teeth. In general, the density change after the loss of the teeth is maximum in the back of the upper jaw and minimum in the front part of the lower jaw.

The trabecular and cortical bone in the body is constantly being modified by modeling or remodeling. (Enlow DH 1963) The modeling presents independent sites of formation and resorption and causes a change in the shape or size of the bone. Remodeling is a process of resorption and formation in the same site, which replaces the previously existing bone and mainly influences the internal turnover of the bone, including those areas where the teeth are missing or the bone is close to an endosseous implant . (Roberts WE 1984 Garretto LP 1995) These adaptive phenomena have been associated with modification of the mechanical stress and the environmental tension, preaviously defined in host bone. (Rhineland FW 1974 Currey JD 1984) The higher is the magnitude of the stress applied to the bone, the higher is the tension observed in the bone. (Bidez MW 1992) The modeling and remodeling of bone are mainly controlled, in part or totally, by the mechanical environment of the tension.



### 3.3 Bone adaptation to mechanical tension

In general, the density of the alveolar bone evolves as a result of mechanical deformation due to micro-tensions, Frost proposed a model of four histological patterns for compact bone, related to adaptation to mechanical stress (Frost HM 1989, 1990) In fact, the bone can reduce tensions through apposition or reduction, formation or resorption, and varying the modulus of elasticity or stiffness modifying the mineral content (Cowin SC 1976, 1976, 1978) Depending on the amount of microtension experienced, different areas have been described for bone: pathologic overload area, low overload area, adaptation window and the acute disuse window (Figure 7). These four categories can also be used to describe the response of the trabecular bone in the maxillary.

The bone in the acute disuse window lose mineral density and disuse atrophy occurs because the modeling of new bone is inhibited, while the remodeling is stimulated, with a gradual net loss of bone. The bone microtension for negligible loads is reported from 0 to 200 units of microtension ( $\mu\epsilon$ ). This phenomenon may occur throughout all the skeletal system, as evidenced by a 15% decrease in the cortical lamina and extensive loss of trabecular bone resulted by the immobilization of a limb for 3 months (Kazarian LE 1969). During bone disuse a decrease in the density of the cortical bone of 40% and a decrease in the density of the trabecular bone of 12% have been reported. (Minaire MC 1974 Uthoff HK 1978) Interestingly a bone loss similar to disuse atrophy was associated to microgravity environments in outer space, because the bone microtension, which is the result of Earth's gravity, is not present in space environment "in weightlessness". (DJ Simmons 1981) In fact, an astronaut that lived in the Russian space station Mir for 111 days lost about 12% of his bone mineralization. (Ingebretsen M 1997 Oganov VS 2004)

The adaptation window between 200 and 2500 microtension units represents a balance between modeling and remodeling and bone conditions are maintained at that level. The bone, in this environment of tensions, remains in a stationary state, and this can be considered the homeostatic window of health. From the histological point of view, this bone is basically lamellar. In the area of physiological load, which corresponds to the adaptation window, every year about 18% of the trabecular bone and 2-5% cortical bone are remodeled. (Roberts EW 1987) In these conditions, the lamellar bone can support millions of load cycles, more than those that can normally occur during life. This is the ideal tension range that should be get around the intraosseous implant. In the adaptation window of the bone the turnover is necessary, as Mori and Burr showed the remodeling of the bone for fatigue damage regions of microfracture within the physiological interval. (Mori S 1993)

The low overload area (from 2500 to 4000 (1500/3000) microtension units) causes a higher percentage of fatigue micro-fractures and increases the rate of cell turnover in the bone. Consequently, the resistance and the density of the bone at the end may decrease. Typically, in this range the bone, from the histological point of view, is interlaced or in repair. This may be the state of a bone when an endosseous implant is overloaded while the bone interface attempts to change the tension environment. During the repairing process, the interlaced bone is weaker compared to the mature, lamellar and mineralized, bone. (Roberts WE 1984) So, it is necessary to be careful while the bone is loaded in the medium overload zone, because the "safety interval" for bone strength during repair processes is reduced. (Garretto LP 1995)

When the micro-tensions are greater than 4000 units, the zones of pathological overload are reached. (Frost HM 1989) In these conditions a fatigue failure in 1000 cycles, which can be easily reached in a few weeks of normal activities, could be produced.

The fracture of the cortical bone occurs between 10,000 and 25,000 microtension units (deformation of 1-2%). Then, the pathological overload may start at microtension levels between 20 and 40% of the extreme resistance to physical

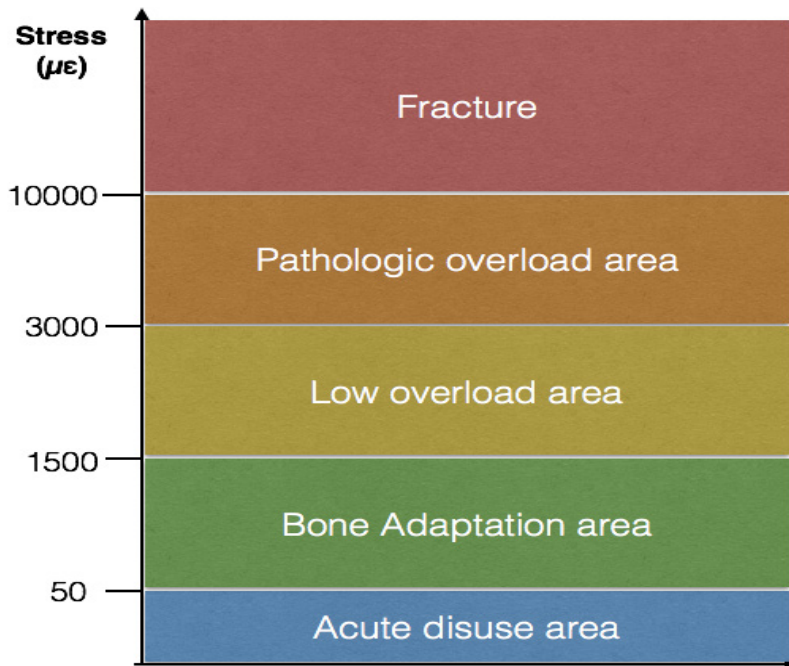
fracture of the cortical bone. The bone may be reabsorbed in this area and form fibrous tissue, or when present, interlaced repairing bone, as a large percentage of replacement is required.

The loss of marginal bone and the eventual failure of an implant, highlighted during the implant load, may depend on the fact that the bone is in a pathological overload condition.

Subsequently Turner (Turner CH 1988 1998) has summarized the rules that rule the bone adaptation as follows: the dynamic load (not static) determines bone adaptation; the load in a short term has an anabolic effect, while a duration increase decreases the bone adaptation; abnormal tensions evoke bone adaptation while it get used to the routine tensions and the remodeling ceases.

More recently the process of cellular mechanotransduction has been analyzed in detail. This is a multistep process that includes mechanical coupling (translation of mechanical forces into signals perceived by the sensorial cells), biochemical coupling (conversion of the mechanical signal into a biochemical signal that brings a response from cells, like gene activation), signal transfer from sensorial cells to effector cells and subsequent effector cells response (Duncan RL 1995). Other studies have shown that osteocytes immersed in the bone matrix inside lacunae can act as mechanoreceptors helping in the transduction of mechanical signals into biochemical, since they are in communication with osteocytes and osteoblasts in periosteal and endosteal space. (Turner CH 1998, Cowin SC 1991, Burger EH 1999 Westbroek I 2000, Vezeridis 2006).

Figure 7. Frost diagram



### 3.4 Masticatory dynamic

After understanding the importance of the intensity of the forces applied on skeletal system in general, and in particular on the interface between bone and implant surface, we analyze how these forces are applied and what is their size.

In humans the masticatory system consists in the capacity of the lower jaw to move related to the skull, to which is connected by two symmetrical joints, the temporomandibular joints (TMJ), with a great freedom of movement, through the action of the mastication muscles.

Six pairs of muscles are crucial in the mandibular movement.

The masseter, the medial pterygoid and temporal muscles elevate the mandible; between them two, the masseter deep fascicle and the temporal rear fascicle, have also the ability to determine retraction movements. The external pterygoid muscle determines the protrusion of the jaw. The geniohyoid and, particularly, the digastric muscle have an action of lowering and retraction of the jaw. (Herring 2007, Hanman 2008)



The jaw has six degrees of freedom of movement, three translational and three rotational oriented in the three axes (Bagar, Osborn, 1984; Koolstra 2002), although it is not simple to recognize functional movements in their complexity in a combination of translational and rotatory axes (Figure 8). To carry out these movements all the muscles mentioned above are active; some moving, some balance, others finally stabilize, interchanging themselves in their role according to the progression of the movement. In close coordination with them, the neck muscles stabilize the skull and hyoid bone, in order to build stable bases from which opening and closing muscles can act.

Each muscle action produces a translation of the jaw along its line of action and a rotation around an axis perpendicular to the direction, passing through the center of jaw mass, thus generating a moment. (Figure 9) (Koolstra 1995 and 2002)

The loads on the jaw muscle may be important and include a shear force dorsal-ventral, torsion along the major axis of the jaw and cross-section, that increases in intensity in the direction from rear to front (Hart RT 1992).

Because insertions of the jaw elevator muscles are located at the back, the front jaw experiences a great moment of forces, even in the absence of occlusal loads, caused by the bending of the vestibular-lingual bone. So we expect higher densities in the anterior mandible than in the posterior as shown by studies of the properties of human toothed jaw bones (Schwartz-Dabney CL 2003, Peterson J 2006). Despite in the posterior mandible are present closing forces considerably higher (2-3 times) compared to the front area, the apparent density and the extreme resistance of bone are lower overall. (Bidez MW 1992) Therefore, to disperse these occlusal loads the rear molar teeth possess a big and multiroots structure.

Many studies have found dimensional changes of the jaw during the activity attributing the action to the masticatory muscles. (De Marco 1974 Grant 1986 Fischman 1990)

One of the most common changes is the medial convergence, which occurs distally to the chin holes, during the movements of opening and protrusion. It is mainly due to the junctions of the internal pterygoid muscles to the medial branch

of the mandible. The amplitude of the contraction was measured in 0.8 mm in the area between the first molars and up to 1.5 mm in the sites from branch to branch. (De Marco 1974 Grant 1986 Fischman, 1990).

While chewing in the balancing side a bending in the sagittal plane, with tensional stress along the alveolar process, and a twist occur (Figure 10). On the working side the body receives a twist along its long axis; muscle strength tends to rotate outward the lower edge of the mandible and inwards the alveolar process, while the torsional moment associated with the occlusal force has the opposite effect. Therefore, the portion of the body of the mandible between these two torsional moments undergoes the maximum stress and also a dimensional variation. (Dechow 2000) The jaws of patients with prosthetic implant had 19% torsion dorsal-ventral, this was confirmed by Hobkirk et al. (Abdel-Latif HH 2000) The magnitude of this deflection increases with the decrease of the bone size, then in mandibles with greater resorption, and with the increase of the masticatory force, in case of parafunction. Miyamoto et al. in a study have identified the mandibular bending as the primary cause of the posterior implants, in mandibular full-arch fixed prostheses on linked implants. This is due to the fact that linked implants rigidly fixed, in a restoration of the entire jaw, are subject to a considerable lateral force, buccal-lingual, during the opening and parafunction (Miyamoto 2003, Zarone 2003) as bending is opposed by prosthesis.

Figure 8. Forces operating on the mandible (Koolstra 2002)

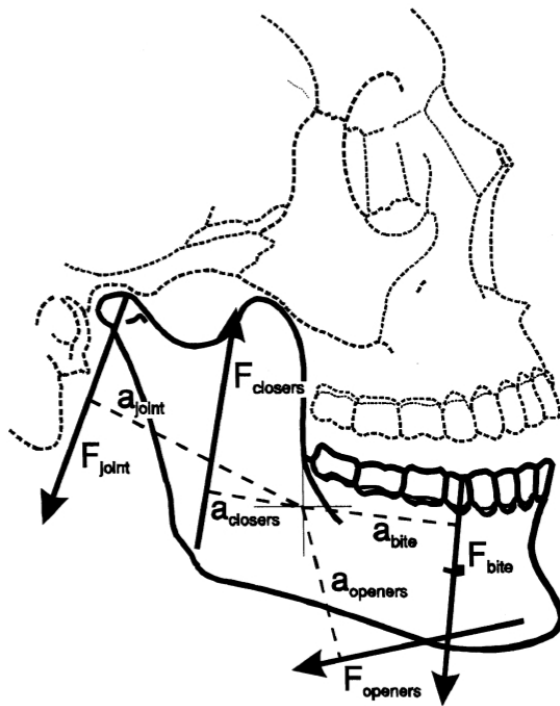


Figure 9. Force and torque generated by a muscle (masseter) in respect to the centre of jaw mass of the mandible

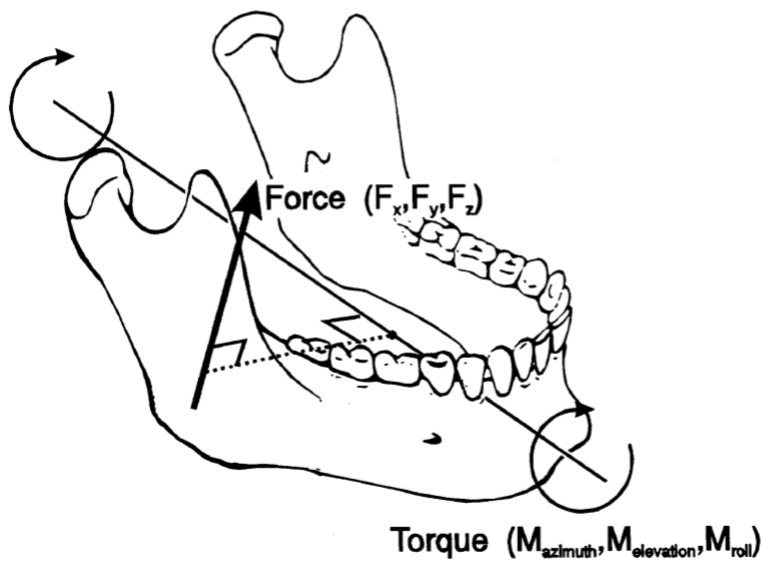


Figura 10 Stress distribution on the balancing side during unilateral mastication (Misch 2002)

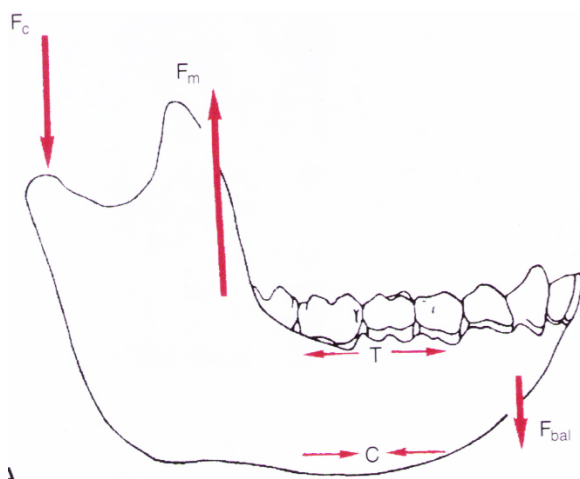
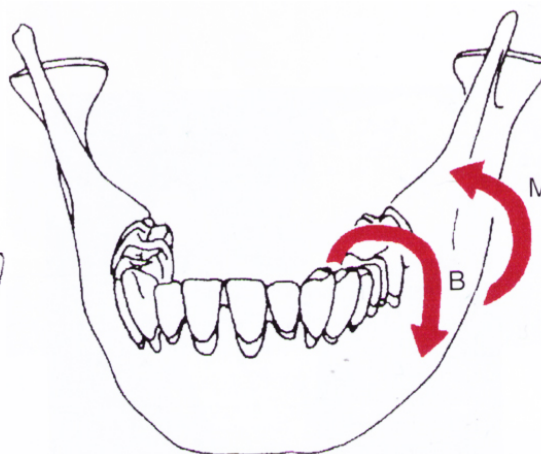


Figura 11 Stress distribution on the working side during unilateral mastication (Misch 2002)



### 3.5 Physiological and parafunctional masticatory forces

The "natural" forces more exercised against the teeth and then against the implants are present during mastication. (Picton 1969, 1971)

In the posterior regions these forces are predominantly perpendicular to the occlusal plane, of short duration and occur only for short periods during the day. They are included between 2.2 and 20 kg approximately, in particular less than 2.2 kg / cm<sup>2</sup> registered by tension measurers on inlay (Scott 1966). The real-time application of the chewing forces on the teeth is about 9 minutes per day (Graf 1969). Perioral muscles and tongue exert a more consistent and more light force on the teeth or on implants in the horizontal direction. These forces reach about 0.2 to 0.35 kg / cm<sup>2</sup> during swallowing (Proffit, 1978). An individual swallows on average 25 times per hour while awake and 10 per hour during sleep for a total of 480 times a day (20 minutes / day). (Graf 1969) The maximum closing force is different than the bite force, is highly variable between individuals and depends on

the state of the teeth and the masticatory musculature. Several studies on different samples of populations have tried to measure the extent of this force obtaining variable results (Tables 1 and 2).

Table 1. Mean of maximum masticatory force in different rehabilitations

<b>Authors</b>	<b>Natural teeth or type of rehabilitation</b>	<b>Maximum chewing force average</b>
Carr and Laney, 1987.	Conventional prosthesis Implant-supported prosthesis	59 N 112,9 N
Momeburg and Proschel, 2002.	FDP of 3 implant-supported units: Single implant: Front Single implant: Rear	220 N 91 N 12 N
Fontijn-Tekamp et al., 1998...	Implant-supported prosthesis Molar region Incisal region	Unilateral 50-400 N 25-170 N
Mericske-Stern and Zarb, 1996	Total prosthesis / implant- supported prosthesis	35-330 N
van Eijden, 1991..	canine tooth second premolar second molar	469±85 N 583±99 N 723±138 N
Braun et al., 1995	Natural teeth	738±209 N (male>female)
Raadsheer et al., 1999	Man teeth Woman teeth	545,7 N 383,6 N

Table 2. Maximum closing force

Maximum closing force							
Reference	Age years	N°	Incisive	Canine	Premolar	Molar	Comments
Braun et al. 1995	26-41	142				710 N	Among premolars and molars; 789 males; 596 female subjects
Van Eijden 1991	31,1(± 4,9)	7		323-485 N	424-583 N	475-749 N	Second premolars and second molars left and right (only males)
Dean et al. 1992	Adult	57	150 N			450 N	Converted from figures
Bakke et al. 1990	21-30 31-40 41-50 51-60 61-70	20 20 20 17 8				572 N 481 N 564 N 485 N 374 N	Measured on the first molars on the right and left
Braun et al. 1996	18-20					176 N	First molars or first premolars

Table 2 shows the maximum closing forces that, as guessed, are greater in the molar rather than in the premolar, canine or incisive area (Mansour, 1975). In fact, in a study of Chung considering 339 implants, operative for 8.1 years in 69 patients, the posterior implants showed an average of 3.5 turns of bone loss per year compared to the anterior implants (Chung 2005).

These forces are not expressed by patients routinely even if there are conditions relative to the patient that may increase the risk of occlusal overload on implant prosthesis.

The main factors are the parafunctions as bruxism, clenching and tongue's push.

Bruxism mainly concern horizontal wear rather than functional, as it consists in a friction rub between incisal and occlusal surfaces of the lower and the upper arch. It is the most common oral parafunction, reported in approximately 10% of cases (Glass 1993, Lavigne 1994) although many of individuals concerned are not conscious. The forces involved are more intense, between 4 and 7 times higher than normal, with longer duration, from lateral direction rather than vertical and characterized by shear more than compression. (Misch 2002) These forces may develop while the patient is awake or more commonly when is asleep, generating an increased load in the system for several hours a day. In patients with implants that also suffer from severe bruxism complications are frequent, such as fractures, prosthetic loosening of the abutment screw, fractures and implant crestal bone loss that can lead to implant failure.

The clenching, often included in the term 'bruxism' according to the dental literature, is a parafunction which generates a constant force exerted by an occlusal surface on the other, without any lateral movement. The lower jaw can be at any position before the static load, there are also combinations of bruxism and clenching. The direction of the load may be horizontal or vertical, the forces involved are much greater than the physiological loads related to bruxism, but the forces generated are directed more vertically with respect to the occlusal plane, at least in the posterior regions of the mouth. Clenching does not produce as many wear surfaces as in bruxism and it is more difficult to diagnose (Alderman 1971, Dawson 1989, Misch 2002). Even clenching, as bruxism, affects the occurrence of complications at implant level as detailed above.

The parafunctional push of tongue is a non natural force exerted on the teeth during swallowing. Although the push of tongue is of a lower intensity than other parafunctional forces, it is horizontal and can increase stress on the transmucosal implant site. (Misch 2002) Apart from that parafunctions the force can be influenced by the size of the patient, age, sex and skeletal position. (Braun 1995, Raadsheer 1999, Fontijn-Tekamp 1998)

A brachycephalic, with a massive head shape, can generate a force three times higher than a regular one. (Koc 2011)

In edentulous patients during years the maximum closing force decreases while muscular atrophy progresses. (Carr 1987) After the implant placement this strength can increase by 300% in three years (Fontijn-Tekamp 1998, Raadsheer 1999, Morneburg 2002).

### 3.6 Implant Failures and complications

Several studies and literature reviews observe that the most frequent implant complications and failures occur after the system load for biomechanical reasons, mainly due to an overload. (Goodacre 2003, Oh 2002, Jividen 2000, Lekholm 1986, Lang 2000, Tonetti 1994, Heitz-Mayfield 2004) (Tables 3 and 4)

Table 3 Mechanical complications (Goodacre 2003)

<b>Mechanical implant complications</b>		
	<b>Number Placed / affected</b>	<b>Mean incidence</b>
Overdenture loss of retention / adjustment	376/113 prostheses	30%
Esthetic veneer fractur (resin)	663/144 prostheses	22%
Overdenture relines	595/114 prostheses	19%
Overdenture clip / attachment fracture	468/80 prostheses	17%
Esthetic veneer fracture (porcelain)	258/36 prostheses	14%
Overdenture fracture	570/69 prostheses	12%
Opposing prosthesis fracture	168/20 prostheses	12%
Acrylic resin base fracture	649/47 prostheses	7%
Prosthesis screw loosening	4501/312 screws	7%
Abutment screw loosening	6256/365 screws	6%
Prosthesis screw fractures	7094/282 screws	4%
Metal framework fractures	2358/70 prostheses	3%
Abutment screw 13 fractures	160/244 screws	2%
Implant fractures 12	157/142 implants	1%



Table 4 Common complications (Goodacre 2003)

<b>Most common implant complications (10% or greater incidence)</b>		
	<b>Number Placed / affected</b>	<b>Mean incidence</b>
Overdenture clip / attachment loosening	376/113 prostheses	30%
Implant loss in the maxilla from radiation therapy	217/55 implants	25%
Hemorrhage-related complications	379/92 patients	24%
Resin veneers fracture / fixed partial dentures	663/144 prostheses	22%
Implant loss with maxillary overdentures	1103/206 implants	19%
Overdenture relins needed	595/114 prostheses	19%
Overdenture clip / attachment fracture	468/80 prostheses	17%
Loss Implant in Type IV bone	1009/160 implants	26%
Porcelain veneers fracture / fixed partial dentures	258/36 prostheses	14%
Overdenture fracture	570/69 prostheses	12%
Opposing prosthesis fracture	168/20 prostheses	12%
Implant loss in smokers	1668/178 implants	11%
Implant loss implants with short (10 mm or less)	2754/272 implants	10%
Implant loss with maxillary fixed complete dentures	4559/443 implants	10%
Esthetic complication with prostheses	493/47 prostheses	10%

In the surgical procedure some failures may be experienced due to overheating in osteotomy preparation, excessive pressure or twisting force on the bone-implant interface during implant placement or implant micro-movement during osseointegration. (Brunski 1979) Recent researches show how the surgical phase determines a successful connection in more than 95% of cases, regardless of the implant system used. (Goodacre 2003)

In some cases the implant can fail soon after the integration in what was described by Misch and Jividen as "failure during the initial load." (Misch 2005) The cause of this failure is usually an excessive stress on the bone-implant connection rather

than the retention of bacterial plaque. (Isidor 1996, 1997) It depends on the amount of forces applied to the prosthesis (Brunski 1989, Bidez 1992, Van Steenberghe 1994, Oh T-J 2002) and on the density of the bone around the implants (Leckolm 1986, Gunne 1994, Snauwaert 2000, Goodacre 2003) and can affect 15% of implant restorations. (Creugers 1994, Oh T-J 2002, Goodacre 2003). The loosening of the abutment screw was found in the total percentage of 6% of the prosthetic implant, especially in single tooth crowns (25%) rather than fixed prostheses and overdentures with multiple units (3%). Factors that can lead to this complication is the presence of lever arms from extensions or greater height of the crowns. (Kallus 1991, Boggan 1999).

The most common complications are stress-fractures of different dental materials of the prosthetic system. The materials follow a fatigue curve which depends on the number of cycles and on the intensity and direction of the force. The most common stress-fractures are those on resin crowns (22%) followed by the junctions of overdentures (17%), the ceramic crowns (14%) and bases in acrylic resin (7%). These data are also confirmed in a study of Francetti et al. (Francetti et al. 2008) in which 62 patients rehabilitated with fixed mandibular prostheses type Toronto, on 4 implants, showed a fracture of the temporary acrylic resin in 11% of cases.

Less common are fractures of the prosthetic screws (3%), of metal structures (3%), of the screws pillar (2%), that usually have a larger diameter than prosthetic ones, and of the implant body (1%), condition reported mostly in long-term failures. The prosthesis decementation occurs far more likely when loads are applied chronically on cement interface or when there are shear forces.

A condition that occurs most frequently is the marginal bone loss. Although it was widely described in the crestal region of successfully osseointegrated implants, regardless of the surgical approaches, it is recognized as a pathological symptom which can lead to implant failure. This bone loss is usually higher in the first year of prosthetic loading and then stabilize; it was quantified by Adell et al. with an average of 1.2 mm during the first year and 0.05 to 0.13 mm per year in subsequent years. (Adell 1981) Based on these data Albrektsson proposed as

criteria, for a successful implant, a bone resorption of 1.5 mm for the first year and of 0.2 mm per year in subsequent years. (Albrektsson, Zarb 1986) The current hypothesis for the cause of crestal bone loss vary between the reflection of bone during surgery, the osteotomy preparation for implantation, the position of the microgap between the abutment and the implant body, the micro-movements of the body of the pillar, the bacterial invasion, the establishment of a biological width and the stress factors. (Adell 1981 1986, Albrektsson, Zarb 1986, Tonetti 1994, Misch 1995, 2005).

The role of occlusion is controversial. Some authors claim that the loss of peri-implant bone without the implant failure is associated mainly to biological formations or complications. (Lang 2000, Heitz-Mayfield 2004) Others suggest the correlation between the reduction of crestal bone and occlusal overload. (Rosenberg 1991, Karolyi 1991, Oh T-J 2002, Misch 1995, 2005) Many authors have finally concluded that the occlusal trauma is a factor related to bone loss, even though the presence of bacteria is a necessary condition. Misch et al. in a review of the literature on cell biomechanics, principles of engineering, finite element studies, animal studies and clinical studies support that the occlusal overload contributes to marginal bone loss. (Misch 2005) This statement considered the response of bone tissue to excessive loads at the interface between the titanium and the cortical bone, which has a modulus of elasticity between 5 to 10 times lower. Several studies on photoelastic the three-dimensional finite element show that the greater intensity of the stress occurs around the implant crestal region (Bidez 1992, Kilamura 2004, Duyck 2001, Natali 2006). If nothing is done to reduce the force factors that produce loss of peri-implant bone a failure of the implant can occur. The more the distance increases between the occlusal surface and the bone crest the more the vertical lever arm increases, therefore the stress intensity between the bone crest and the implant surface will be greatly enhanced.

# Chapter 3

## FINITE ELEMENT ANALYSIS

---

### 3.1 Definition of Finite element analysis

The finite element method (FEM) or finite element analysis (FEA), in mathematics is a numerical technique for finding solutions to boundary value problems for partial differential equations.

It was first introduced in 1943 by Richard Courant (Choi 2014) and was comprehensively applied in engineering, particularly in the early 1960s by the aerospace industry and its use has spread.

In the 1970s FEM was introduced in orthopedic biomechanics in order to assess the stresses and deformations in human bones during functional loadings and in 1976, Weinstein et al. (Weinstein AM 1976) were the first researcher to use it in oral implantology.

Since then, this method was widely used to analyze the designs of implants, prosthetic components and interactions at bone-implant interface. (Pesqueira 2014)

The FEM technique to obtain a solution to a complex mechanical problem, consists in dividing the problem domain into a collection of much smaller and

simpler domains in which the field variables can be interpolated with the use of shape functions. (Geng 2001)

So instead of seeking a solution function for the entire domain. one formulates the solution functions for its finite element and combines them properly to obtain the solution to the whole structure.

The steps followed are generally constructing a finite element model, followed by specifying appropriate material properties, loading and boundary conditions so that the desired settings can be accurately simulated. (Trivedi 2014)

The success of FE modeling in implant dentistry depends on the accuracy in simulating the geometry and surface structure of the implant, the material characteristics of the implant and bone, the loading and support conditions as well as the biomechanical implant\_bone interface

### **3.2 Creating a model of living and non-living structures**

A finite element model is constructed to represent the physical problem that has to be evaluated, by dividing solid objects into several elements that are connected at a common nodal point. Each element is assigned appropriate material properties corresponding to the properties of the object being modeled. The first step is to subdivide the complex object geometry into a suitable set of smaller 'elements' of 'finite' dimensions.

When combined with the 'mesh' model of the investigated structures, each element can adopt a specific geometric shape (i.e., triangle, square, tetrahedron, etc.) with a specific internal strain function. Using these functions and the actual geometry of the element, the equilibrium equations between the external forces acting on the element and the displacement occurring at each node can be determined.

The features of the model should resemble the physical properties of the actual structure as closely as possible, with respect to dimension and material properties. (Geng 2001)

The model could be either a 2D or a 3D model, depends on the intricacy of the problems which are to be addressed, the level of accuracy required, applicability of the results and the complexity of the structures involved in the analysis. (Romeed 2006) 3D models are considered more realistic and more representative of human anatomy, restorations and implant components and although they involve a higher level of difficulty in mesh refinements, their level of accuracy is much superior while capturing the geometry of complex structures.

3D models can be manually constructed or generated from imaging options such as a CT scan or an MRI.

Computed tomography offers another advantage for realistic modeling in not only the development of anatomic structures, but also the inclusion of material properties according to different bone density values. (Cahoon 1994)

Most FEA studies most studies assume a uniform density value for cortical and cancellous bone.

However some of them, as for example Bellini et al. 2009 (Bellini 2009), develop two meshes with different elastic properties in which cortical bone can be layered around the cancellous bone or can be neglected altogether in order to simulate weak bone properties similar to those found in the posterior maxilla. (Figure 1)

To develop more realistic models, different studies (Arisan 2012, Lee 2011, Turkyilmaz 2008) suggest future studies include variable density properties obtained from bone density values measured in Hounsfield Units or from other advanced data obtained from computed tomography scans performed with individual patients.(Figure 2)

Implant and abutment components can be imported into the FE module being scanned and digitally reconstructed or can be manually drawn from precise geometric measurements acquired from the manufactures. (Moeen 2014)

In most studies the models are considered to have an isotropic behavior, since it is not possible to quantify the whole anisotropic structure of a bone with current techniques (Doblare 2004, Bayraktar 2013).

An isotropic material indicates that the mechanical response is similar regardless of the stress field direction. It requires Young's modulus ( $E$ ) and Poisson's ratio ( $\nu$ )

values for the FE calculation. The elastic, or Young's modulus ( $E$ ), is defined as stress/strain ( $s/e$ ) and is measured in simple extension or compression. It is a measure of material deformation under a given axial load. Poisson's ratio ( $\nu$ ) is the lateral strain divided by axial strain, thus representing how much the sides of a material deform as it is tested.

Figure 1. Example of the process of creating two different meshes for cortical and cancellous bone

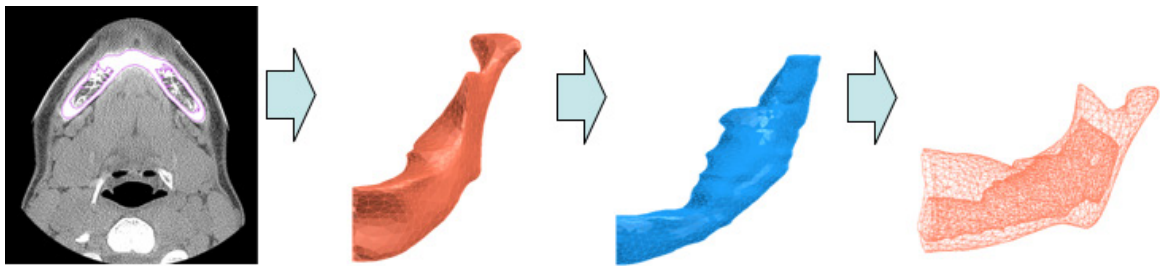
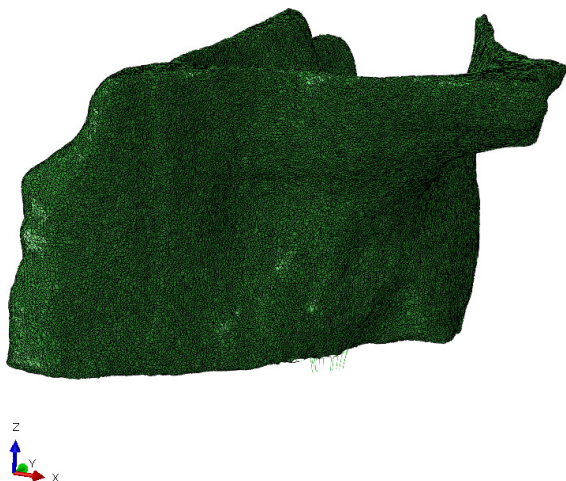


Figure 2. Example of a 3d model of a mandible reconstructed from TC scans



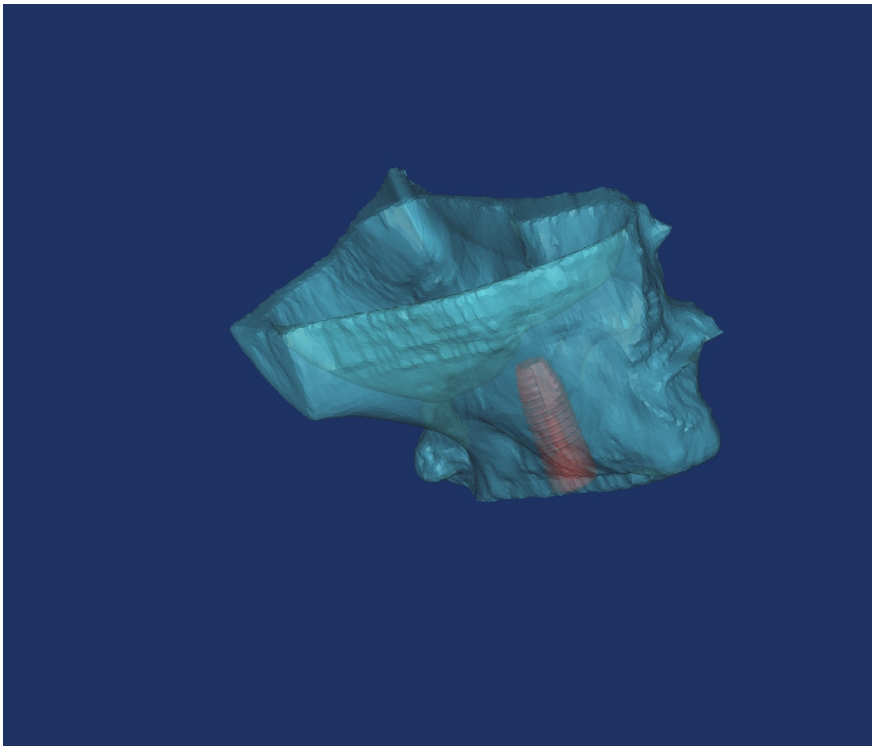
### 3.3 Interfaces

The following step is to assemble all the elements to obtain the finite element model of the structure. (Figure 3)

Previous FEA studies employed linear static models with the assumption that bone and implant are perfectly bonded to each other. (Geng 2004) In reality, dental implants never have a total osseointegration, with the whole surface area perfectly bonded to the surrounding bone. The bone-implant contact (BIC) values may change according to the jaw, placement of the region of the implant, healing time, implant design, and surface structure. Comparative studies show different BIC levels changing from 13% to 80% percent. (Wennerberg 1996, Galli 2005)

In most FEA studies, even the interface between prosthetic materials is assumed to be 100% bonded, including the cement thickness. (Geng 2001, Sagat 2010) Therefore implant, abutment, abutment screw, framework, and porcelain structures are considered to be a single unit.

Figure 3. Example of 3D Maxilla mesh with a dental implant mesh embedded in it





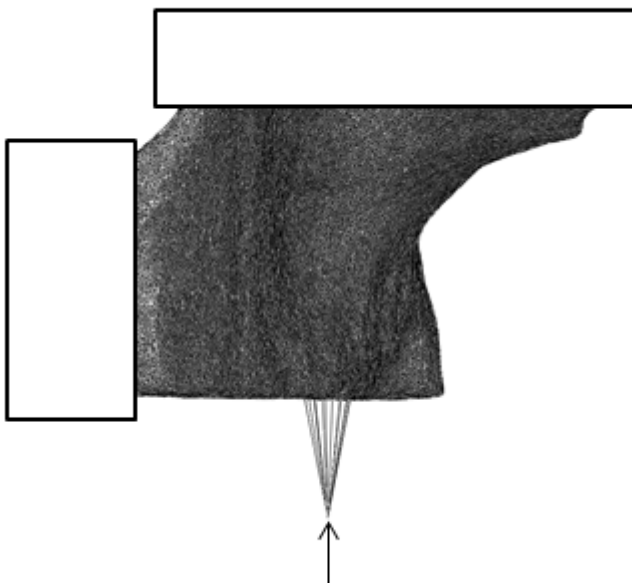
### 3.4 Loading conditions and boundaries

Even if the muscle activity and craniofacial morphology should be included in the model because they affect the occlusal load in actual clinical situation, it is presently difficult to simulate individual muscle forces to FEA modeling. And since the distribution of stress and strain is effective only in the region of loading the entire quadrant of bony segment need not be modeled.

To guarantee the validity of the simulation, boundaries with zero displacement or rotation should be positioned at nodes which are at a reasonable distance away from the region of interest so that there is no overlapping between the stress and strain fields associated with the induced reaction forces. (Moeen 2014) (Figure 4)

Loading can be axial and non-axial. An axial force is transmitted down through the long axis of the implant and hence compresses the anchorage unit which is favorable. Non-axial or horizontal loading transmits tensile stresses which try to separate the components and induces a bending movement which is considered potentially harmful.

Figure 4. Boundaries nodes at the extremities of the 3d model of the maxilla



### 3.5 Analysis of the stress

To evaluate the effect of loading forces on the peri-implant region or prosthesis structures, in FEA studies related to implant dentistry, usually the values are presented as either von Mises stress (equivalent tensile stress), minimum principal stress, and maximum principal stress. (Geng 2001, Meric 2012, Sagat 2010, Bayraktar 2013, Moeen 2014)

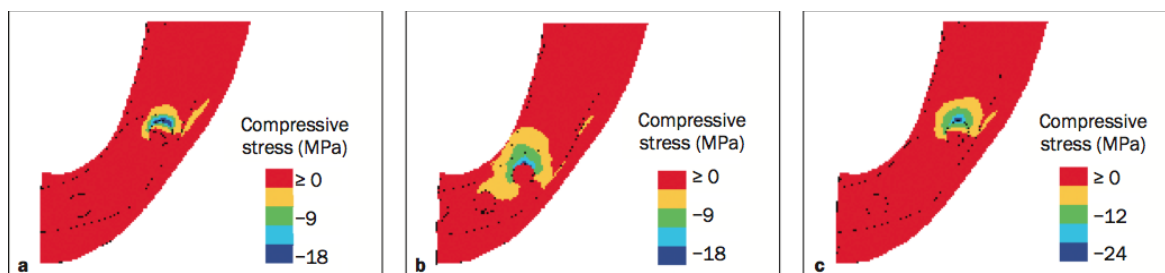
The von Mises criteria refer to a formula for combining the three "principal stresses" (that can be calculated in any point, acting in the x, y and z directions) into an equivalent stress, which is then compared to the yield stress of the examined material. (Bayraktar 2013)

The maximum principal stress is a positive value indicating the highest tension. The minimum principal stress is a negative value indicating the highest compression.

Most of the previously published studies have used von Mises stress as an analysis criterion which usually deals with ductile materials having equal compressive and tensile strength such as aluminum or steel. However when representing brittle materials such as bone, ceramics or cements maximum and minimum principal stresses would better indicate the magnitude of stress concentrations and the distributions as this offers the option of distinguishing between tensile and compressive stresses by positive and negative signs respectively. (Moeen 2014)

The stress is frequently represented by color figures, figure 5 represent an example of minimum principal stress distribution in a model of mandible with three different implant configurations (Bellini 2009).

Figure 5. Graphical representation of minimum stress distribution in the mandible (Bellini 2009)



### 3.6 Other biomechanics studies in Dentistry

The application of engineering knowledge in dentistry has helped the understanding of biomechanics aspects related to dental implants.

Several techniques other than FEA have been used to evaluate the biomechanical load on implants among that the most used are photoelastic stress analysis and strain-gauge analysis.

#### Photoelastic Analysis

Photoelasticity was introduced in dentistry by Noona in 1949. (Sevimay 2005)

Since then, this method has been widely used in dentistry, and in particular in oral implantology since 1980. (Haraldson 1980)

The photoelastic analysis technique is based on the optical property of certain colorless plastic materials that, when subjected to stress and deformation present alterations on the refraction indices promoting color change and the creation of fringes. (Pesqueira 2014)

Unlike the analytical methods of stress determination, photoelasticity gives a fairly accurate picture of stress distribution even around discontinuous materials. The method is as an important tool for determining the critical stress points in a material and is used for determining stress concentration factors in irregular

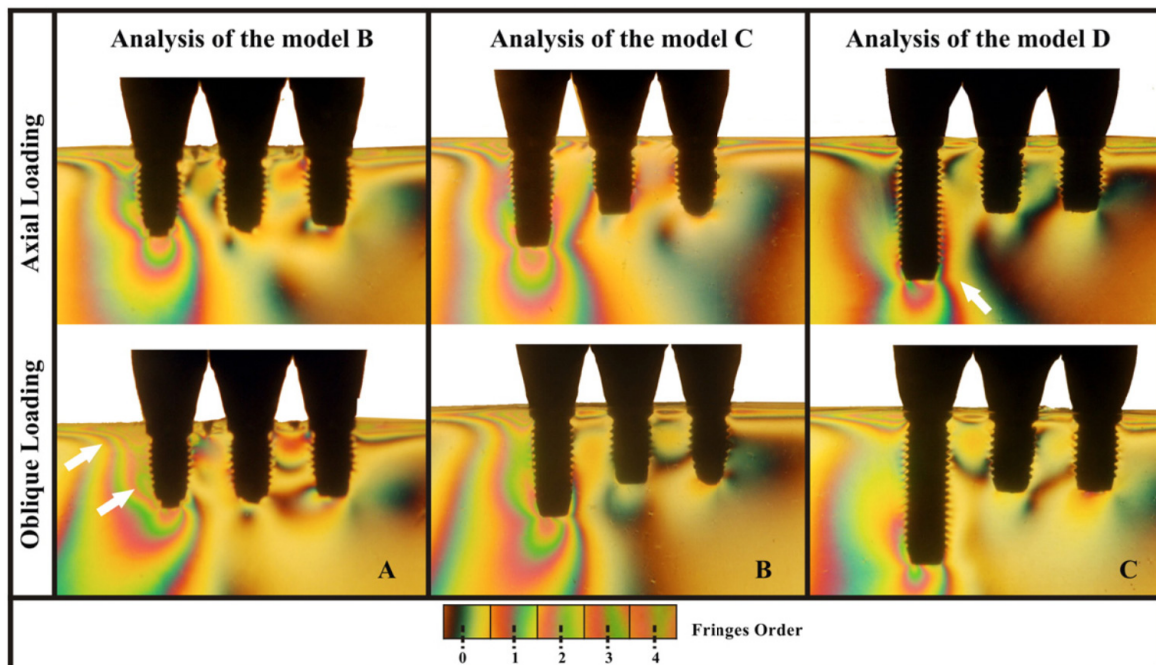
geometries.

The colorful fringes are the visible optical expression of the applied forces within a model. The interpretation of the obtained data is based on the colors and the extent of the fringes that indicate the location and amount of stress in the photoelastic model.

Photoelastic stress analysis has limitations in its capacity to model the nonhomogeneous and anisotropic characteristics of bone. Another limit is the limit of applied external force, which may not exceed the resistance of the photoelastic material. (Cehreli 2004) However, it has been used extensively and successfully in dentistry to study the interaction of tissue response and physical characteristics of prosthetic restorations and implants. (Assuncao 2009)

An example of a photoelastic experiment about stress distribution in dental implants is shown in Figure 6. (Pellizzer 2015)

Figure 6. Example of a photoelastic analysis (Pellizzer 2015)



## **Strain-gauge Analysis**

A strain gauge is a small electric resistor that under slight deformation modifies the resistance created in its current. (Francetti 2015, Pesqueira 2015)

It measures the deformation of an object where it is applied. The captured electrical signal is sent to a data acquisition board, turned into a digital signal and read by a computer.

The gauges are able to precisely record the deformation of any object subjected to stress in which they can be attached on.

Foil gauges typically have active areas of about 2 to 10 mm and if they are correctly installed strains can be measured up to at least 10%.

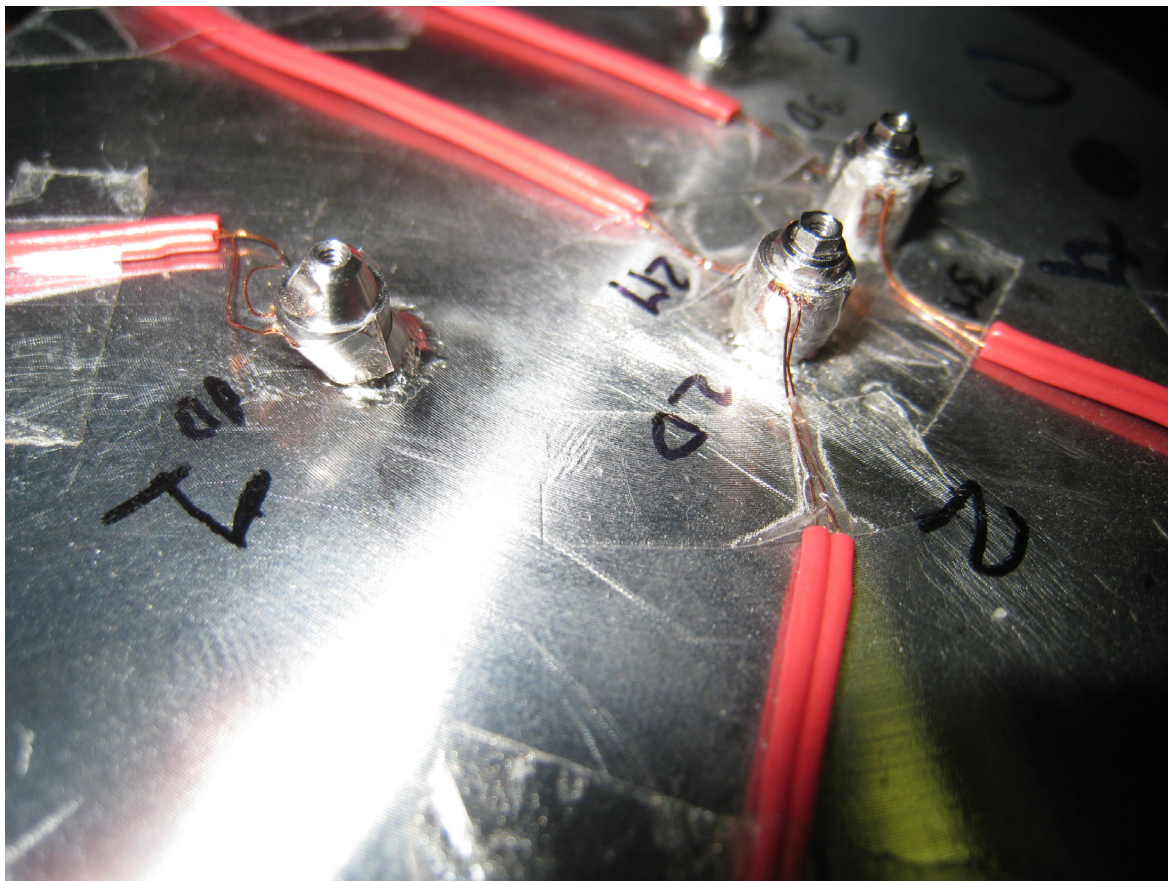
In most cases, the orientation of the strain gauge is significant. (Suedam 2009)

Strain-gauge analysis has been extensively used to evaluate the biomechanical loads on implants for accurate clinical prediction." The application of this method on dental implants could provide both in vitro and in vivo measurements strains under static and dynamic loads. (Assuncao 2009)

The main limitation of this technique is that the measurements are limited to the area where the gauge is bonded.

An example of strain gauges is shown in Figure 7 representing a strain gauges attached on the abutments in an in-vitro experiment to evaluate different implant and prosthetic configurations. (Francetti 2015)

Figure 7. Example of strain gauges experimental model (Francetti 2015)



# Chapter 4

## SHORT IMPLANTS

---

### 4.1 Anatomic Issues

After tooth extraction the alveolar bone could undergo a process of resorption that in some cases could result in a severe deficit.

The volume of the alveolar bone deficiency can affect the horizontal component alone, the vertical component or it can be combined (or vertical and horizontal). Cawood and Howell in 1988 (Cawood and Howell 1988) made a descriptive classification of atrophy of the alveolar edentulous process (Figure 1).

The extent of resorption that occurs is not predictable and show some interindividual differences.

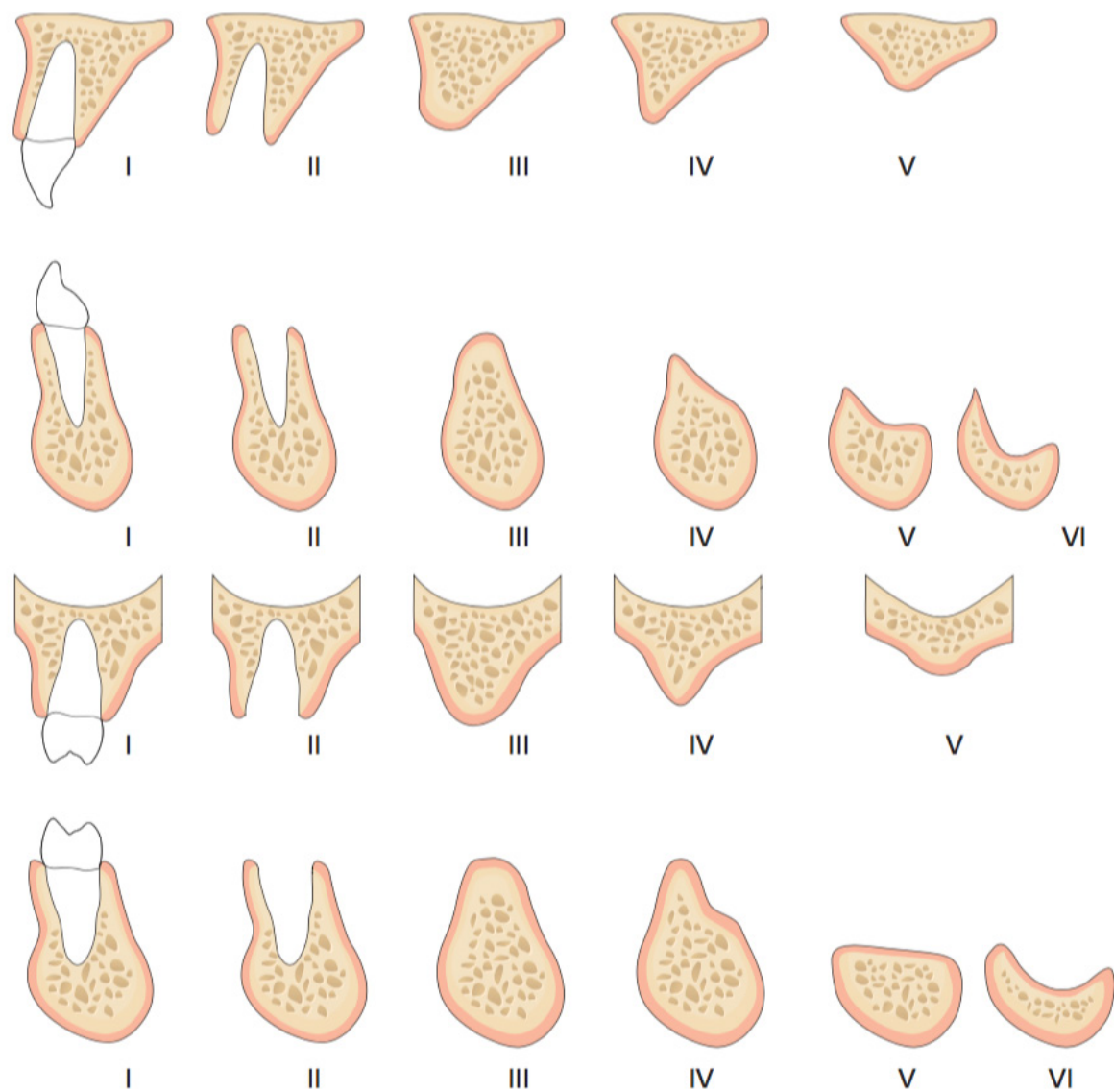
In particular in the posterior regions of jaws the presence of anatomical boundaries may limit the available bone volume to place implants (Pommer 2011):

- In the maxilla low lying maxillary sinuses in association with alveolar bone resorption
- In the mandible the position of the inferior alveolar nerve and canal.

Therefore in some situations the bone quantity is not sufficient to place a standard length implant in the correct positions.

Clinical solutions to these problems involve alveolar ridge augmentation procedures or the use of short implants. (Atieh 2012)

Figure 1. Classification of alveolar bone atrophies by Cawood and Howell (Barone and Bianchi 2013)





## 4.2 Early mistrust and caution in using short implants

There is no general consensus about the length threshold to consider an implant short. The classification of “short implant” lengths in the existing literature is varied and ranges 5–10 mm. (Srinivasan 2014).

A recent literature review stated that in the past long implants were considered more desirable (Pommer 2011).

Firstly there was early evidence that short Branemark implants (6-10 mm) with traditional machined surfaces had an inferior survival rate compared with longer implants. (Wyatt 1998, Friberg 1991, Attard 2003, Weng 2003, Bahat 2000)

Friberg et al (Friberg 1991) following 4641 consecutively placed Branemark machined implants concluded that a preponderance of failures could be seen among the shortest fixtures (7 mm) compared with the longer 10-mm to 20-mm fixtures.

Wyatt et al (Wyatt 1998) followed 230 machined Brénemark implants up to 12 years and of the 7-mm implants placed, 25% failed, whereas the 10-mm fixtures had an 8% failure rate and the 13-mm and 15-mm implants had failure rates of 5% and 2% respectively.

Bahat (Bahat 2000) followed a total of 666 implants placed in the posterior maxilla from 5 to 12 years and the 17% of the 3.75-mm diameter short implants, including 7 and 8.5 mm length, failed.

In 2003 Attarb and Zarb (Attarb 2003) showed a 15% failure rate for 7-mm implants, whereas 11-mm and 13-mm implants had failure rates of 6% to 7%.

Weng and colleagues (Weng 2003) reported on a multicenter prospective clinical study evaluating the success of 1179 3i machined surface implants for up to 6 years. Of the 1179 implants, 48.5% were considered short ( $\leq 10$  mm). These short implants accounted for 60% of all failed implants, with a cumulative success rate of only 88.7%. The 10-mm long implants accounted for 10% of the failures, whereas the 8.5-mm and 7-mm long implants accounted for 19% and 6% of failures respectively.

Secondly, Ante's law states that the total periodontal membrane area of the

abutment teeth must equal or exceed that of the teeth to be replaced. (Ante 1926) From that law, the radiographic calculation of the crown/root ratio (CRR) was used to decide a tooth's suitability as an abutment. A variety of ratios are reported in the literature. A CRR of 1:2 was considered ideal, but is a difficult condition to be found in clinical reality. Shillingburg and colleagues in 1997 suggested that a CRR of 1:1.5 was optimal and a ratio of at least 1:1 necessary for a satisfactory result. Even though Ante's law has lately been disapproved (Lulic 2007) the concept of longer roots being better abutments than short roots still prevails. In this context short dental implants were considered wrong.

### **4.3 Implant surface**

Recently research progressed on the surface technology of dental implants is leading to textured or rough-surface implants.

Considering the classical success criteria (Smith and Zarb 1989) of 1.5 mm of crestal bone loss in the first year and no more than 0.2 mm of bone loss per year in succeeding years, then short implants would effectively become even shorter, potentially increasing the negative effects.

These criteria for success were proposed in 1989 when most implants had only a machined/turned surface. With the introduction of rough surfaces, these old criteria are no longer valid.

The systematic review on implant surface roughness and bone healing of Shalabi et al (Shalabi 2006) presented a positive relationship between bone-to-implant contact and surface roughness. Wennerberg and Albrektsson (Wennerberg and Albrektsson 2009) concluded in their systematic review that surface topography influence bone response at the micrometre level and might influence bone response at the nanometre level.

Renouard and Nisand (Renouard and Nisand 2006) reviewed 53 clinical studies of the impact of implant length and diameter on survival rates. They found that 12 of these studies indicated an increased failure rate with short implants, which was

associated with operator experience, routine surgical preparation (irrespective of bone density), machined surface implants, and placement in areas of poor bone density. Other 22 papers showed comparable survival rates between short and long implants when rough-surface implants and adapted surgical protocols based on bone density were used.

Pommer and colleagues (Pommer 2011) indicated that short rough-surfaced implants showed significantly lower failure rates than machined implants. Balshe et al (Balshe 2009) found in their retrospective study of 2182 machined surface implants versus 2425 rough-surfaced implants that there was no statistical difference in the 5-year survival rates (94% vs 94.5% respectively). However, when implants of less than or equal to 10 mm were evaluated separately, the estimate survival was 93,7%, whereas for smooth-surface implants it was only 88.5%.

#### **4.4 Biomechanical issues**

In general, the use of short implants has not been recommended by some because it is believed that occlusal forces must be dissipated over a large implant area in order for the bone to be preserved. Finite element modeling (FEM) analyses have shown that the occlusal forces are distributed primarily to the crestal bone rather than evenly throughout the entire surface area of the implant interface. Since masticatory forces are light and fleeting, these forces should normally well-tolerated by the bone even with short implants. (Lum 1991)

Himmlova et al (Himmlova 2004) simulated implants variations in length from 8 mm to 18 mm and diameters from 2.9 mm to 6.5 mm. The maximum stress concentration was at the top 5 to 6 mm of the implant and there was little difference in area affected by maximum stress with the 8 mm versus the 17-mm implant. The difference in stress was only 7,3%. On the contrary, stress reduction continued to decrease as implant diameter increase. Maximum stress values in the 6.5 mm diameter implant were almost 60% less than those of the narrow 2.9

mm implant. This simulation showed that the diameter was more important for stress distribution than length.

Baggi et al (Baggi 2008) analyzed the effect of implant diameter and length on stress distribution, including crystal bone loss, using 5 commercially available implant designs. They concluded that implant diameter can be considered to be a more effective design parameter than implant length.

About crown-implant ratio (CIR) in a systematic review Blanes et al (Blanes 2009) conclude that CIR did not affect peri-implant crestal bone loss.

However Urdaneta et al (Urdaneta 2010) observed that excessive CIR had no negative effect on the periimplant bone loss but caused more significant prosthetic complications, such as screw loosening and porcelain fracture.

#### **4.5 Analysis of clinical success**

Telleman et al (Telleman 2011) conducted a systematic review of the posterior zone of partially edentulous patients. Their report included 29 studies totaling 2611 short (5-9.5 mm) implants. They analyzed multiple variables including implant length, rough versus machined surface, maxilla versus mandible, and smokers versus nonsmokers.

They concluded that increasing length from 5 mm to 9.5 mm improved overall survival. The survival rates were 5 mm (93.1%), 6 mm (97.4%), 7 mm (97.6%), 8 mm (98.4%), 8.5 mm (98.8%), 9 mm (98.0%), and 9.5 mm (98.6%). There was a 29% improvement of rough surfaces compared with machined surfaces. The difference in the failure rate of maxillary implants (generally lower density bone) than mandibular implants was substantial at 100%. When studies included heavy smokers (215 cigarettes/d) versus strictly excluding smokers were examined, the estimated failure rate was 57% lower.

Atieh and colleagues (Atieh 2012) showed a noteworthy increase in the 3-year to 4 year cumulative survival rate as implant length increased from 5 mm implants (89,9%) to 6 mm

(96.6%), 7 mm (95.6%), 8 mm (99.2%), and 8.5 mm (98.2%). There was an overall acceptable 5-year cumulative survival rate of 98,3% for short implants compared with 97.7% for standard length implants.

Nisand and Renouard (Nisand and Renouard 2014) recently reported a structured review of short implants ( $\leq 8$  mm) versus longer implants. For the short implants 29 case series for a total of 9780 implants were included. The overall cumulative survival rate was 96.67% of implants. They also studied long implants, analyzing 5 reviews comprising 58,953 implants with cumulative survival rates ranging from 93.1% to 99.1%.

At this time, 6 mm is accepted as the minimum implant length, because of its acceptable success rates (Telleman 2011, 97.4%, and Atieh et al 2012, 96.6%), then the minimum height of remaining bone that would be acceptable can be calculated adequately in respect to the anatomic boundaries.

## **4.6 Surgical Protocol**

The surgical protocol used for the insertion of short implants is similar to the ones used for longer implants.

Al-Marshood et al (Al-Marshood 2011) found that moderately rough threaded implants placed in undersized osteotomies showed a greater bone-to-implant contact than those placed using standard surgical methods. It would appear that avoiding over-instrumentation of osteotomies will improve implant stability and the overall performance of both machined and rough-surfaced short threaded implants. (Deporter 2013)

Adapted surgical protocols to increase the primary stability have been suggested by several authors. (Tawil and Younan 2003, Fugazzotto 2004, Renouard and Nisand 2006, Nisand and Renouard 2014)

Considering that usually short implants need to be positioned in the posterior part of jaws where there is commonly low bone density this technique is even more suggested.

It has been suggested that operator experience, with short implants may be a reason for the different reported outcomes with short implants between studies (Renouard and Nisand 2006)

Although it may seem to require a simpler procedure than a long implant, there is a learning curve and short implants are best not to be inserted by novice surgeons. Surgeons must be totally comfortable with the basics of implant surgery so that attention can be directed toward modification of the drilling protocol as needed to compensate for changes in bone density while still being aware of implant three-dimensional positioning.

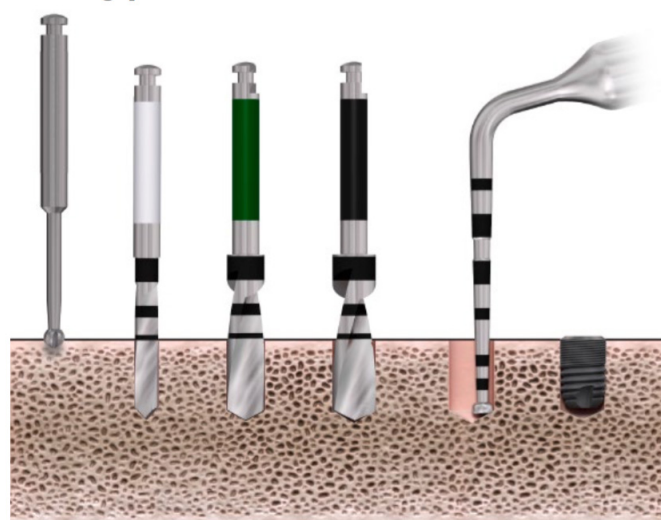
In Figure 2 it is schematically shown the surgical protocol for Astratech Osseospeed 6mm long implants (Dentsply Implants, Molndal, Sweden), that correspond to the ones that are going to be evaluated in this research.

In a clinical situation with a bone volume between 7-8 mm above the inferior alveolar nerve a mucoperiosteal flap was elevated. (Figure 3)

Then osteotomies were made and their inclination verified through the use of direction pins.(Figure 4, Figure 5) Three implants with 6 mm length and 4 mm diameter (Figure 6) were inserted with the platform at bone level (Figure 7 and Figure 8) and the flap was sutured.

Figure 2. Drilling protocol for short implants

**Drilling protocol – STANDARD**



Guide Drill	Twist Drill 2.0	Twist Drill 3.2	Twist Drill 3.7	OsseoSpeed™ TX 4.0 S 6 mm
-------------	-----------------	-----------------	-----------------	---------------------------

Figure 3. Mucoperiosteal flap elevation

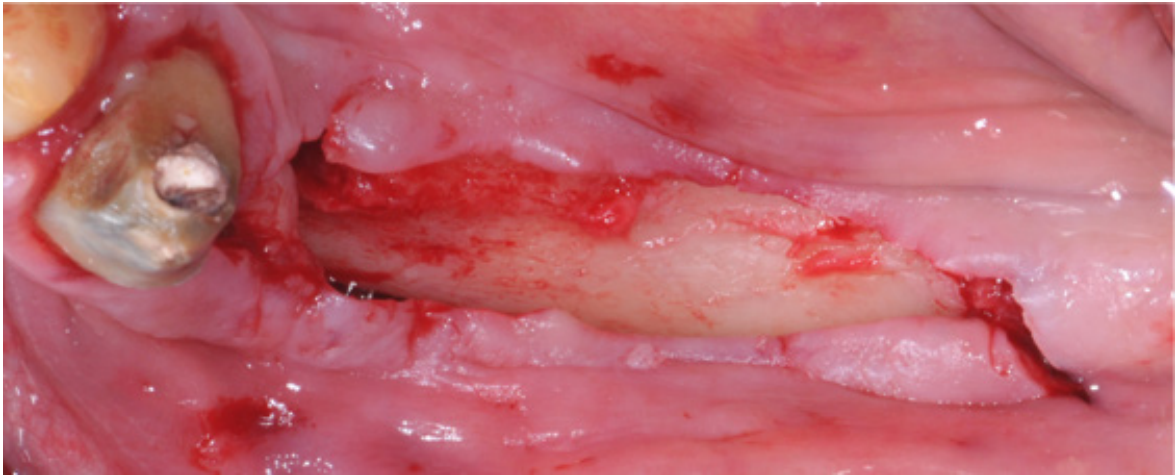


Figure 4. Direction pins do indicate the direction of the osteostomy - occlusal view

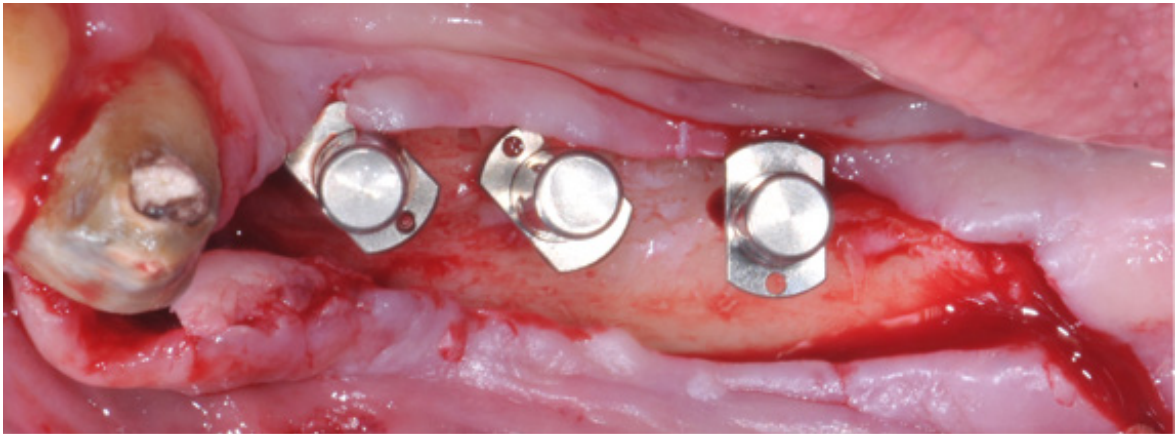


Figure 5. . Direction pins do indicate the direction of the osteostomy - lateral view

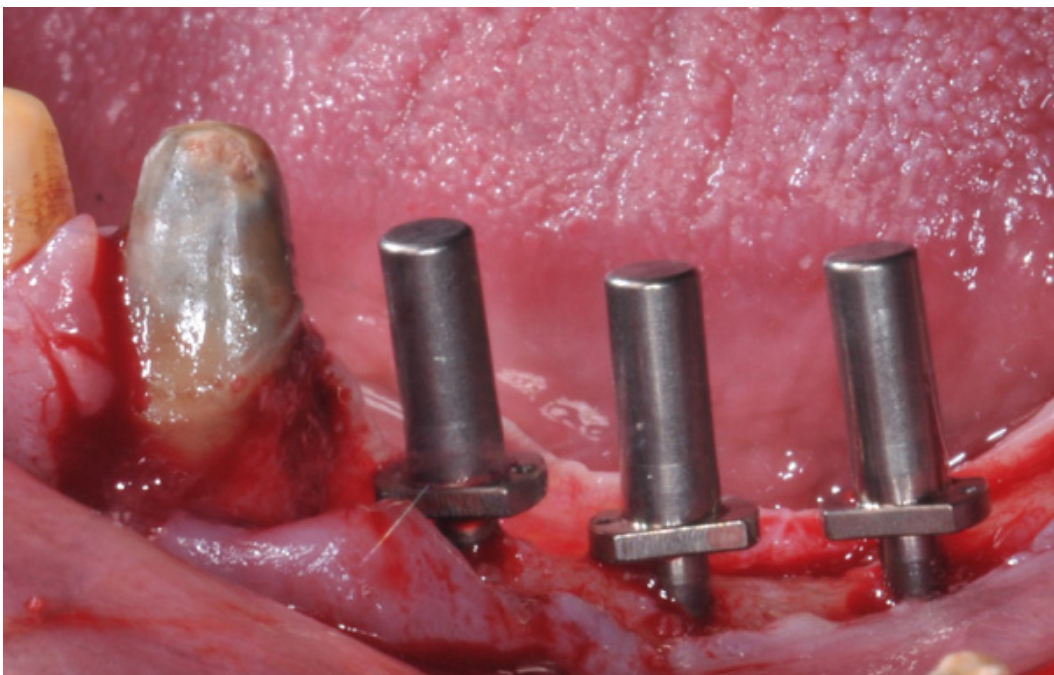


Figure 6. 6 mm length and 4 mm diameter implant

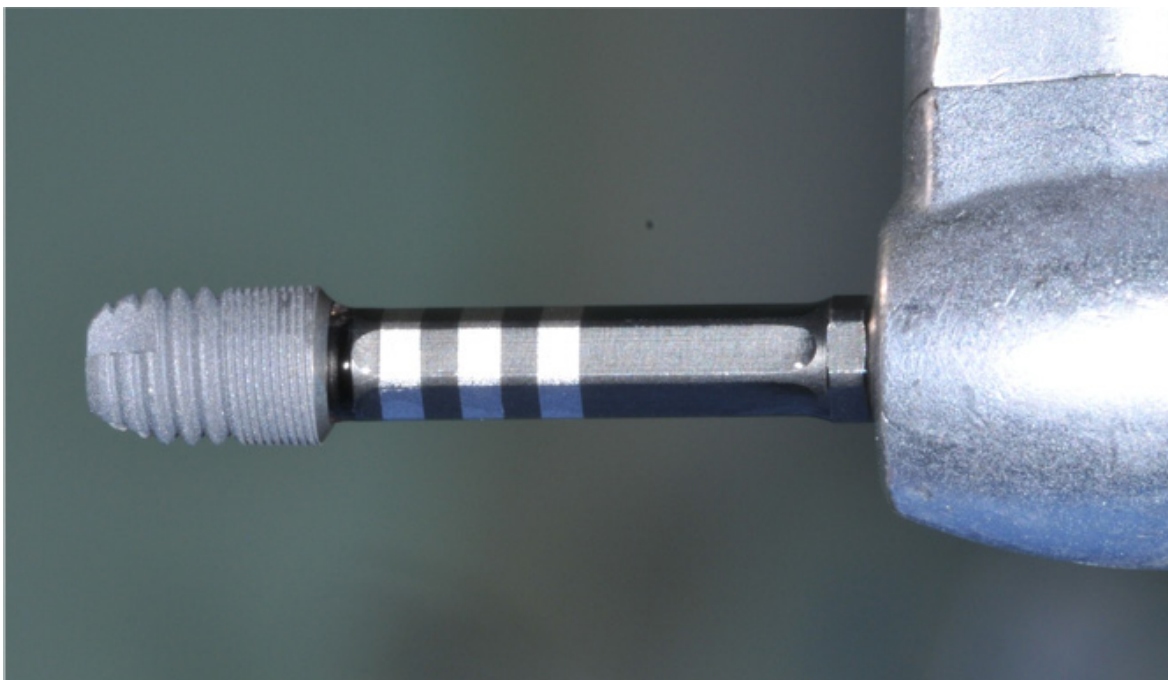


Figure 7. implant positioning

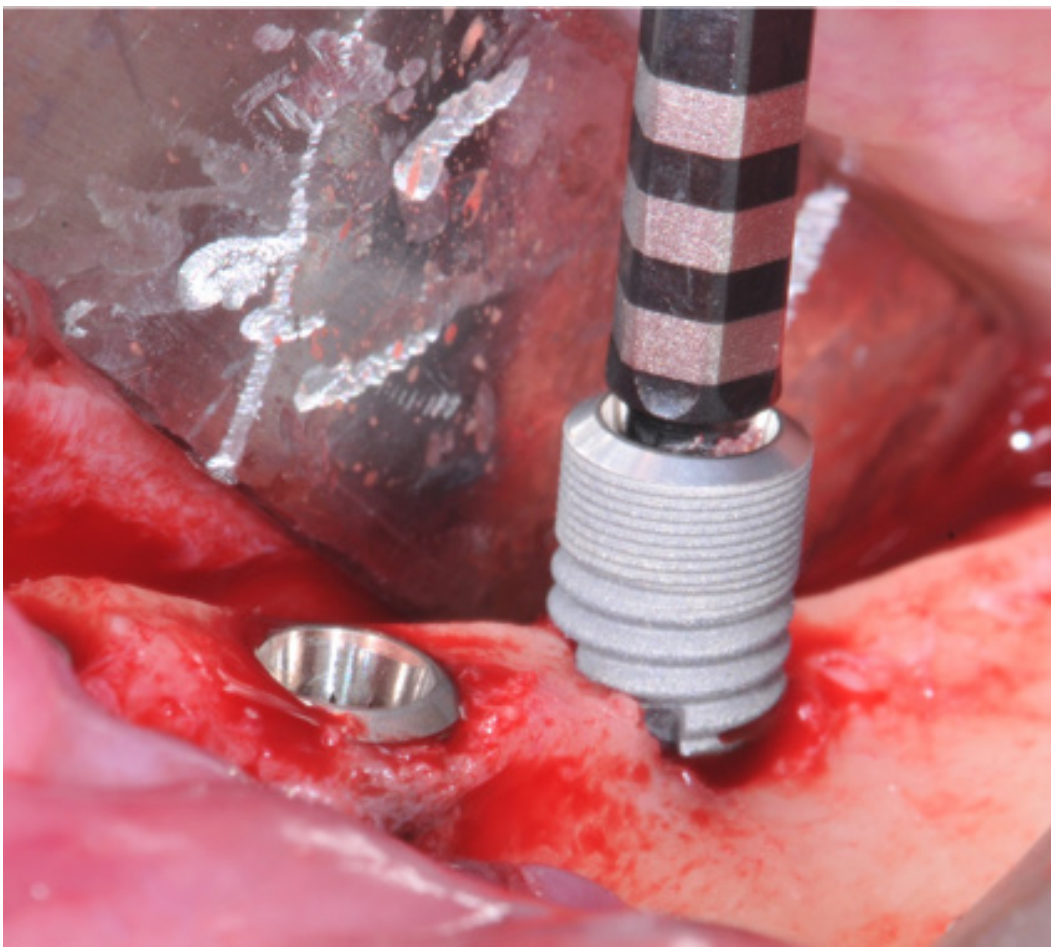
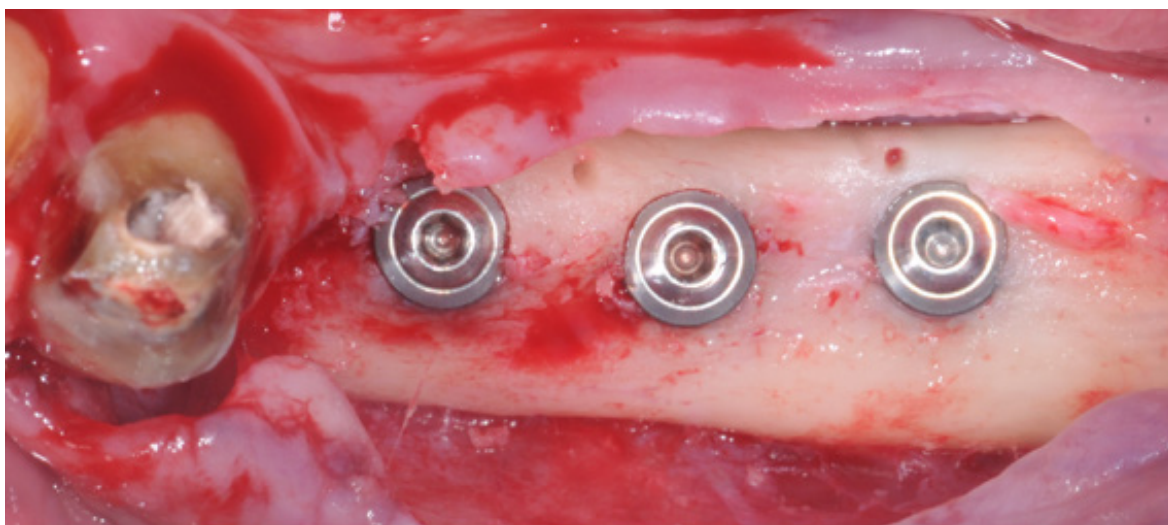




Figure 8. Occlusal view three short implants positioned at bone levels



#### 4.7 Bone augmentation procedures

To overcome the anatomical problems due to insufficient bone volume, as an alternative to short implant placement in order to be able to place standard length implants in the prosthetic correct position, advanced surgical techniques were developed.

To increase the alveolar bone height, guided bone regeneration, block grafting, maxillary sinus floor grafting and distraction osteogenesis procedures were performed. To bypass vital structures such as the inferior alveolar nerve, nerve transpositioning techniques were used.

All of these advanced surgical procedures can be challenging, technique sensitive, time consuming, costly and can increase surgical morbidity and prolong overall treatment time.

A systematic review by Milinkovic and Cordaro (Milinkovic and Cordaro 2014) of different alveolar bone augmentation procedures for partially and fully edentulous jaws documented the mean implant survival rate (MISR) and the mean complication rate (MCR) for vertical augmentation procedures, including guided

bone regeneration (GBR), bone blocks (BBS), and distraction osteogenesis (DO). In partially edentulous patients with GBR, the MISB ranged from 98.9% to 100%, with an MCR 13.1% to 6.95%. BBs had a MISR of 96.3% and MCR of 8.1%. The greatest vertical gain was noted with DO, but it also had the highest MCR (22.4%) and MISR (98.2%). In fully edentulous patients, the BB MISR was only 87.75% and the MCR was highly variable, depending on whether the different donor sites or recipient sites were being analyzed. The overall MQR was calculated as 21.9%. For Le Fort I grafts, the MISB was 87.9%, with MCR ranging from 24% to 30%. With sinus graft there are multiple different complications possible, including intraoperative and postoperative complications. Moreno Vazquez et al. (Moreno Vasquez 2014) evaluated the complications in 200 consecutive sinus lift procedures and reported that the most common intraoperative complication, at 25.7%, was schneiderian membrane perforation. Previous reports note a range of 7% to 56% in the rate of perforation. After surgery, 19.7% had some type of complication. The most frequent were wound infection (7.1%), sinusitis (3.9%), and graft loss (1.6%).

For atrophic mandibles, if the remaining posterior vertical alveolar bone is considered inadequate for 10 mm or longer implants, the only option is either vertical grafting as outlined previously or inferior alveolar nerve transpositioning surgery. Hassani et al (Hassani 2015) evaluated initial postoperative sensory impairment after inferior alveolar nerve transposition of almost 100% of patients. Normal sensory function returned in 84% of cases with 16% of patients left with a permanent and irreversible condition. Neurosensory disturbances are so prevalent with this procedure that many surgeons consider sensory disorders as normal and predictable postsurgical state.

Nisand and Renouard in 2014 (Nisand and Renouard 2014) reviewed multiple studies comparing short implants with standard length implants with various vertical augmentation procedures and found similar survival rates. However, the use of short implants resulted in faster and lower-cost treatment with reduced morbidity.

# Chapter 5

## OBJECTIVES OF THE STUDY

---

The aim of this study was to evaluate the influence of the following parameters on the stress distribution in the bone-implant interface in a three-unit bridge in the posterior mandible by means of finite element analysis:

- Short vs regular length implants
- Two or three implants to support a three-unit bridge in the posterior mandible
- Influence of crown height
- Different forces directions over the crowns
- If the use of short implants with longer crowns could be a viable option compared to longer implants and shorter crowns under a biomechanical point of view

# Chapter 6

## MATERIALS AND METHODS

---

### 6.1 Development of the finite element model

The 3D geometry of an edentulous mandible was reconstructed from CT scans using Mimics 17.0 (Materialise, Leuven, Belgium). The anatomical symmetry allowed for the reconstruction of half the mandible. After surface meshing, a volumetric tetrahedral mesh was generated, which resulted in 1988708 linear tetrahedral elements and 362188 nodes. (Figure 1)

The grey value (GV) was used to calculate the density and in turn the elastic modulus, by applying the following empirical formula:

$$\rho = 1017 * GV - 13.4$$

$$E = 5925 * \rho - 388.8$$

where GV is grey value,  $\rho$  is the density and E is the elastic modulus.

The range of GVs was divided into 10 equally sized intervals, each of that represents a set of material properties. Elastic moduli resulted in the range of 1.23 to 23.39 GPa (Table 1).

**Table 1: Material properties assigned for bone.**

MATERIAL	YOUNG'S MODULUS (GPa)	POISSON RATIO
Mat1	1.20	0.34
Mat2	3.59	0.34
Mat3	5.99	0.34
Mat4	8.38	0.34
Mat5	10.77	0.34
Mat6	13.17	0.34
Mat7	15.56	0.34
Mat8	17.96	0.34
Mat9	20.35	0.34
Mat10	22.74	0.34

The low values (<3GPa) represented materials like trabecular bone and adjacent soft tissues; the intermediate values (3-16 GPa) represented cortical bone; the high values (>16 GPa) represented the tooth enamel and dentin. This procedure has been validated and suggested by other authors. (Xin 2013, Moeen 2014)

CAD file of two different implants were provided by Dentsply Implants (Molndal, Sweden) and tetrahedral meshes were generated using Ansys ICEM (Ansys Inc., Canonsburg, PA, USA). The dimensions of the implants (OsseoSpeed™, Astra Tech, Dentsply Implants) were 4 mm diameter x 11 mm length (regular length implants) and 4 mm diameter x 6 mm length (short implants) (Fig.2).

FEMs of the mandible and the implants were exported to ABAQUS software (Version 6.10; Dassault Systèmes, Providence, RI, USA) for the analysis.

A superstructure representing the porcelain crown was built using 16 beam elements connecting the head of the implant to a node located in the centre of the implant at crown height. The mechanical properties of implants and crown are listed in Table 2.

**Table 2: Material properties assumed for implants and crown.**

MATERIAL	YOUNG'S MODULUS (GPa)	POISSON RATIO
Titanium	106.33	0.34
Porcelain	68.90	0.28

Figure 1: view from above of the 3-D reconstruction of half mandible

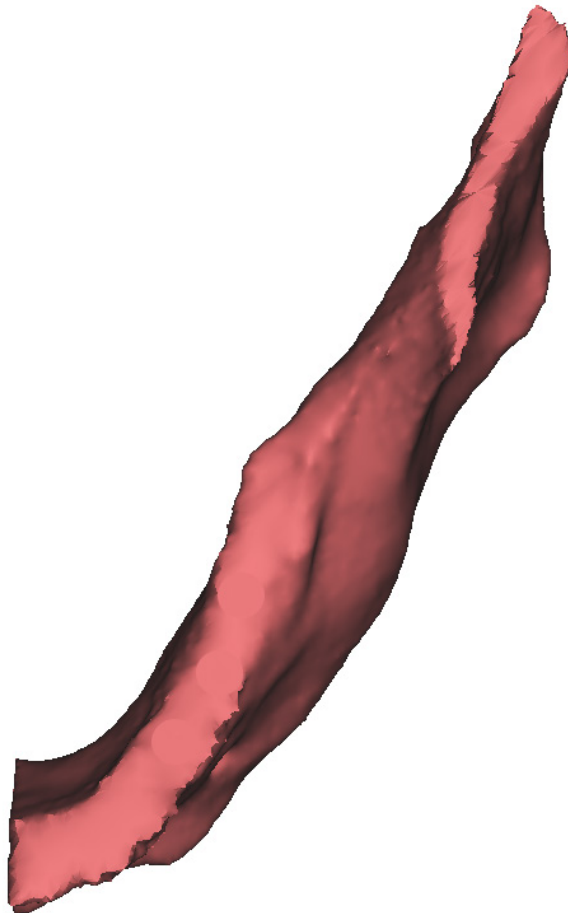
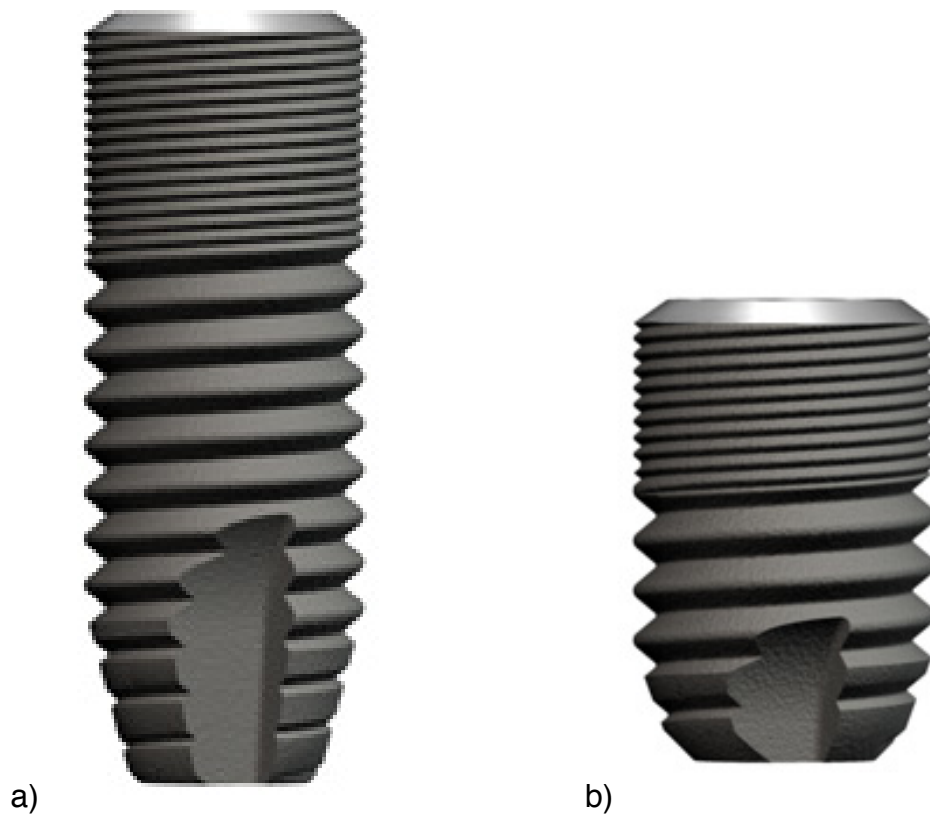


Figure 2: Graphic representation of a) 4 mm x 11 mm and b) 4 mm x 6 mm Astra Tech AB OsseoSpeed™ Implants



## 6.2 Experimental configurations

Six different configurations have been compared:

LS2) two regular length implants to support a three-unit bridge with 8 mm height crowns

LS3) three regular length implants to support a three-unit bridge with 8 mm height crowns

SS2) two short implants to support a three-unit bridge with 8 mm height crowns

SS3) three short implants to support a three-unit bridge with 8 mm height crowns  
SL2) two short implants to support a three-unit bridge with 13 mm height crowns  
SL3) three short implants to support a three-unit bridge with 13 mm height crowns

A schematic representation of the six configurations are shown in Figure 3

The three single implant-crown different configurations are represented in Figure 4.

Implants have been placed in II premolar, first molar and second molar position for configurations with 3 implants (LS3, SS3 and SL3), while for configurations with 2 implants they were placed in II premolar and II molar position.

Implants in the II premolar position were labeled Imp1, in the I molar position were labeled Imp2 and in II molar position were labeled Imp 3 (Fig.5).

In each configuration the 3 nodes at the centre of the crown at crown height were connected together with two beam elements and the whole superstructure was considered as a unique structure completely bonded.

The translational degrees of freedom of the implant nodes were kinematically constrained to the corresponding degrees of freedom of the closest nodes of the mandible, thus realizing a fully bonded integration. A symmetry boundary condition was applied to the nodes belonging to the plane of symmetry. Furthermore, the nodes belonging to the sagittal, transverse and frontal plane were fully constrained.

A vertical and 45° inclined concentrated load of 200 N representing the masticatory force was applied to the node of each crown simultaneously (Fig. 6).

Two set of elements were created to facilitate postprocessing of the peri-implant stresses (Fig. 7): the first one included the whole bone-implant interface within a distance of 1.5 mm, whereas the second had the same thickness but included only the coronal area, with a height of 2.5 mm.



Figure 3: Graphical representation of the six configurations. The numbers express the measurements in mm.

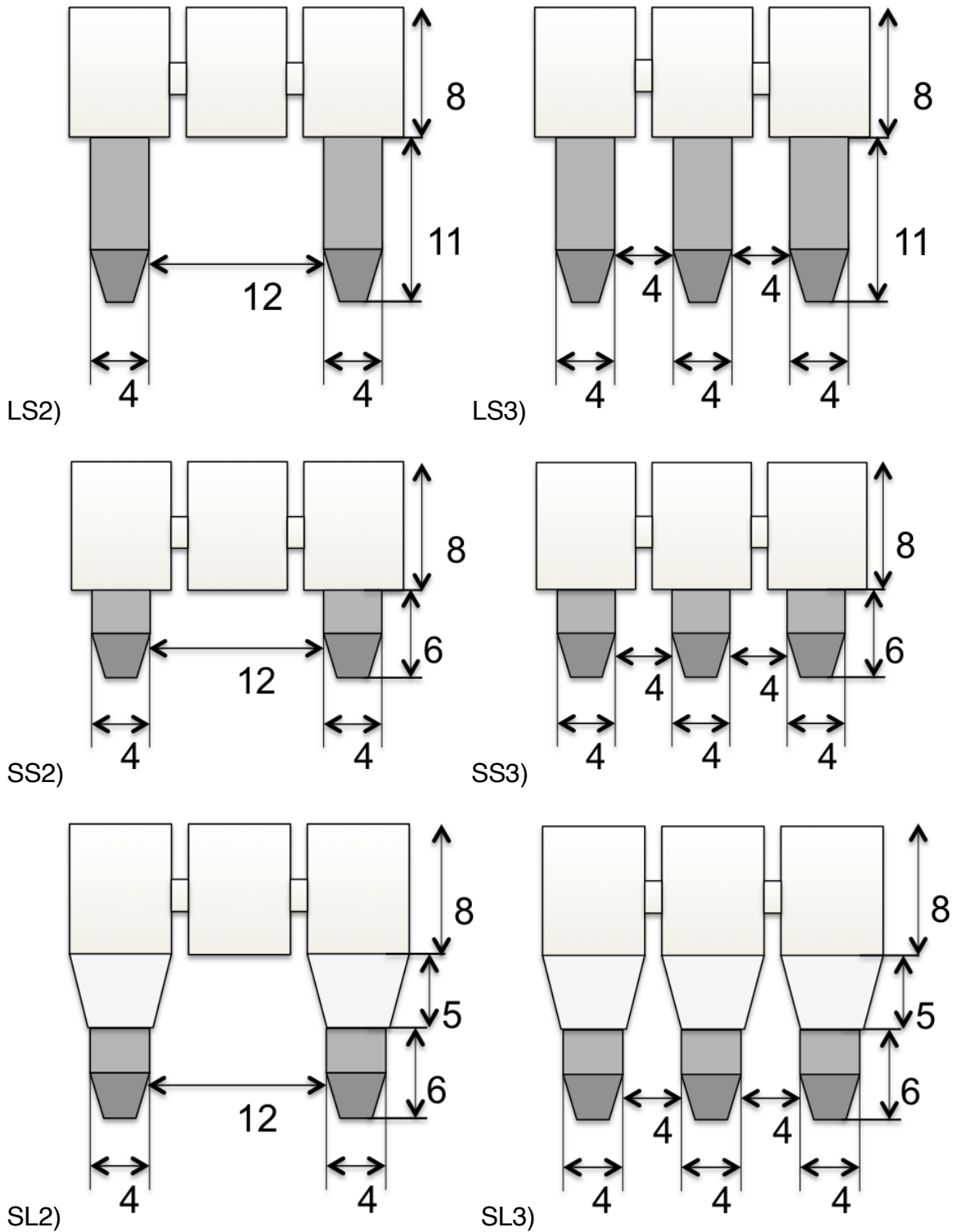


Figure 4: 3D models of the single implants and crown built using beam elements: a) Long implant and 8 mm crown; b) short implant and 8 mm crown; c) short implant and 13 mm crown.

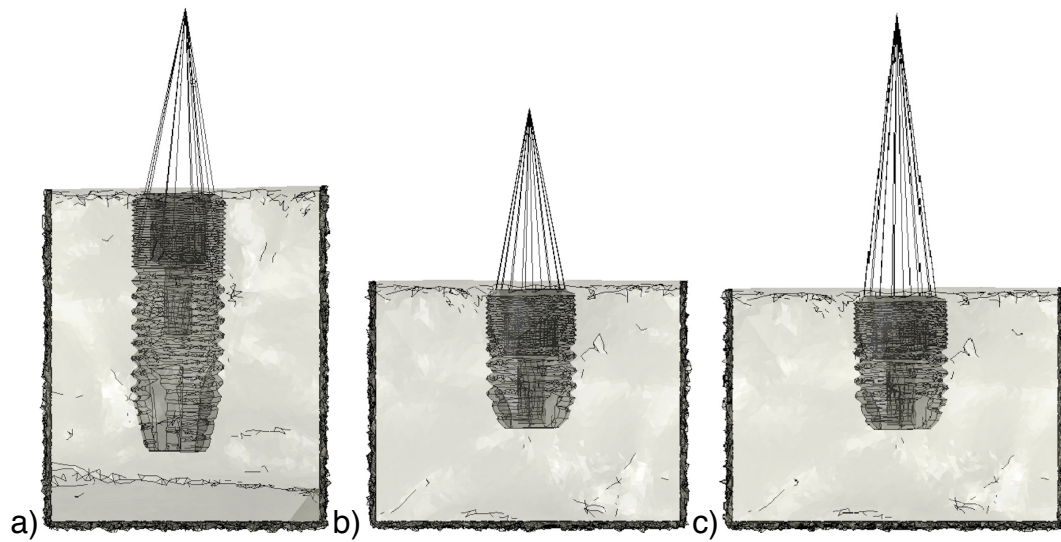


Figure 5: 3D model of LS3 configuration. The implants are numbered based on their position.

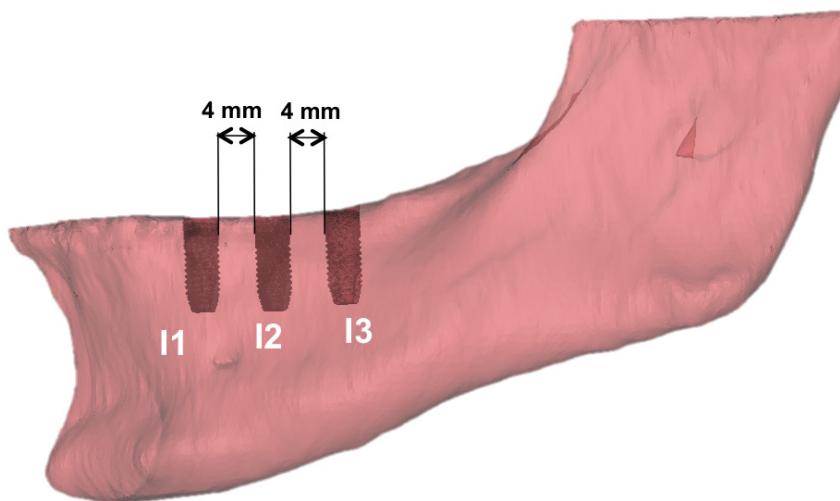


Figure 6: Load application point and direction. "B" stands for "buccal" and "L" stands for "lingual"

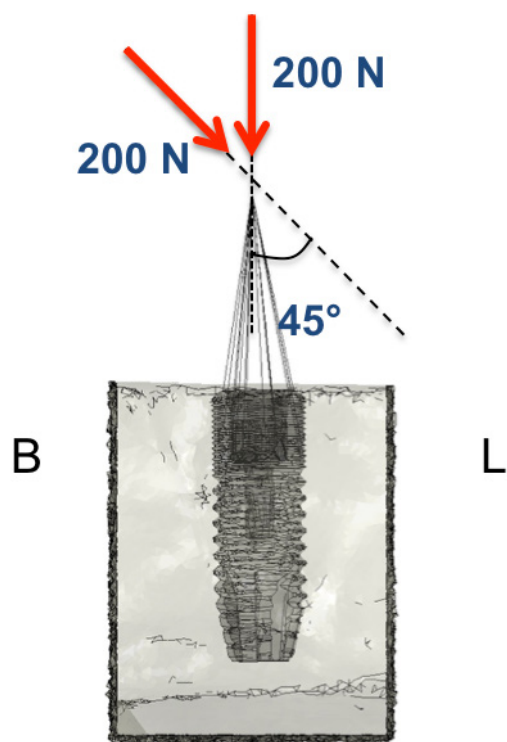
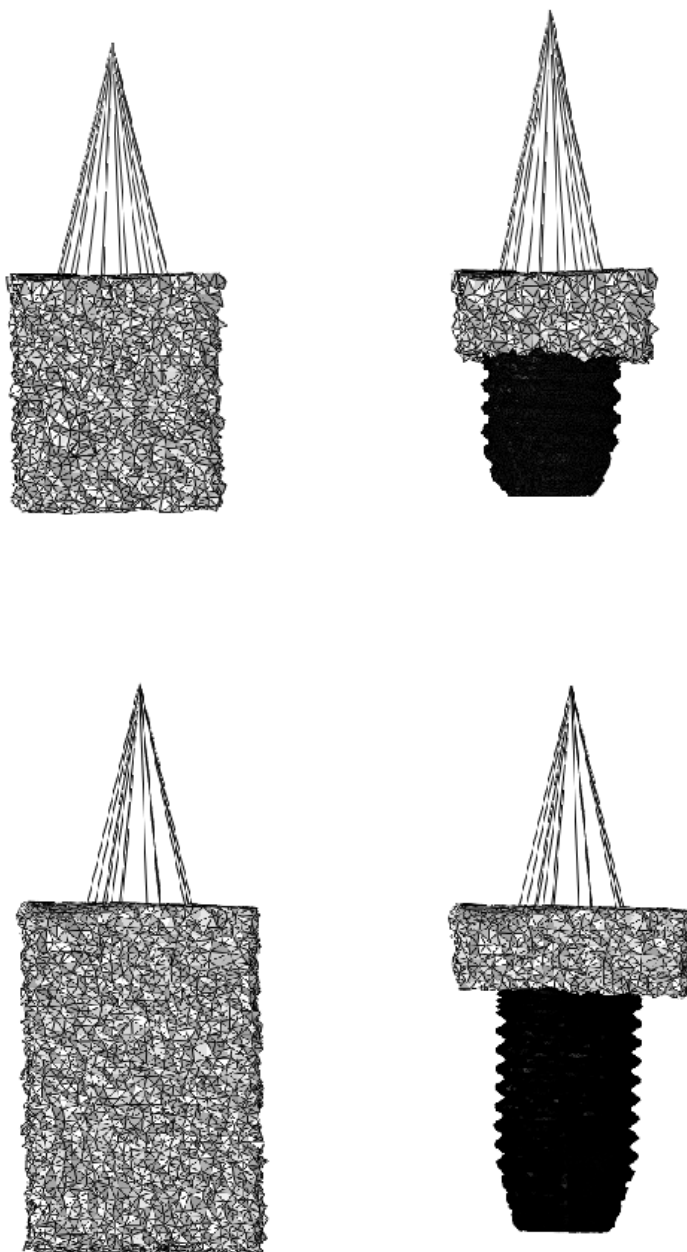


Figure 7: Graphical representation of the considered area around the implants. In the first column it is represented the whole bone-implant interface (1,5 mm thick) while in the second column the apical 2,5 mm. The first row represent short implants and the second row regular length implants.



### 6.3 Data analysis

Static analysis was performed and simulation results were evaluated in terms of Von Mises stressed, maximum and minimum principal stresses and the nodal displacement of the point of application of the masticatory force of all implants of all configurations.

All parameters have been analyzed in terms of maximum and minimum values, first, second and third quartiles (Q1, Q2 and Q3), considering both the whole bone-implant thickness or the coronal area to make the results of the different configurations more comparable.

# Chapter 7

## RESULTS

---

For what concerns the LS2 configuration, the data about Von Mises stress, maximum principal stress and minimum principal stress for the whole bone-implant interface are summarized in Table 1, while the ones regarding just the coronal area are presented in Table 2.

Table 3 presents the the data about Von Mises stress, maximum principal stress and minimum principal stress for the whole bone-implant interface of all implants in configuration LS3. The data concerning just the coronal area are presented in Table 4.

For what concerns the SS2 configuration, the data about Von Mises stress, maximum principal stress and minimum principal stress for the whole bone-implant interface are summarized in Table 5, while the ones regarding just the coronal area are presented in Table 6.

Table 7 presents the the data about Von Mises stress, maximum principal stress and minimum principal stress for the whole bone-implant interface of all implants in configuration LS3. The data concerning just the coronal area are presented in Table 8.

For what concerns the SL2 configuration, the data about Von Mises stress, maximum principal stress and minimum principal stress for the whole bone-implant interface are summarized in Table 9, while the ones regarding just the coronal area are presented in Table 10.

Table 11 presents the the data about Von Mises stress, maximum principal stress and minimum principal stress for the whole bone-implant interface of all implants in configuration LS3. The data concerning just the coronal area are presented in Table 12.

Figures from 1 to 6 show Von Mises stress, maximum principal stress and minimum principal stress under axial loading conditions for each configuration, while figures from 7 to 12 show the same parameters under tilted load.

Under axial load the stress values were almost identical between the configurations with short implants and different crown length (SS2 and SL2, SS3 and SL3).

The graphical representations of the Von Mises stress distribution are shown in this chapter through a longitudinal slice that includes all implants and a paraxial slice for each implant for every examined configuration. (Fig.13)

Figures from 14 to 19 show Von Mises stress distribution under axial load for every configuration while for the 45° tilted load the stress distribution is displayed in figures from 20 to 25.

In all loading conditions the stress is more concentrated at coronal level but this fact is more evident under tilted load.

Therefore the data about the coronal interface were considered more comparable. Considering that the highest values of Von Mises stress, maximum principal and minimum principal stresses could be influenced by the models' irregularities and imperfections, Q3 for Von Mises and maximum principal stresses and Q1 for minimum principal stress were considered a more reliable and comparable parameters.

The graphs presented in figure 26, figure 27 and figure 28 summarize the stress of each implant in every configuration under axial load through respectively the Q3

values of Von Mises stress and maximum principal stresses and Q1 of minimum principal stress.

The graphs presented in figure 29, figure 30 and figure 31 summarize the stress of each implant in every configuration under tilted load through respectively the Q3 values of Von Mises stress and maximum principal stresses and Q1 of minimum principal stress.

The stress values calculated in the configurations under tilted load were on average 6 times higher for Von Mises stress, 4 times higher for minimum principal stress and 23 times higher for maximum principal stress.

The increase of stress parameters values in SS configurations respect to LS configuration were on average of the 40%.

Even the average increase of stress values in SL configurations respect to SS configuration was about the 42% under tilted load.

Configurations with 2 implants were recorded to undergo about the 50% more of stress on average than the respective 3 implants configurations.

The highest stress values were observed in the SL2 configuration while the minimum stress values were found in LS3.



Table 1. Stress values (in Mpa) for the LS2 configuration with the whole bone-implant interface.

LS2		WHOLE BONE-IMPLANT INTERFACE			
		AXIAL LOAD		TILTED LOAD	
		Imp 1	Imp 3	Imp 1	Imp 3
VON MISES	Min	0,14	0,21	0,57	0,25
	Q1	1,46	1,31	4,88	2,35
	Q2 (Median)	2,13	1,74	9,88	4,74
	Q3	2,83	2,26	17,06	11,79
	Max	21,20	24,77	137,38	183,41
MAX PRINCIPAL	Min	-10,13	-11,32	-56,13	-68,04
	Q1	0,25	0,15	2,43	0,78
	Q2 (Median)	0,52	0,33	4,66	1,79
	Q3	1,03	0,53	7,85	4,30
	Max	13,58	6,35	125,36	251,17
MIN PRINCIPAL	Min	-23,05	-32,36	-156,26	-241,61
	Q1	-2,27	-2,14	-9,70	-5,64
	Q2 (Median)	-1,66	-1,50	-4,62	-2,80
	Q3	-1,15	-1,08	-1,88	-1,56
	Max	2,34	0,93	47,57	99,86

Table 2. Stress values (in Mpa) for the LS2 configuration with the coronal bone-implant interface.

LS2		CORONAL BONE-IMPLANT INTERFACE			
		AXIAL LOAD		TILTED LOAD	
		Imp 1	Imp 3	Imp 1	Imp 3
VON MISES	Min	0,14	0,21	1,13	0,69
	Q1	1,69	1,75	13,82	9,57
	Q2 (Median)	2,47	2,38	20,88	15,81
	Q3	3,64	3,23	29,94	22,90
	Max	15,75	24,77	137,38	183,41
MAX PRINCIPAL	Min	-10,13	-11,32	-56,13	-68,04
	Q1	0,09	0,00	3,68	2,49
	Q2 (Median)	0,26	0,16	9,00	4,61
	Q3	0,55	0,36	19,68	11,81
	Max	13,58	6,35	125,36	251,17
MIN PRINCIPAL	Min	-23,05	-32,36	-156,26	-241,61
	Q1	-3,40	-3,28	-15,84	-14,78
	Q2 (Median)	-2,36	-2,39	-7,44	-7,37
	Q3	-1,61	-1,74	-4,18	-3,98
	Max	2,34	0,93	47,57	99,86

Table 3. Stress values (in Mpa) for the LS3 configuration with the whole bone-implant interface.

LS3		WHOLE BONE-IMPLANT INTERFACE					
		AXIAL LOAD			TILTED LOAD		
		Imp 1	Imp 2	Imp 3	Imp 1	Imp 2	Imp 3
VON MISES	Min	0,15	0,30	0,26	0,42	0,31	0,16
	Q1	1,54	1,36	1,27	3,78	2,41	1,94
	Q2 (Median)	2,46	1,87	1,64	6,86	4,93	3,67
	Q3	3,36	2,38	2,05	11,64	8,59	7,92
	Max	16,14	17,65	26,71	79,81	68,85	146,54
MAX PRINCIPAL	Min	-4,60	-15,70	-8,53	-45,95	-16,47	-28,10
	Q1	0,21	0,07	0,07	2,27	1,28	0,58
	Q2 (Median)	0,76	0,28	0,26	3,95	2,60	1,27
	Q3	1,49	0,52	0,45	6,43	4,30	2,84
	Max	14,19	17,75	22,99	104,36	120,12	111,47
MIN PRINCIPAL	Min	-13,36	-32,06	-29,90	-108,84	-57,74	-135,92
	Q1	-2,50	-2,19	-2,02	-6,19	-4,88	-4,18
	Q2 (Median)	-1,79	-1,71	-1,44	-3,02	-2,22	-2,29
	Q3	-1,24	-1,28	-1,09	-1,27	-1,00	-1,31
	Max	0,64	3,63	8,52	21,33	53,10	25,89

Table 4. Stress values (in Mpa) for the LS3 configuration with the coronal bone-implant interface.

LS3		CORONAL BONE-IMPLANT INTERFACE					
		AXIAL LOAD			TILTED LOAD		
		Imp 1	Imp 2	Imp 3	Imp 1	Imp 2	Imp 3
VON MISES	<b>Min</b>	0,15	0,33	0,26	1,37	0,96	1,29
	<b>Q1</b>	1,20	1,69	1,69	7,74	5,70	6,41
	<b>Q2 (Median)</b>	1,89	2,28	2,32	12,34	10,14	10,58
	<b>Q3</b>	3,21	2,91	3,18	17,16	15,93	16,12
	<b>Max</b>	16,14	17,65	26,71	79,81	68,85	109,82
MAX PRINCIPAL	<b>Min</b>	-4,60	-15,70	-8,53	-45,95	-16,47	-28,10
	<b>Q1</b>	0,05	-0,07	-0,03	2,77	2,82	1,86
	<b>Q2 (Median)</b>	0,18	0,09	0,10	5,68	4,50	3,63
	<b>Q3</b>	0,53	0,25	0,26	11,16	7,86	8,35
	<b>Max</b>	14,19	17,75	5,74	104,36	120,12	111,47
MIN PRINCIPAL	<b>Min</b>	-13,36	-32,06	-29,90	-108,84	-57,74	-115,52
	<b>Q1</b>	-2,87	-3,09	-3,36	-8,56	-10,12	-9,87
	<b>Q2 (Median)</b>	-1,82	-2,41	-2,42	-4,48	-3,17	-4,94
	<b>Q3</b>	-1,17	-1,81	-1,75	-2,79	-1,49	-2,50
	<b>Max</b>	0,58	3,63	1,20	21,33	53,10	16,74

Table 5. Stress values (in Mpa) for the SS2 configuration with the whole bone-implant interface.

SS2		WHOLE BONE-IMPLANT INTERFACE			
		AXIAL LOAD		TILTED LOAD	
		Imp 1	Imp 3	Imp 1	Imp 3
VON MISES	Min	0,26	0,58	0,98	1,02
	Q1	3,50	3,16	8,34	6,49
	Q2 (Median)	4,74	4,06	15,26	10,79
	Q3	5,97	5,21	23,65	18,45
	Max	40,08	56,58	136,21	135,22
MAX PRINCIPAL	Min	-19,73	-28,09	-92,38	-95,64
	Q1	0,38	0,12	3,15	1,94
	Q2 (Median)	1,04	0,49	6,58	4,03
	Q3	1,91	1,03	11,20	7,64
	Max	26,33	68,17	201,10	140,85
MIN PRINCIPAL	Min	-41,14	-89,27	-191,85	-229,29
	Q1	-5,12	-4,90	-13,86	-10,38
	Q2 (Median)	-3,97	-3,79	-6,83	-5,32
	Q3	-2,88	-2,97	-2,97	-3,24
	Max	4,01	28,17	53,26	31,47

Table 6. Stress values (in Mpa) for the SS2 configuration with the coronal bone-implant interface.

SS2		CORONAL BONE-IMPLANT INTERFACE			
		AXIAL LOAD		TILTED LOAD	
		Imp 1	Imp 3	Imp 1	Imp 3
VON MISES	Min	0,26	0,58	0,98	1,53
	Q1	3,32	3,34	14,70	11,02
	Q2 (Median)	4,89	4,66	22,48	18,08
	Q3	6,33	6,09	32,50	27,54
	Max	40,08	56,58	136,21	135,22
MAX PRINCIPAL	Min	-19,73	-28,09	-92,38	-95,64
	Q1	0,20	0,02	3,81	3,41
	Q2 (Median)	0,74	0,41	8,42	6,20
	Q3	1,43	0,91	18,69	13,87
	Max	26,33	68,17	201,10	140,85
MIN PRINCIPAL	Min	-41,14	-89,27	-191,85	-229,29
	Q1	-5,74	-6,19	-19,26	-18,41
	Q2 (Median)	-4,27	-4,50	-9,10	-7,08
	Q3	-2,98	-3,29	-4,78	-3,60
	Max	4,01	28,17	53,26	31,47

Table 7. Stress values (in Mpa) for the SS3 configuration with the whole bone-implant interface.

SS3		WHOLE BONE-IMPLANT INTERFACE					
		AXIAL LOAD			TILTED LOAD		
		Imp 1	Imp 2	Imp 3	Imp 1	Imp 2	Imp 3
VON MISES	Min	0,14	0,32	0,46	0,97	0,90	0,53
	Q1	2,08	2,26	2,29	6,92	5,18	5,20
	Q2 (Median)	3,09	3,08	2,96	11,75	9,79	9,02
	Q3	4,47	3,93	3,74	17,79	17,40	14,83
	Max	29,41	50,91	40,52	103,76	107,66	104,26
MAX PRINCIPAL	Min	-14,15	-6,30	-13,97	-28,22	-44,21	-47,77
	Q1	0,18	0,00	0,01	3,09	2,14	1,39
	Q2 (Median)	0,66	0,27	0,24	5,97	4,41	3,20
	Q3	1,50	0,68	0,68	9,63	7,06	6,03
	Max	41,88	73,38	64,82	139,98	116,71	149,36
MIN PRINCIPAL	Min	-45,86	-22,66	-46,73	-101,35	-160,35	-159,93
	Q1	-3,69	-3,90	-3,75	-10,20	-11,01	-9,70
	Q2 (Median)	-2,57	-2,97	-2,85	-5,25	-4,16	-4,49
	Q3	-1,72	-2,19	-2,18	-2,45	-1,80	-2,61
	Max	13,39	30,86	21,95	64,49	30,90	68,49

Table 8. Stress values (in Mpa) for the SS3 configuration with the coronal bone-implant interface.

SS3		CORONAL BONE-IMPLANT INTERFACE					
		AXIAL LOAD			TILTED LOAD		
		Imp 1	Imp 2	Imp 3	Imp 1	Imp 2	Imp 3
VON MISES	<b>Min</b>	0,14	0,32	0,46	1,11	1,12	1,41
	<b>Q1</b>	1,80	2,66	2,66	9,68	8,98	9,45
	<b>Q2 (Median)</b>	2,85	3,75	3,61	15,79	15,74	15,04
	<b>Q3</b>	4,60	5,17	4,60	23,09	24,37	22,45
	<b>Max</b>	29,41	50,91	40,52	103,76	104,78	104,12
MAX PRINCIPAL	<b>Min</b>	-14,15	-6,30	-6,25	-28,22	-38,39	-18,84
	<b>Q1</b>	0,06	-0,06	-0,05	3,07	3,42	2,64
	<b>Q2 (Median)</b>	0,41	0,22	0,24	6,86	6,06	4,89
	<b>Q3</b>	1,10	0,59	0,63	12,23	11,00	9,70
	<b>Max</b>	41,88	73,38	64,82	134,99	116,71	146,56
MIN PRINCIPAL	<b>Min</b>	-45,86	-22,66	-17,08	-101,35	-144,90	-91,23
	<b>Q1</b>	-4,10	-5,20	-4,78	-12,97	-16,94	-17,09
	<b>Q2 (Median)</b>	-2,56	-3,78	-3,63	-6,98	-5,63	-6,93
	<b>Q3</b>	-1,51	-2,55	-2,57	-3,97	-2,43	-3,13
	<b>Max</b>	13,39	30,86	21,95	37,14	30,90	37,08



Table 9. Stress values (in Mpa) for the SL2 configuration with the whole bone-implant interface.

SL2		WHOLE BONE-IMPLANT INTERFACE			
		AXIAL LOAD		TILTED LOAD	
		Imp 1	Imp 3	Imp 1	Imp 3
VON MISES	Min	0,28	0,49	0,92	1,65
	Q1	3,39	3,15	11,94	9,99
	Q2 (Median)	4,63	4,05	20,94	15,99
	Q3	5,91	5,11	32,31	26,44
	Max	41,87	53,78	176,89	183,04
MAX PRINCIPAL	Min	-18,51	-26,13	-124,06	-131,78
	Q1	0,34	0,11	4,67	3,36
	Q2 (Median)	1,00	0,48	8,91	6,23
	Q3	1,87	1,02	15,61	11,85
	Max	38,86	66,95	253,19	173,15
MIN PRINCIPAL	Min	-37,98	-84,33	-257,07	-313,27
	Q1	-5,05	-4,86	-18,41	-14,16
	Q2 (Median)	-3,91	-3,79	-8,82	-7,30
	Q3	-2,83	-2,98	-4,14	-4,46
	Max	3,58	28,04	68,59	44,39

Table 10. Stress values (in Mpa) for the SL2 configuration with the coronal bone-implant interface.

SL2		CORONAL BONE-IMPLANT INTERFACE			
		AXIAL LOAD		TILTED LOAD	
		Imp 1	Imp 3	Imp 1	Imp 3
VON MISES	Min	0,28	0,49	0,92	1,65
	Q1	3,11	3,24	19,75	16,33
	Q2 (Median)	4,67	4,49	31,01	26,04
	Q3	6,16	5,84	45,77	39,67
	Max	41,87	53,78	176,89	183,04
MAX PRINCIPAL	Min	-18,51	-26,13	-124,06	-131,78
	Q1	0,17	0,01	5,46	4,82
	Q2 (Median)	0,68	0,37	11,50	9,35
	Q3	1,38	0,86	27,28	21,76
	Max	38,86	66,95	253,19	173,15
MIN PRINCIPAL	Min	-37,98	-84,33	-257,07	-313,27
	Q1	-5,52	-5,96	-25,63	-25,65
	Q2 (Median)	-4,14	-4,35	-11,45	-9,39
	Q3	-2,85	-3,22	-6,17	-4,59
	Max	3,58	28,04	68,59	44,39

Table 11. Stress values (in Mpa) for the SL3 configuration with the whole bone-implant interface.

SL3		WHOLE BONE-IMPLANT INTERFACE					
		AXIAL LOAD			TILTED LOAD		
		Imp 1	Imp 2	Imp 3	Imp 1	Imp 2	Imp 3
VON MISES	Min	0,13	0,33	0,39	1,42	1,15	0,76
	Q1	2,11	2,26	2,29	9,62	7,27	7,80
	Q2 (Median)	3,09	3,07	2,97	16,11	13,58	13,03
	Q3	4,42	3,92	3,73	24,20	24,10	20,95
	Max	25,77	51,51	36,76	103,76	149,25	139,68
MAX PRINCIPAL	Min	-10,02	-6,26	-13,55	-38,68	-32,51	-41,72
	Q1	0,17	-0,01	0,01	4,30	2,99	2,30
	Q2 (Median)	0,65	0,26	0,23	7,87	5,86	4,75
	Q3	1,50	0,67	0,67	12,93	9,58	9,00
	Max	40,64	68,25	57,96	139,98	156,43	197,79
MIN PRINCIPAL	Min	-38,11	-20,85	-46,68	-144,03	-136,66	-158,08
	Q1	-3,68	-3,88	-3,76	-13,77	-15,04	-13,08
	Q2 (Median)	-2,59	-2,97	-2,86	-6,85	-5,52	-6,02
	Q3	-1,74	-2,20	-2,18	-3,17	-2,44	-3,51
	Max	14,36	28,46	19,10	64,49	49,12	85,59

Table 12. Stress values (in Mpa) for the SL3 configuration with the coronal bone-implant interface.

SL3		CORONAL BONE-IMPLANT INTERFACE					
		AXIAL LOAD			TILTED LOAD		
		Imp 1	Imp 2	Imp 3	Imp 1	Imp 2	Imp 3
VON MISES	<b>Min</b>	0,13	0,33	0,39	1,42	1,76	1,37
	<b>Q1</b>	1,80	2,58	2,67	13,29	12,25	13,30
	<b>Q2 (Median)</b>	2,88	3,65	3,59	21,96	22,33	21,33
	<b>Q3</b>	4,47	5,06	4,54	32,54	35,13	31,89
	<b>Max</b>	25,77	51,51	36,76	103,76	121,39	115,42
MAX PRINCIPAL	<b>Min</b>	-10,02	-6,26	-6,73	-38,68	-32,51	-26,88
	<b>Q1</b>	0,05	-0,09	-0,05	4,50	4,43	3,67
	<b>Q2 (Median)</b>	0,39	0,20	0,23	9,42	7,97	6,90
	<b>Q3</b>	1,08	0,55	0,61	17,20	16,04	14,21
	<b>Max</b>	37,59	68,25	57,96	134,99	156,43	143,86
MIN PRINCIPAL	<b>Min</b>	-38,11	-20,85	-18,55	-144,03	-136,66	-126,95
	<b>Q1</b>	-4,04	-5,18	-4,73	-17,97	-23,85	-23,42
	<b>Q2 (Median)</b>	-2,57	-3,70	-3,63	-9,13	-7,33	-9,25
	<b>Q3</b>	-1,51	-2,52	-2,54	-4,92	-2,97	-4,13
	<b>Max</b>	12,74	28,46	19,10	37,14	49,12	22,77

Figure 1. Box plot graphs for configuration LS2

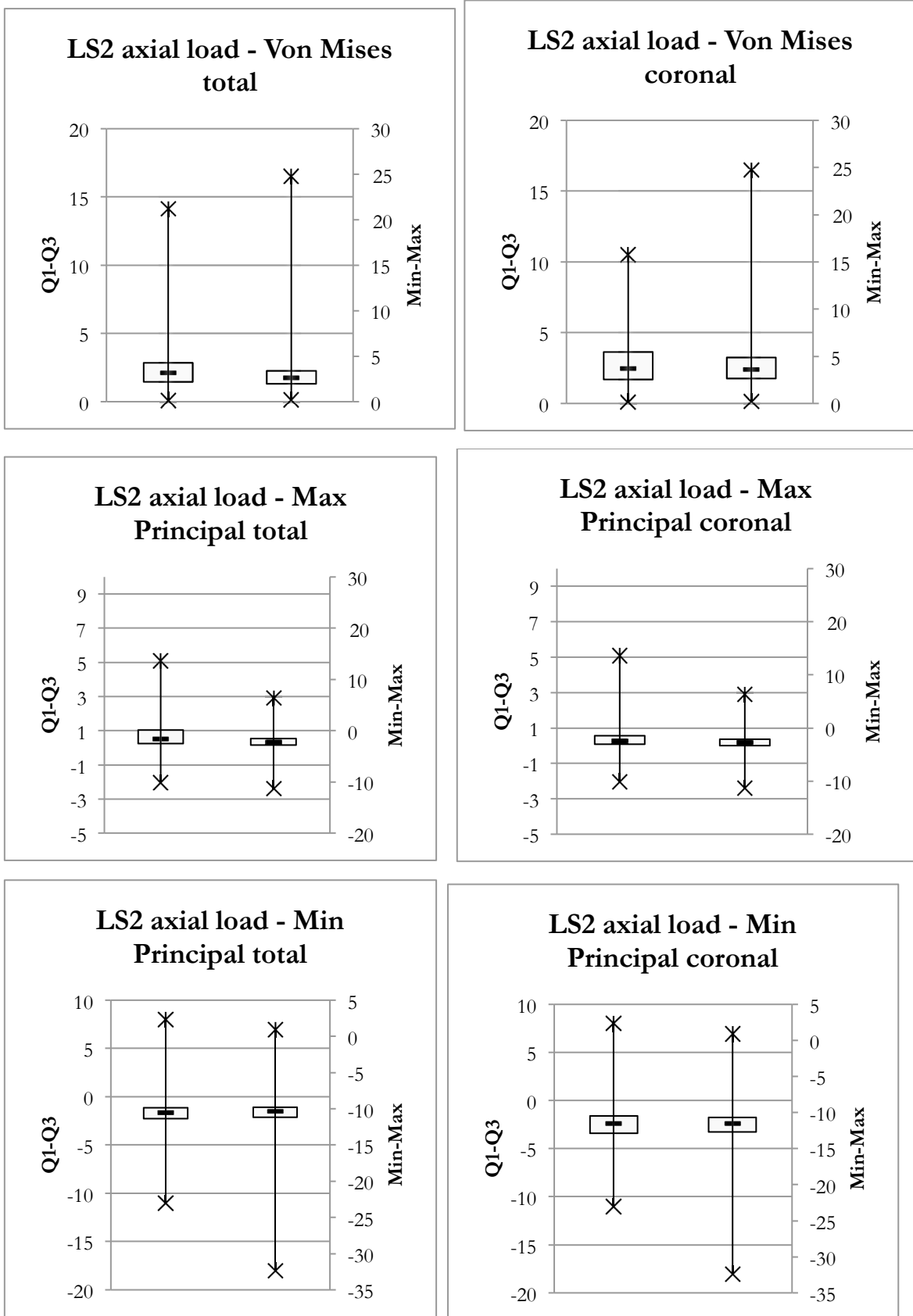


Figure 2. Box plot graphs for configuration LS3

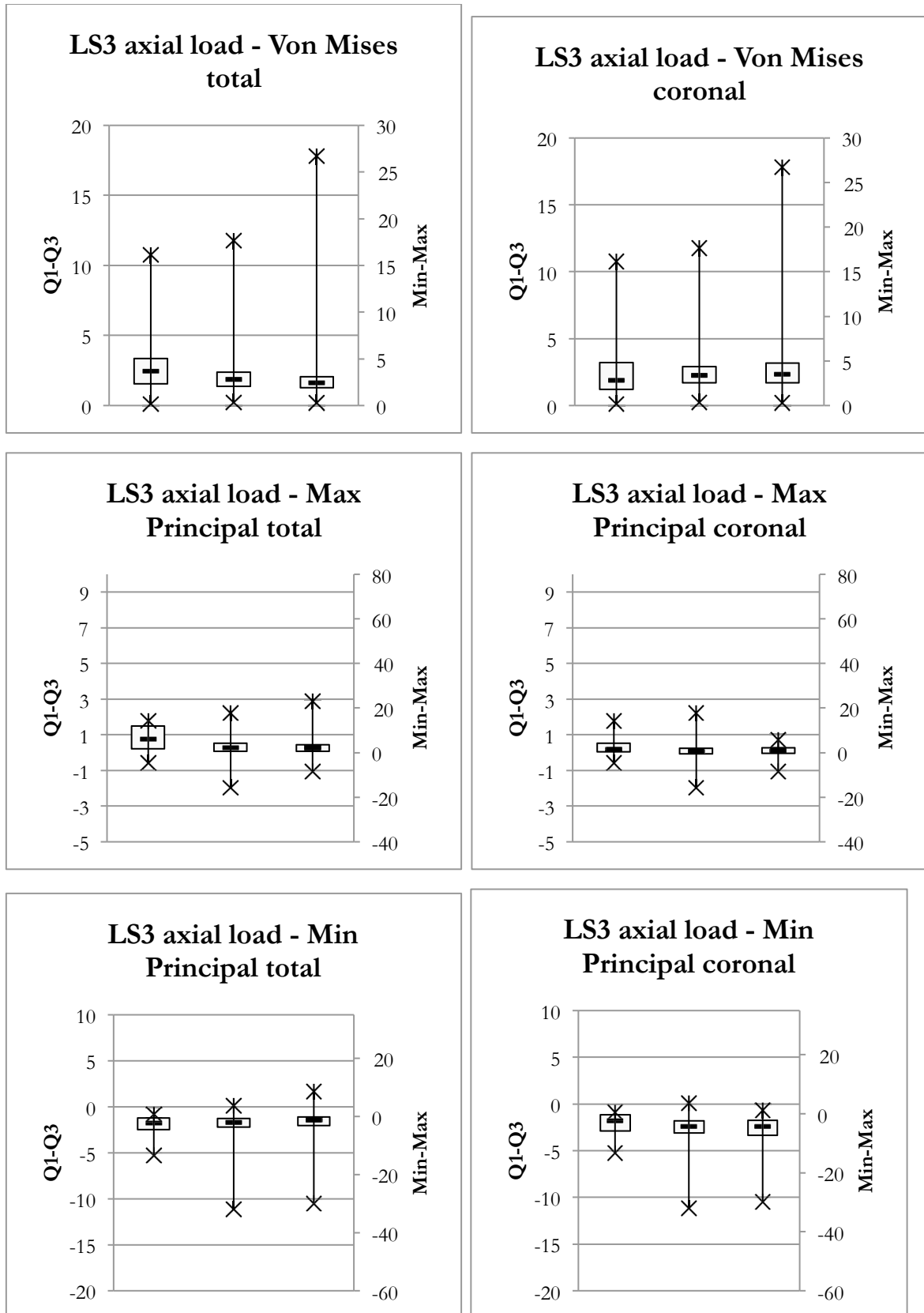


Figure 3. Box plot graphs for configuration SS2

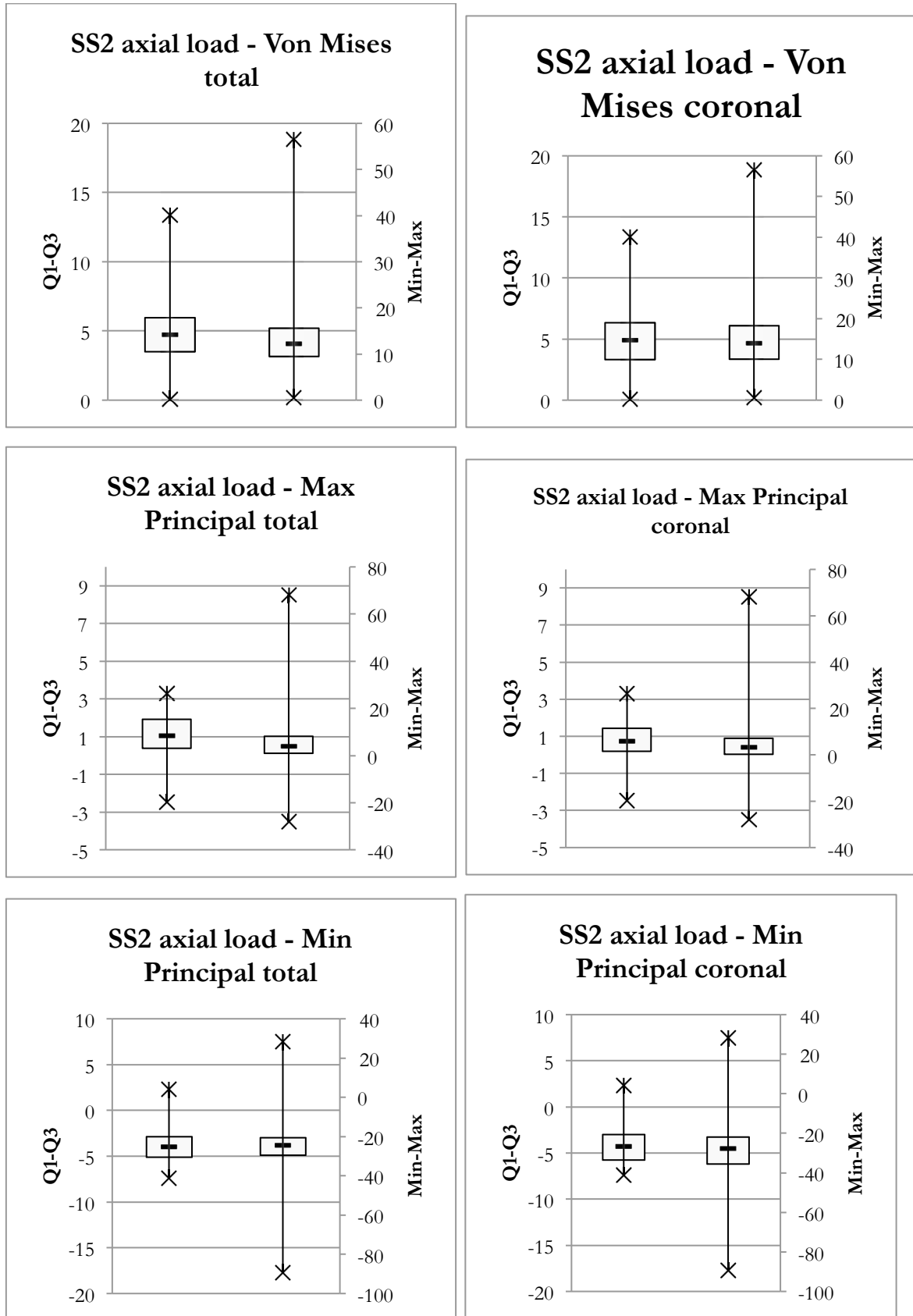


Figure 4. Box plot graphs for configuration SS3

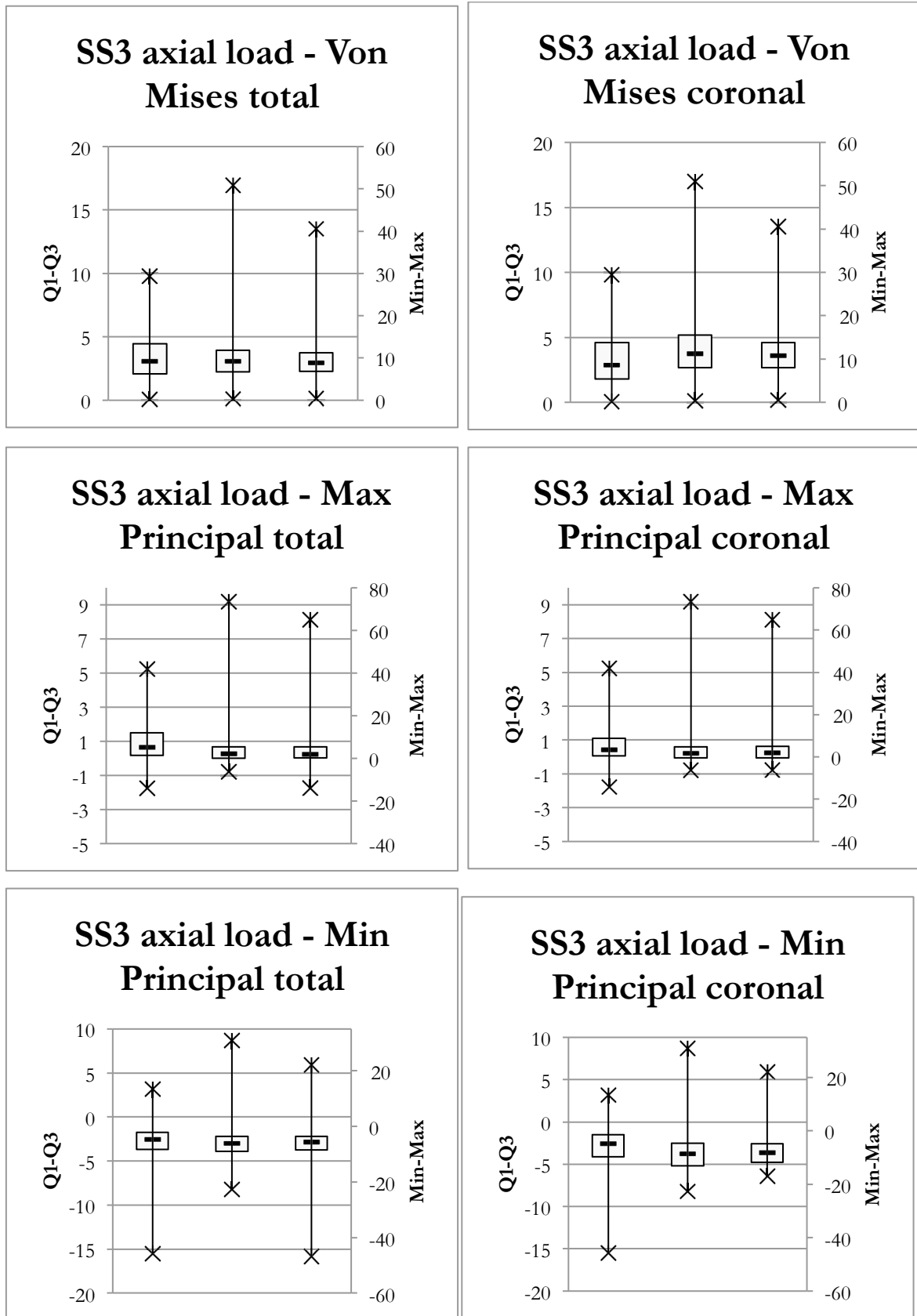




Figure 5. Box plot graphs for configuration SL2

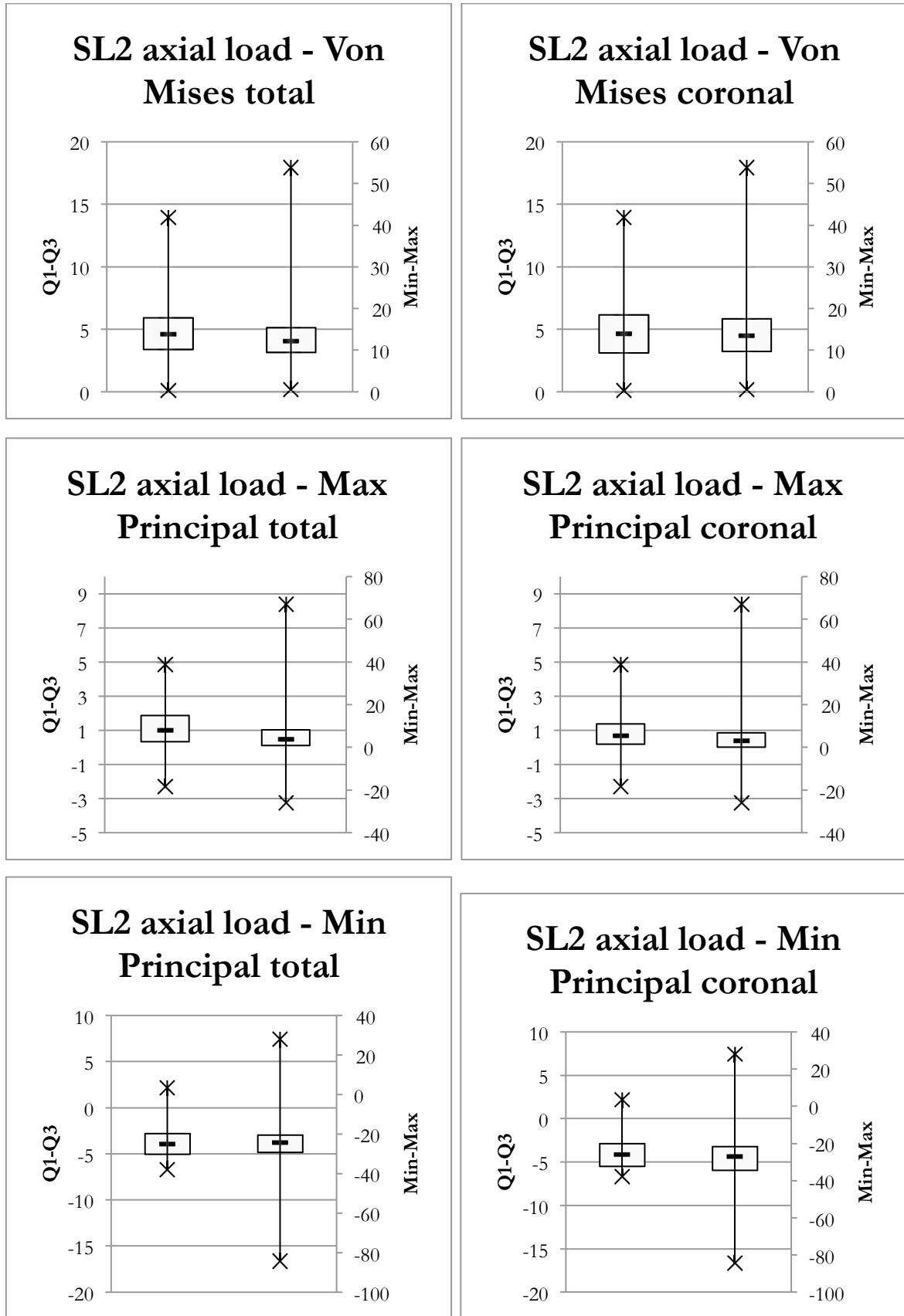


Figure 6. Box plot graphs for configuration SL3

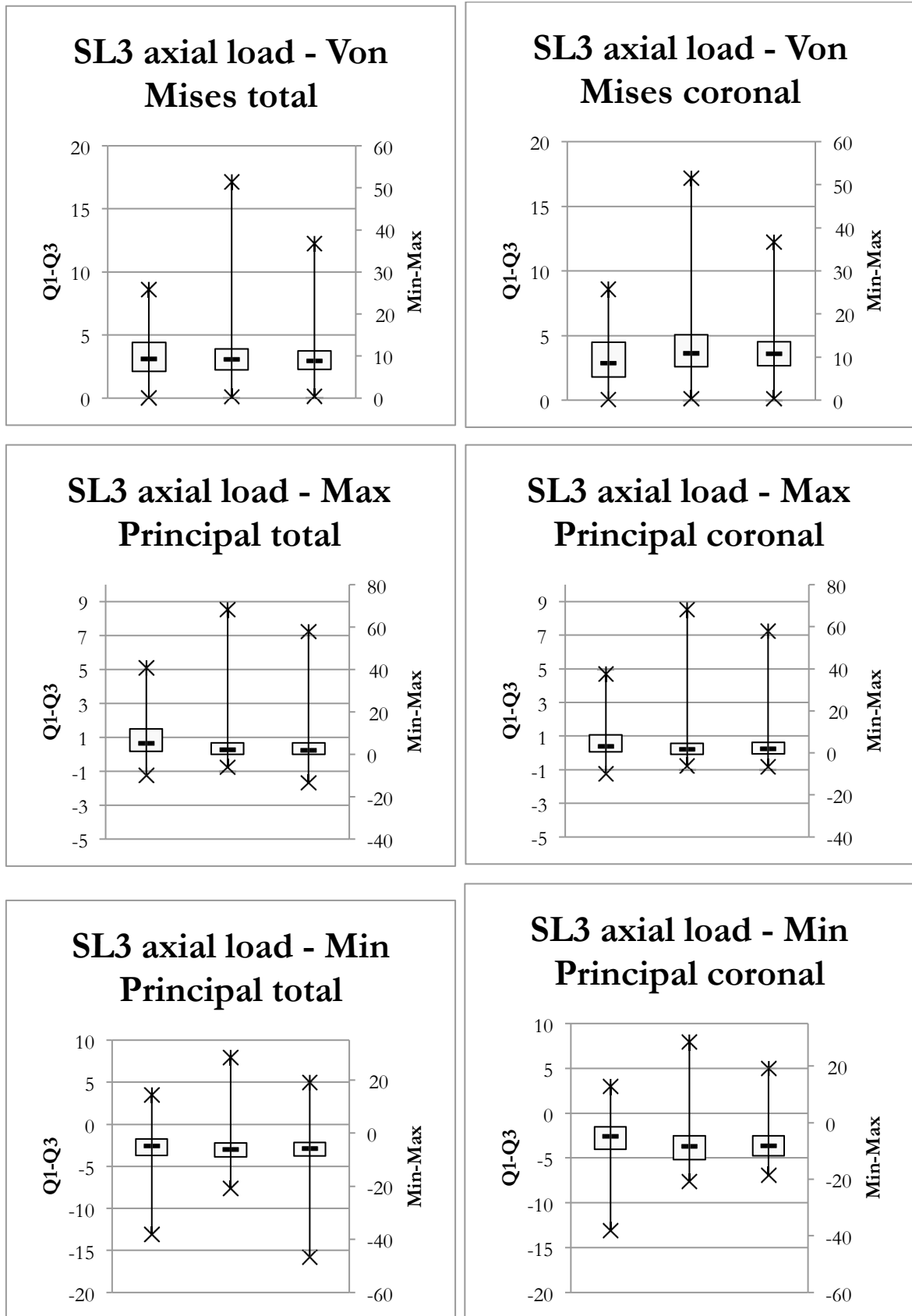


Figure 7. Box plot graphs for configuration LS2

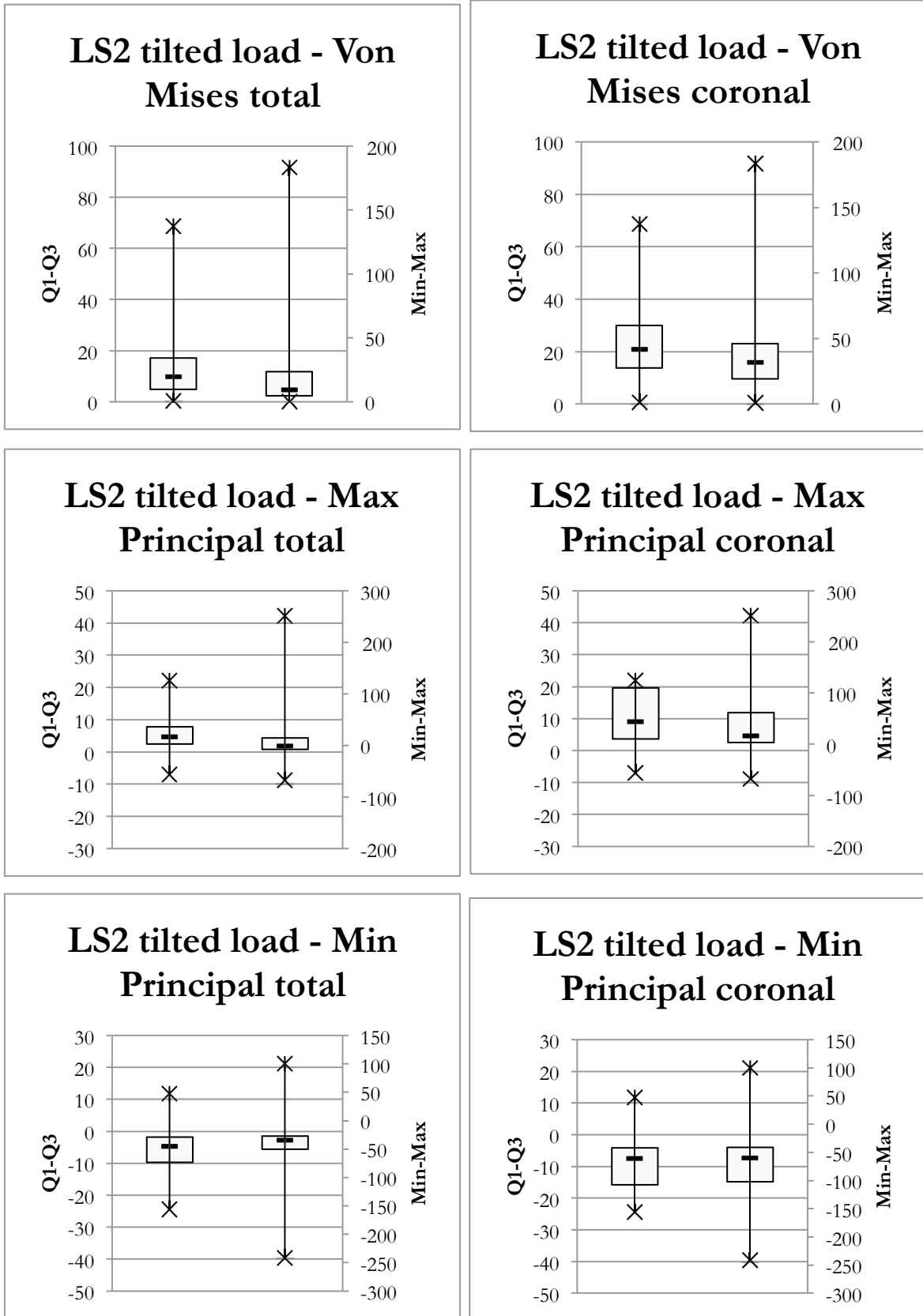


Figure 8. Box plot graphs for configuration LS3

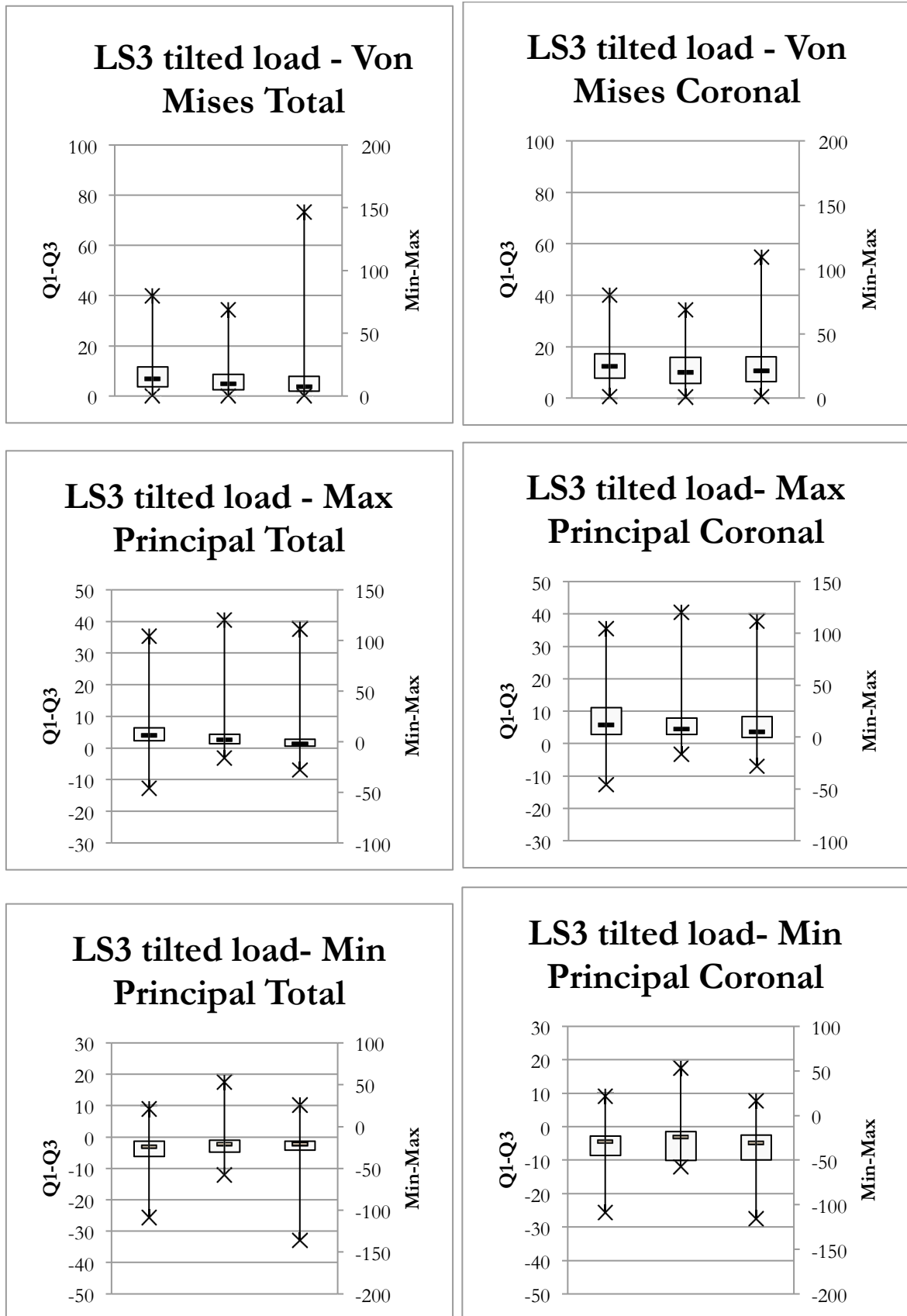


Figure 9. Box plot graphs for configuration SS2

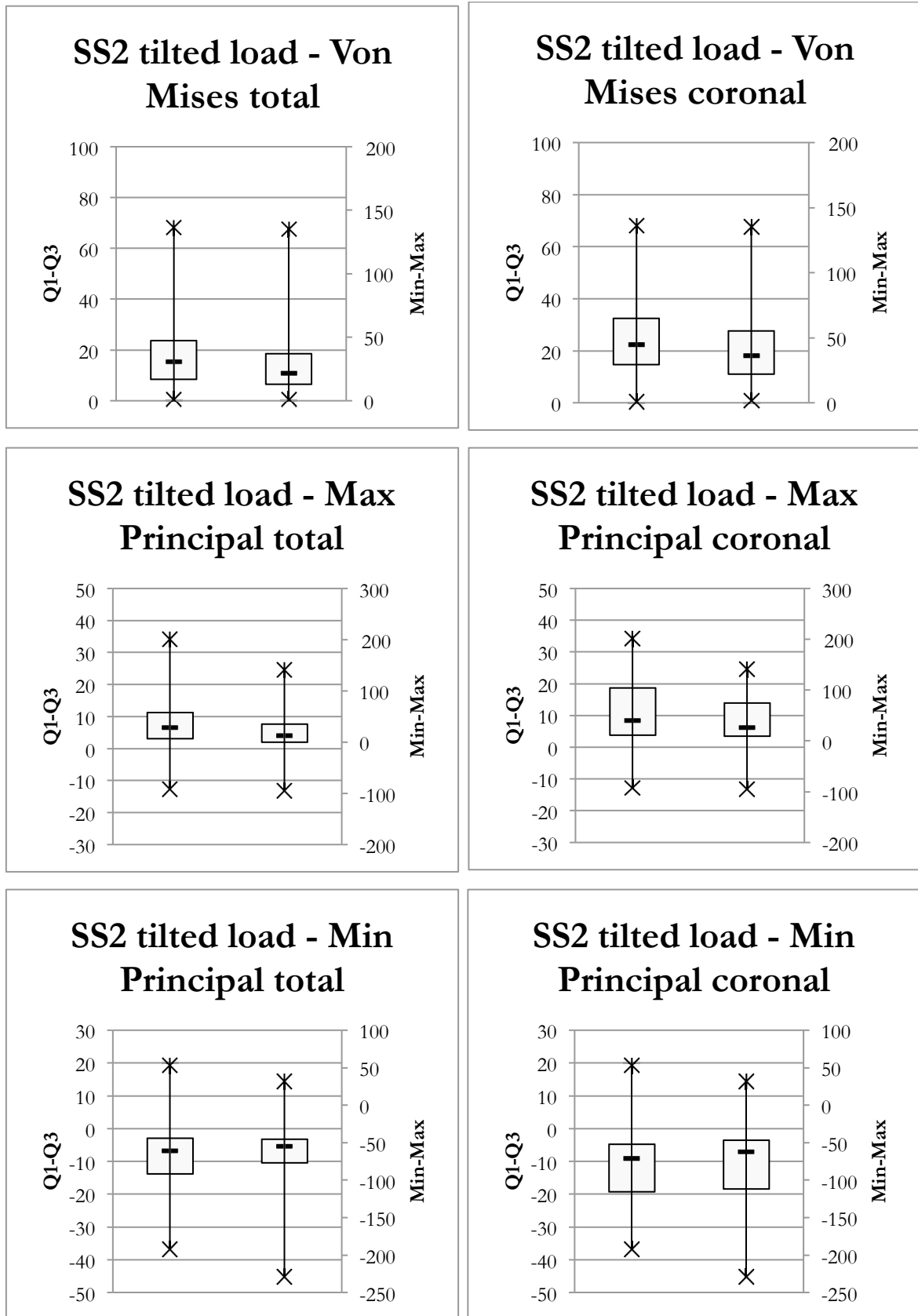


Figure 10. Box plot graphs for configuration SS3

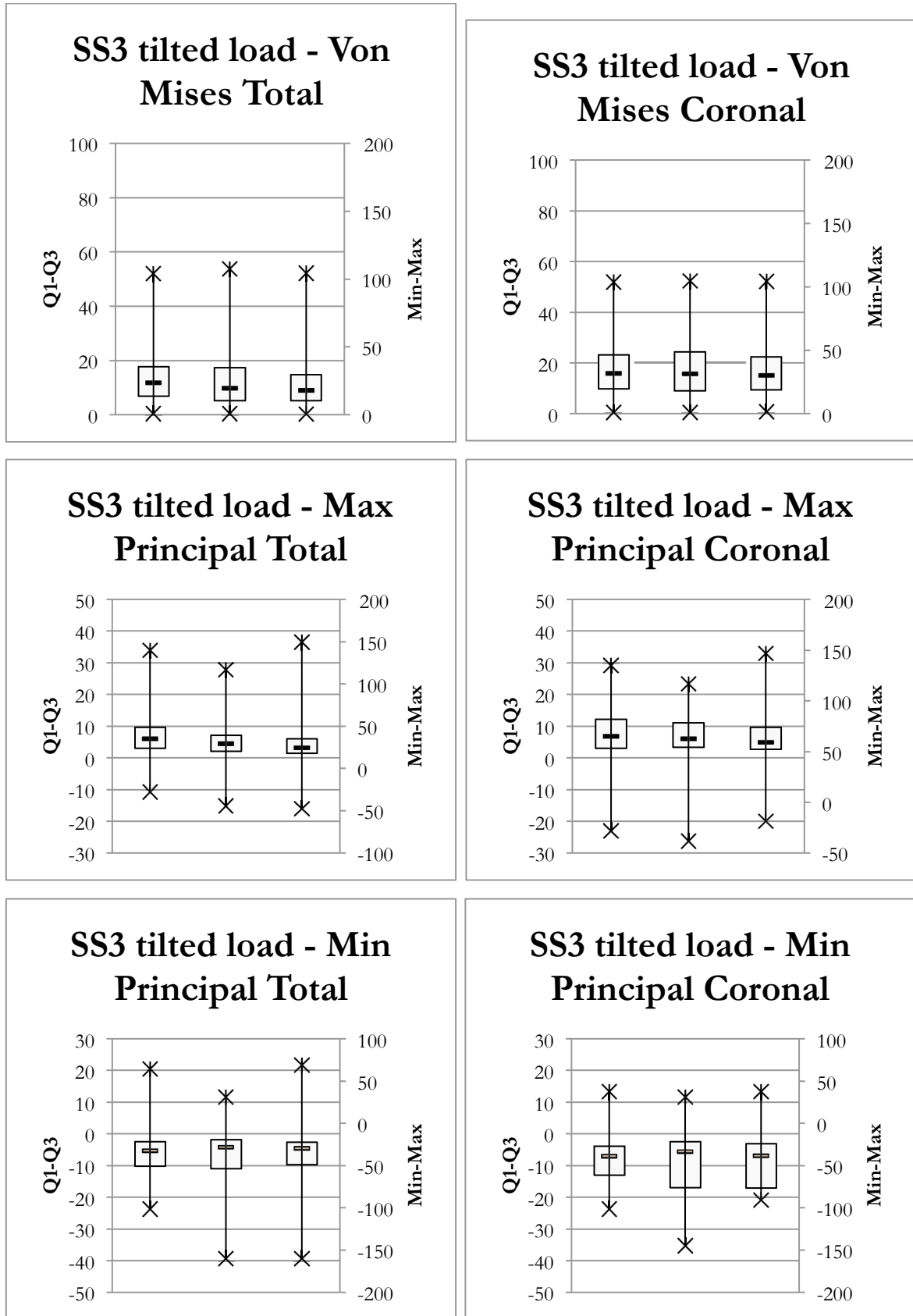


Figure 11. Box plot graphs for configuration SL2

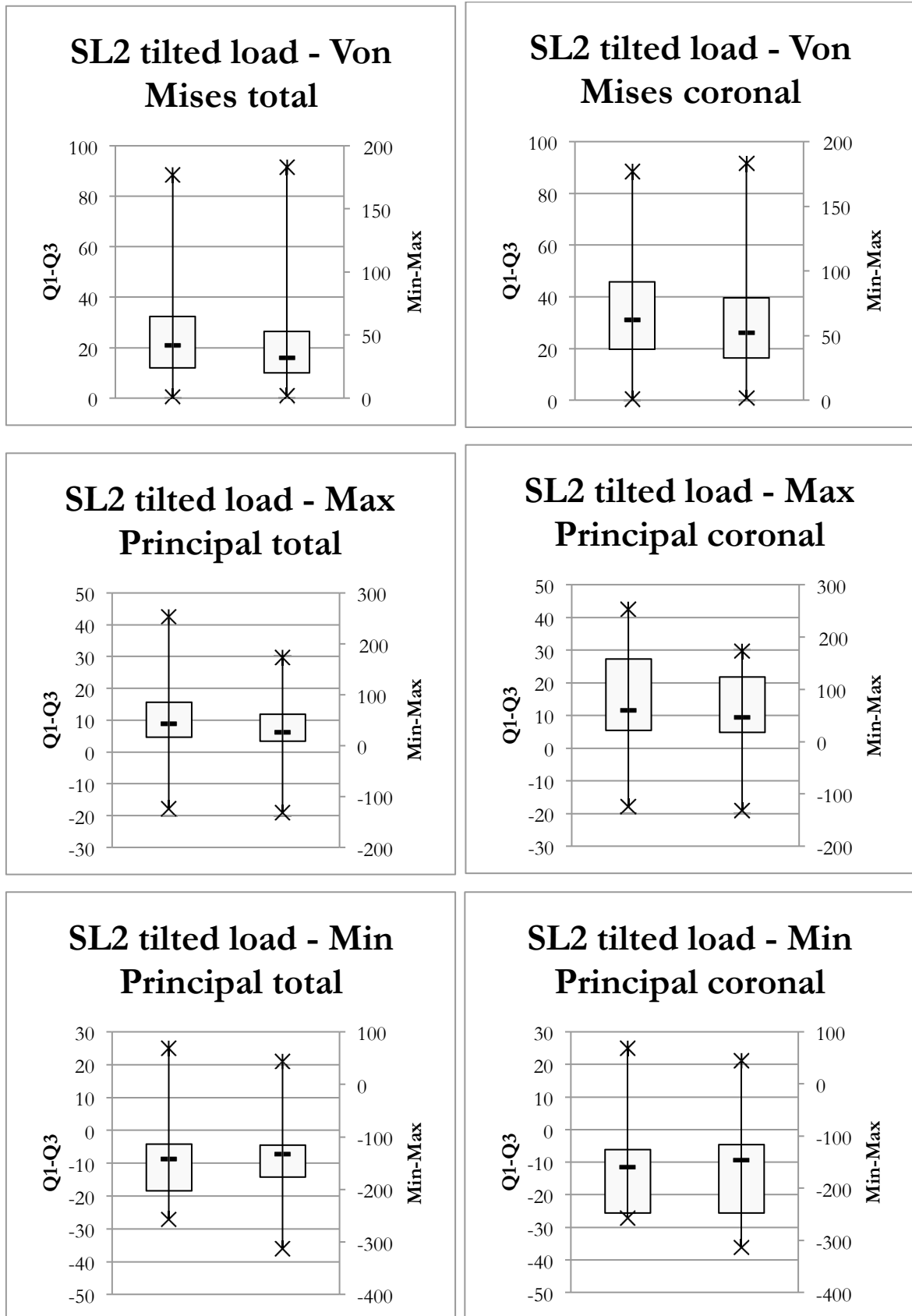


Figure 12. Box plot graphs for configuration SL3

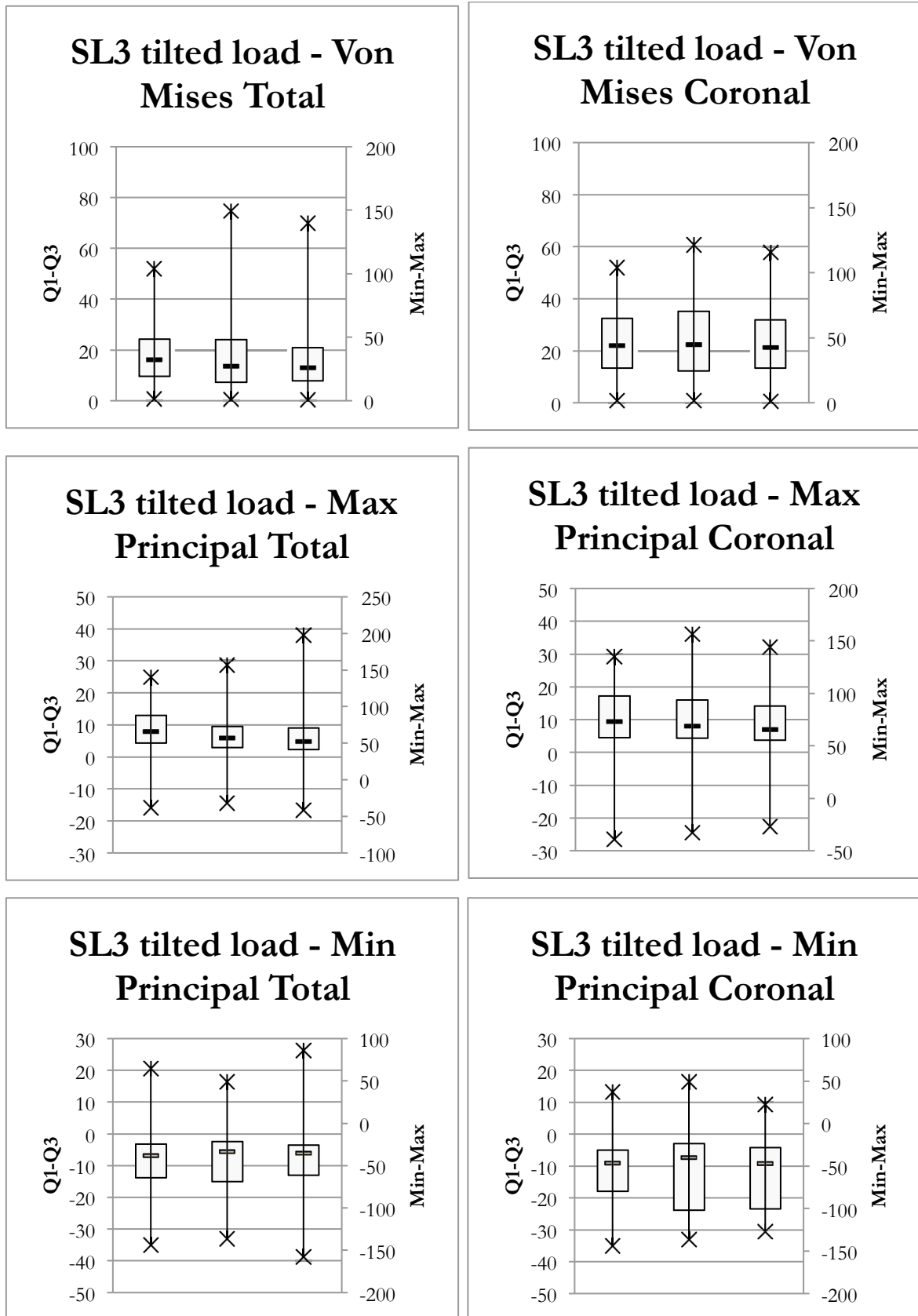




Figure 13. Above view of the 3D model of configuration LS3 to show implants' labels and the lungitudinal and paraxial slices that were used to show Von Mises stress distribution from figure 14 to figure 25.

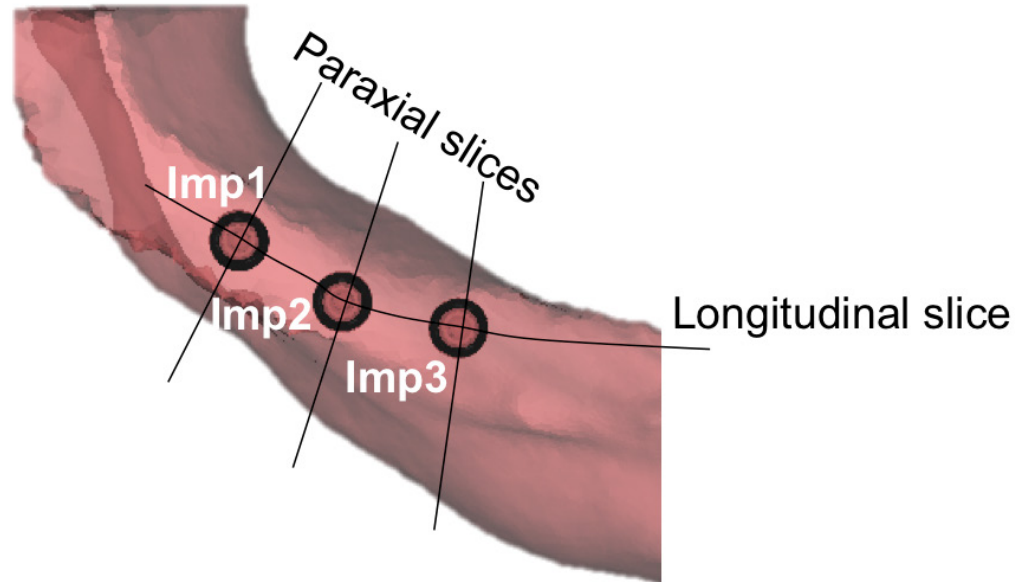


Figure 14. Graphical representation of the Von Mises stress distribution in the LS2 configuration under axial load. (The scale is in MPa)

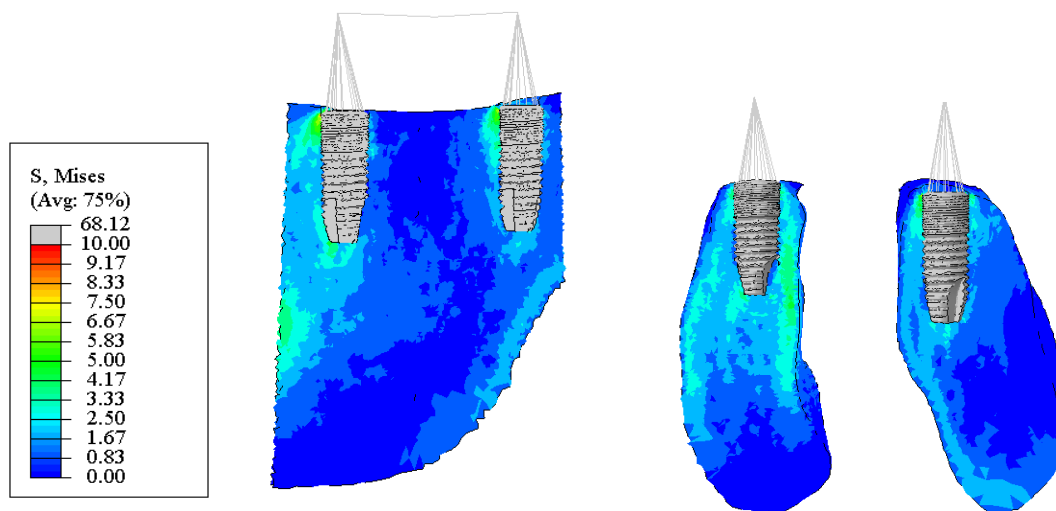


Figure 15. Graphical representation of the Von Mises stress distribution in the LS3 configuration under axial load. (The scale is in MPa)

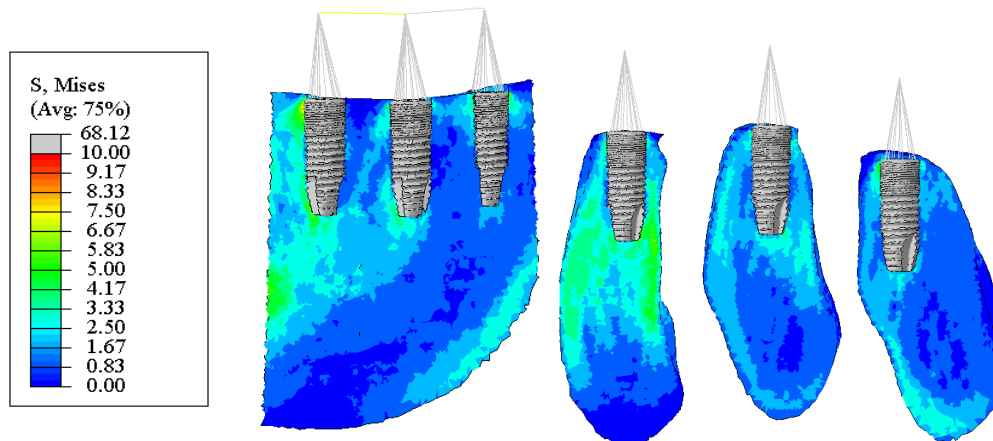


Figure 16. Graphical representation of the Von Mises stress distribution in the SS2 configuration under axial load. (The scale is in MPa)

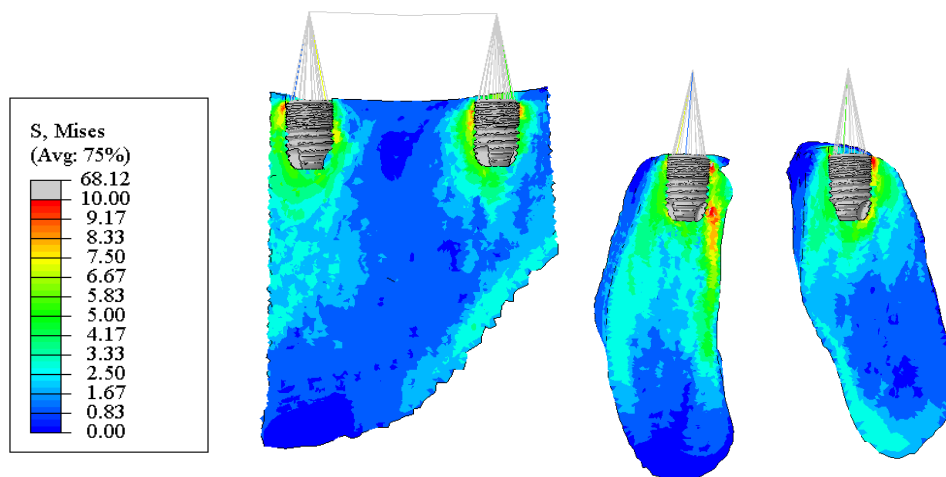


Figure 17. Graphical representation of the Von Mises stress distribution in the SS3 configuration under axial load. (The scale is in MPa)

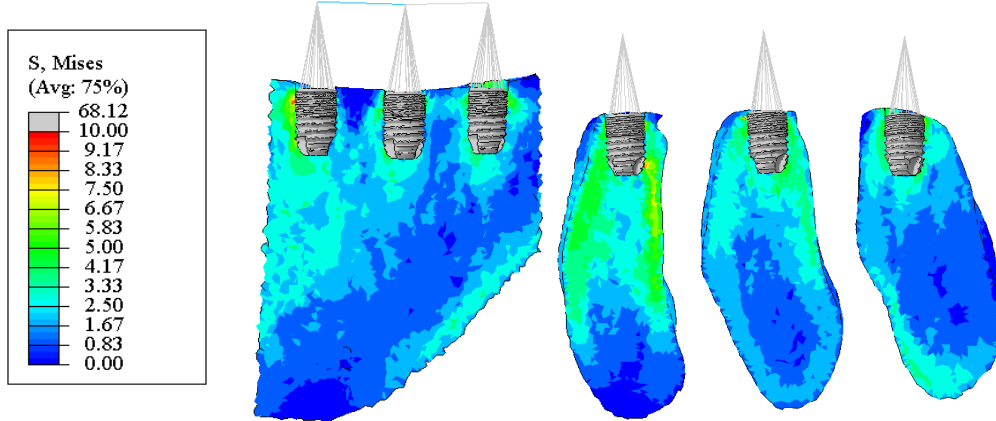


Figure 18. Graphical representation of the Von Mises stress distribution in the SL2 configuration under axial load. (The scale is in MPa)

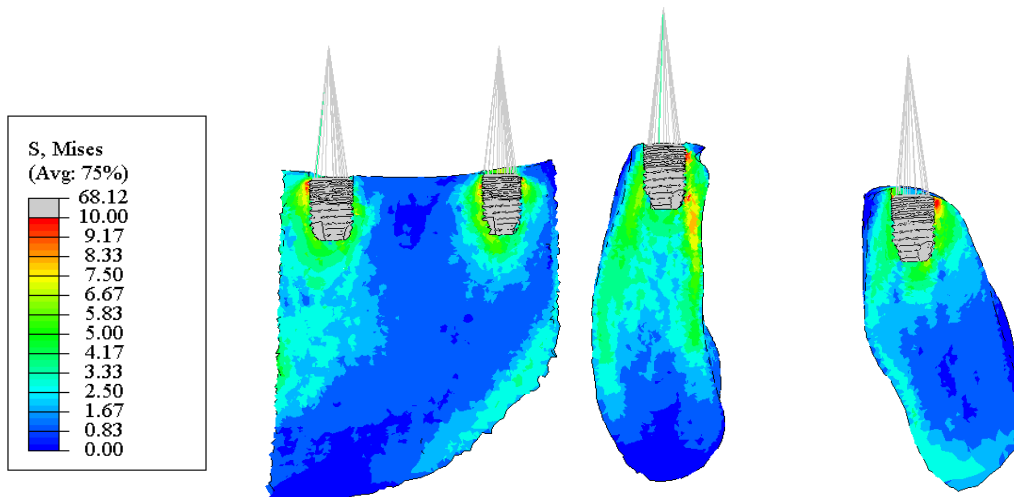


Figure 19. Graphical representation of the Von Mises stress distribution in the SL3 configuration under axial load. (The scale is in MPa)

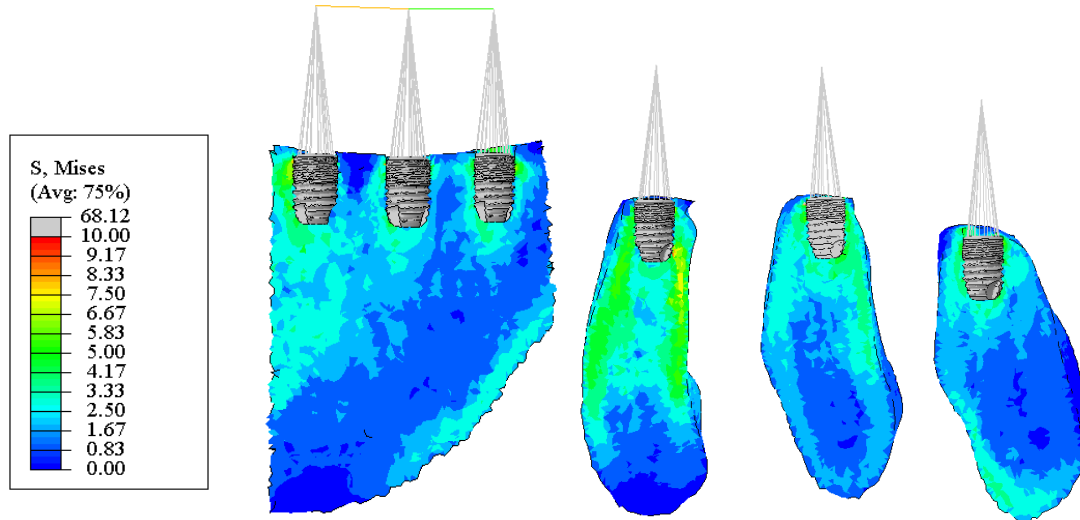


Figure 20. Graphical representation of the Von Mises stress distribution in the LS2 configuration under tilted load. (The scale is in MPa)

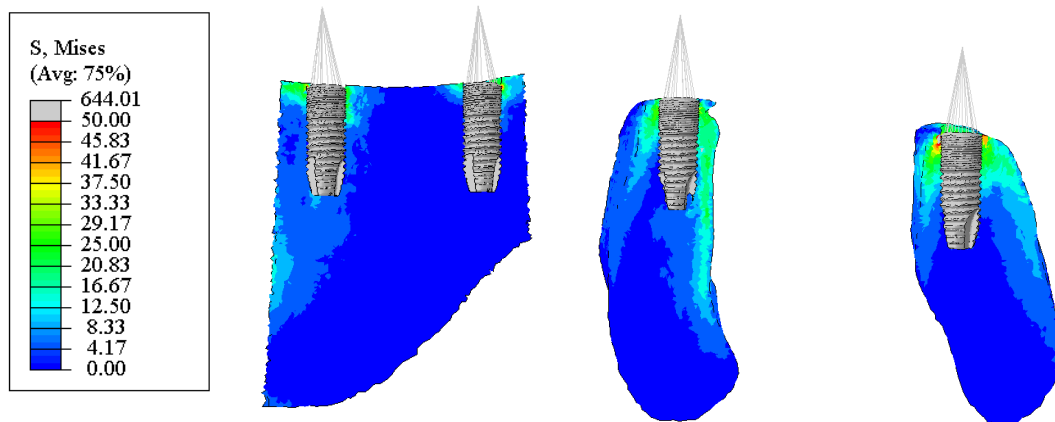


Figure 21. Graphical representation of the Von Mises stress distribution in the LS3 configuration under tilted load. (The scale is in MPa)

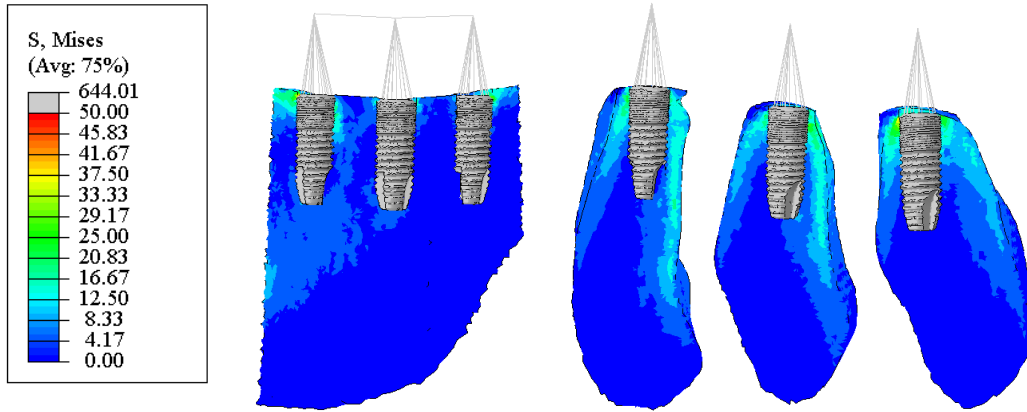


Figure 22. Graphical representation of the Von Mises stress distribution in the SS2 configuration under tilted load. (The scale is in MPa)

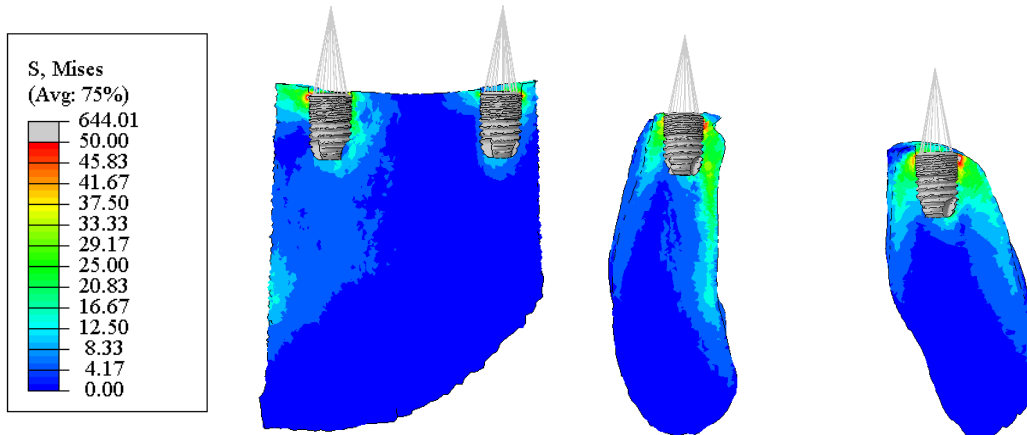


Figure 23. Graphical representation of the Von Mises stress distribution in the SS3 configuration under tilted load. (The scale is in MPa)

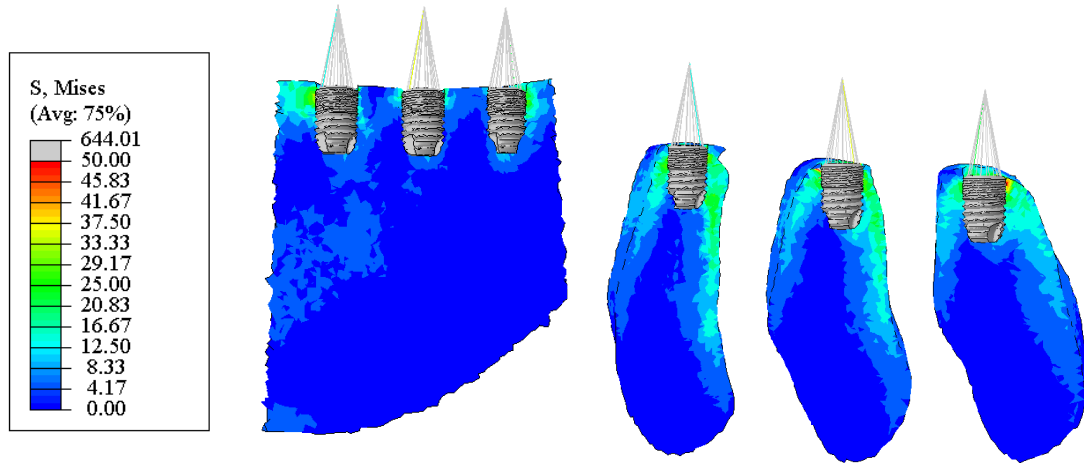


Figure 24. Graphical representation of the Von Mises stress distribution in the SL2 configuration under tilted load. (The scale is in MPa)

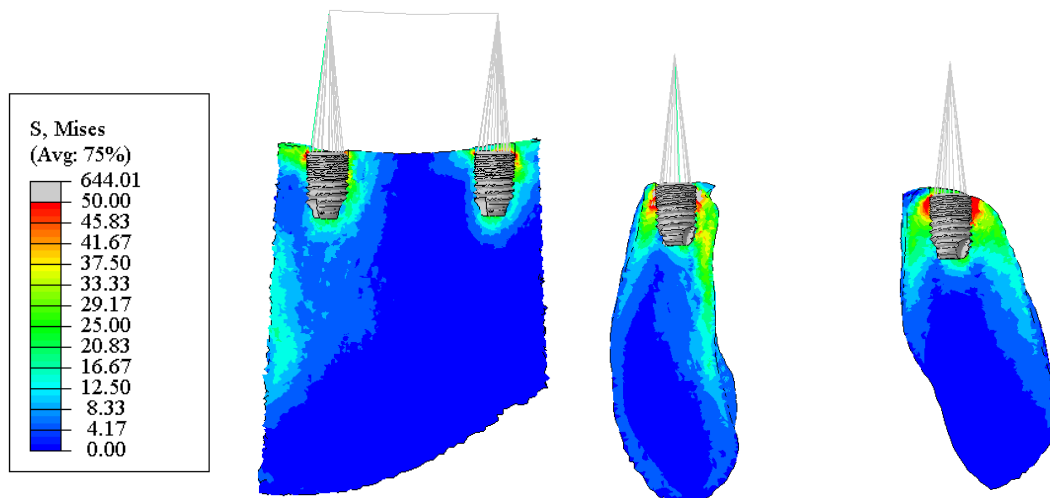


Figure 25. Graphical representation of the Von Mises stress distribution in the SL3 configuration under tilted load. (The scale is in MPa)

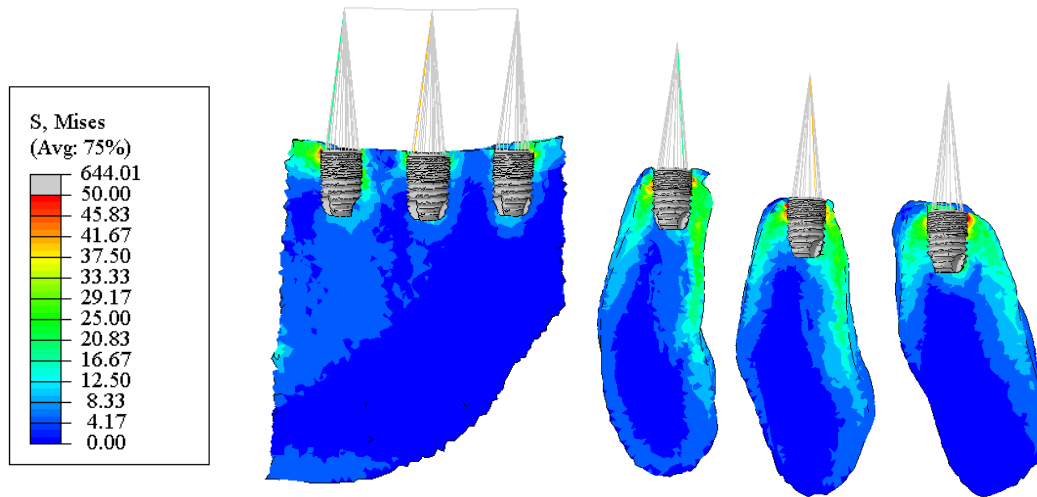


Figure 26. Graph representing the Q3 Von Mises stress for each implant in every configuration under axial load.

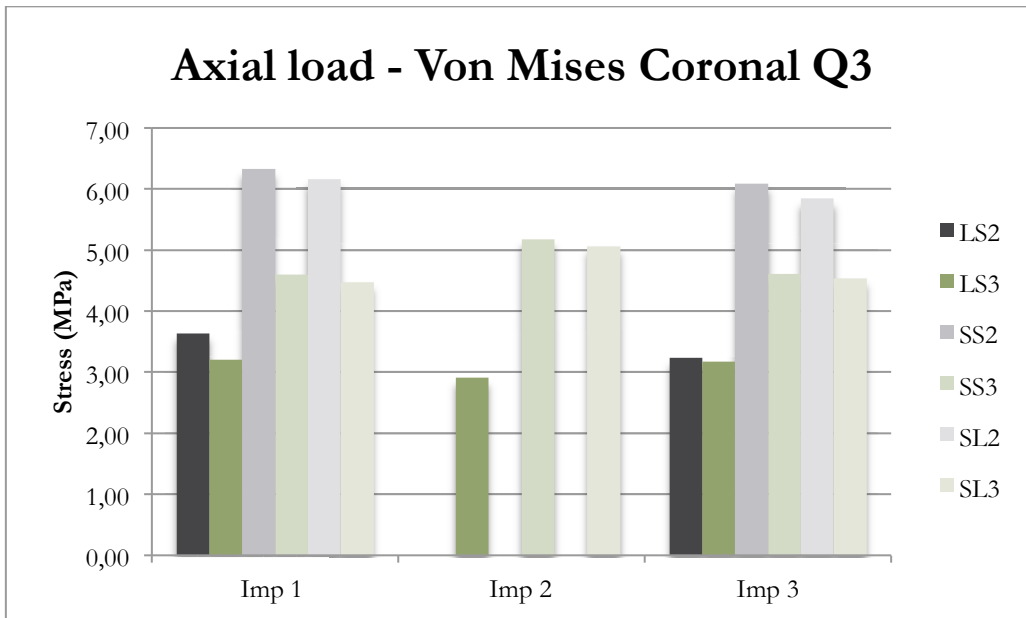


Figure 27. Graph representing the Q3 maximum principal stress for each implant in every configuration under axial load.

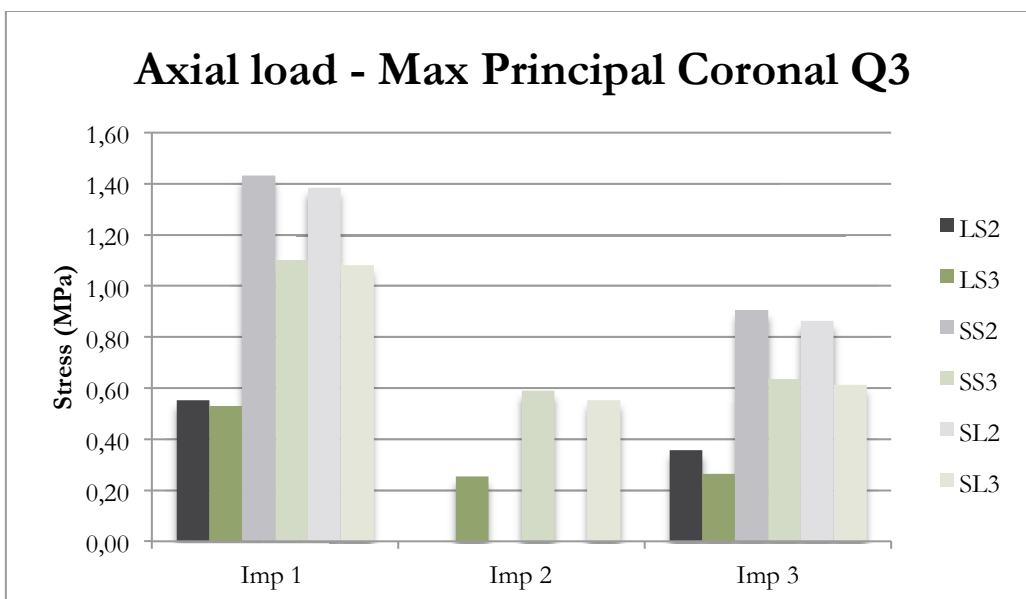




Figure 28. Graph representing the Q1 minimum principal stress for each implant in every configuration under axial load.

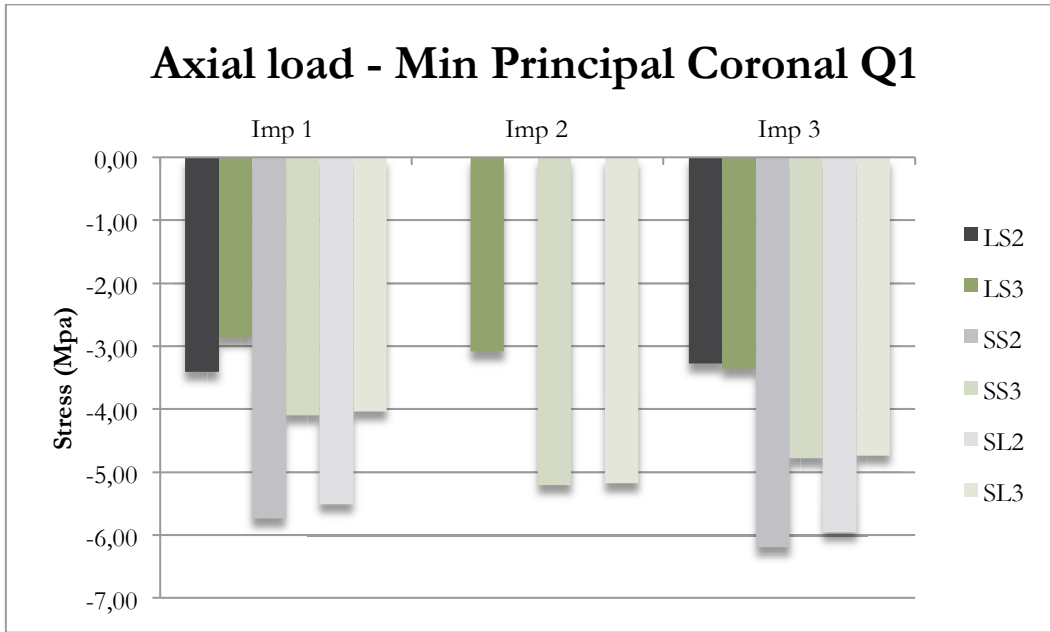


Figure 29. Graph representing the Q3 Von Mises stress for each implant in every configuration under tilted load.

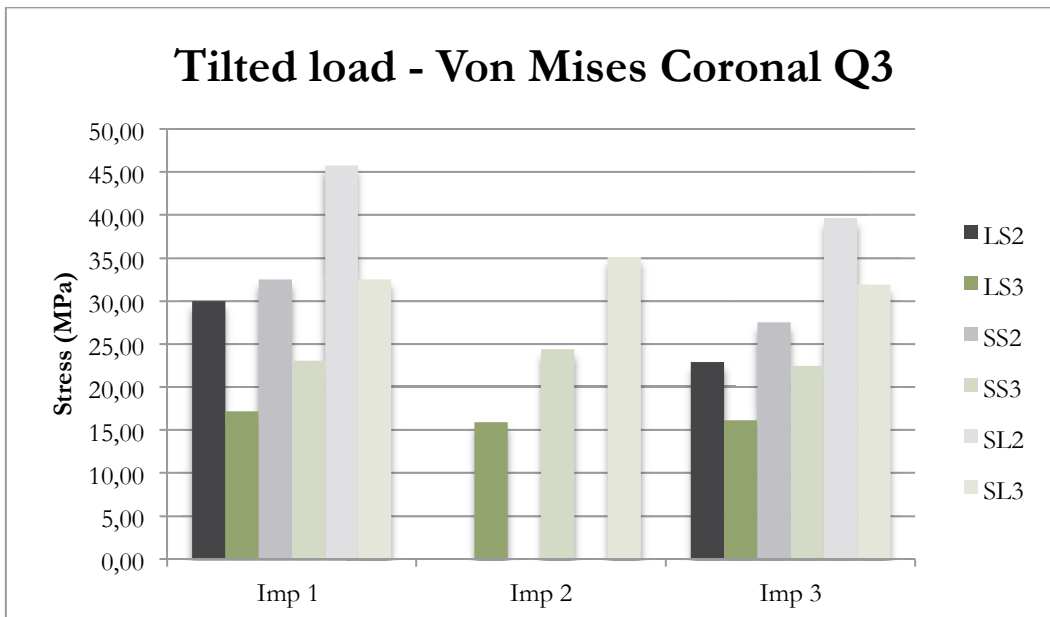


Figure 30. Graph representing the Q3 max principal stress for each implant in every configuration under tilted load.

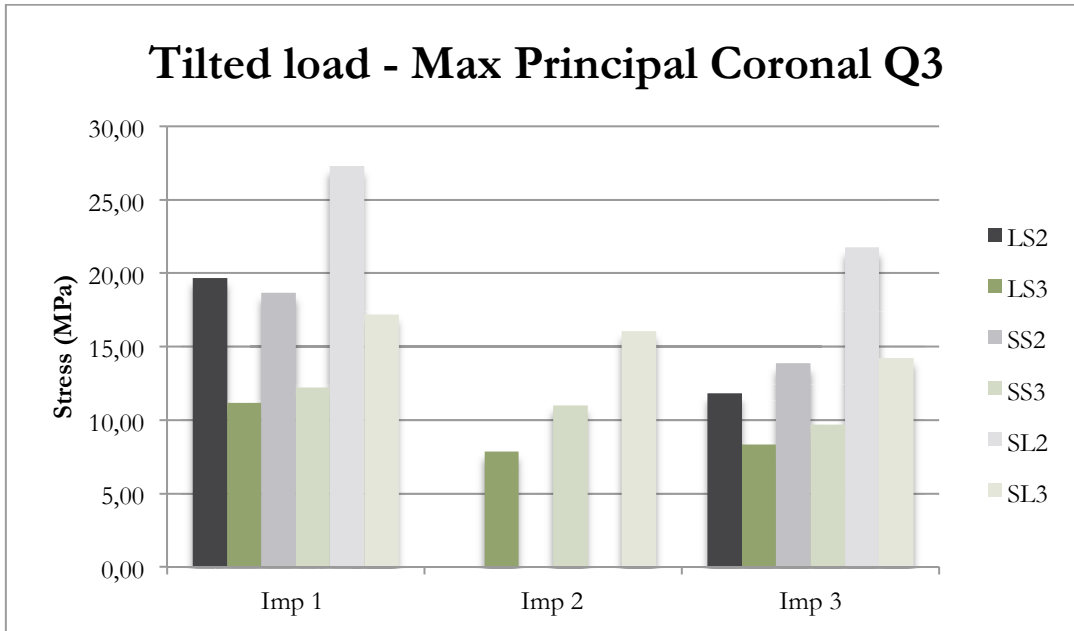
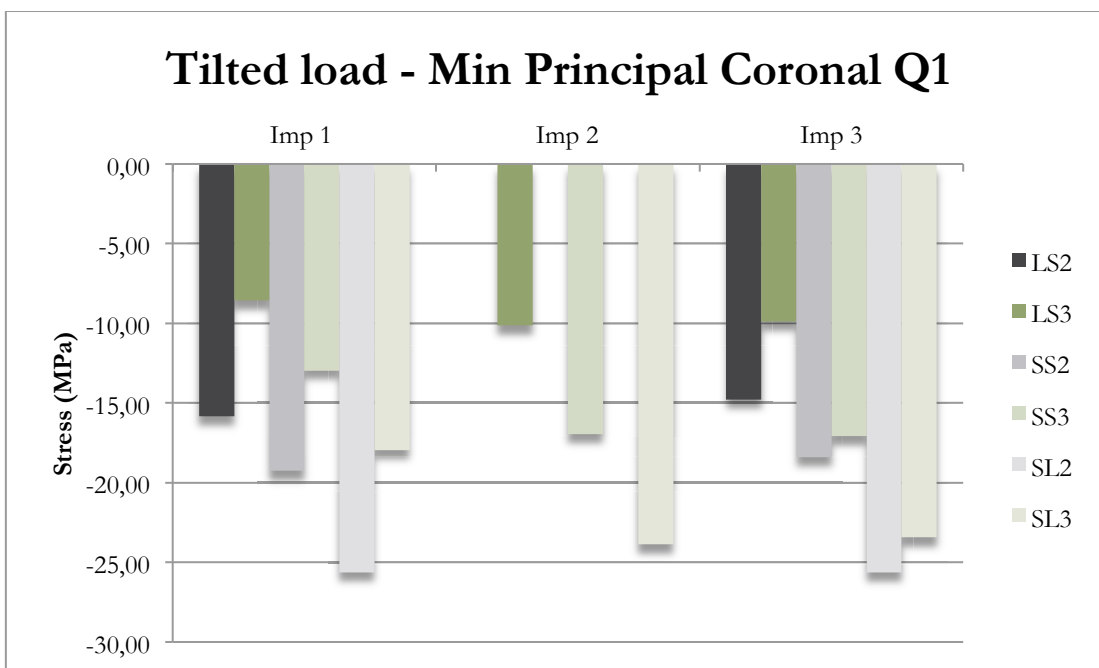


Figure 31. Graph representing the Q1 minimum stress for each implant in every configuration under tilted load.



# Chapter 8

## DISCUSSION

---

### 8.1 Effect of implant stress direction

Many literature studies (Li 2012, Desai 2012, Shigemitsu 2013) considered the jaws composed by two materials only, the cortical and cancellous bone. In the present investigation, bone was modeled in a more realistic way. Material assignment based on grey values allowed for the generation of a model with heterogeneous material properties, which could therefore prevent artifacts related to the sharp border between the cortical and the trabecular regions as suggested by recent studies. (Moeen 2014)

It is interesting that although in this study has not been made a clear distinction between cortical and cancellous bone, in most experimental situations analyzed, the load is dissipated through a large part of the cortical bone.

This is in agreement with the principles orthopedic according to which the loading forces are developed along the axis in which it has a higher density. (Wolf 1892)

That is more evident in the axial load situation, in which the stress distribution is still prevalent in the coronal part of the implants, but not in a marked way, maybe because of the cortical thickness.

However in this situation the load is well dissipated and the stress values at bone-implant level are low in all the studied configurations.

Under oblique load the stress distribution is more concentrated around the coronal part of the implant and it is several times higher than under axial load.

In particular the tension represented by the maximum principal stress is from 15 to 35 times higher.

Although the Q3 values could still be considered physiological even in the most stressed configuration revealed (SL2), lateral forces should be correctly evaluated and avoided and could lead to crestal bone resorption.

This aspect is in accordance with several other biomechanics studies.

Verri et al. (Verri 2014) outlined that lateral forces could lead to not only bone resorption but also to a higher mechanical complications rate as prosthetic screw loosening and fracture, depending on the implant and connection design.

Klindeberg et al. (Klindeberg 2012) suggested that also the occlusal design and the crown cusps inclination could enhance the lateral stress distribution and has to be evaluated.

## **8.2 Effect of implant length**

Current literature supports the validity of short dental implants as a viable option (Fugazzotto 2008; Rossi 2010; Esposito 2011; Srinivasan 2012; Lee 2014)

However some literature reviews suggest that implant surface may influence the survival rate of short implants. The stress/strain patterns differ if there is no complete osseointegration between the bone and implant and a higher stress can be observed with decrease in the percentage of osseointegration. (Chun 2002)

In almost all the research with finite-element analysis implant and bone were bonded together simulating a complete osseointegration.

Biomechanical studies showed that the occlusal forces are distributed primarily to the crestal bone and mostly in the first 4 to 6 mm. (Lum 1991, Himmlova 2004, Chang 2011)

Himmlova et al. (Himmlova 2004) observed a stress reduction of only the 7,3% from a 18 mm long implant and a 8 mm long implant.

These observations are confirmed in the present study. Even if comparing the stress distribution between regular length implants and short implants with the same crown configurations the former underwent about a 50% increase, evaluating only the tilted loading conditions the stress increase was less than 10% on average.

### **8.3 Effect of implant crown height**

Blanes in a systematic review (Blanes 2009) CI ratio did not influence the survival rates of implants but suggested that crown height itself is a potentially more critical factor because an increase in crown height might be more problematic than an equal reduction in implant length.

This observation was confirmed by several biomechanical studies (Klindeberg 2012, de Moraes 2013, Bulaqi 2015)

de Moraes et al. (de Moraes 2013) suggested that the increase in crown height enhanced stress concentration at the implant/bone tissue and increased displacement in the bone tissue, mainly under oblique loading.

Under oblique loads, the use of long crown heights not only increases the stress at the peripheral bone and implant compartments but also causes biomechanical disadvantages, thereby elevating the risk of screw loosening. The use of a suitable crown height could reduce the incidence of biologic and biomechanical complications. (Bulaqi 2015)

Those considerations were partially confirmed by the present study that revealed an average of 42% increase of stress intensity around implants under tilted load comparing the configurations with short implants and short crowns with the respective one with short implants and longer crown.

Considering than the increase of stress was only the 10% under tilted loads

among configurations with short implants respect to regular length with the crown of the same length, the increase of crown length seems to be more influent on the stress values than implant length.

Although the peri-implant bone tissue presented an increase in average stress as the crown height increased, However, the obtained stress and strain values are acceptable as physiologic values in the literature (Baggi 2008; Papavasiliou 1996; Frost 2003).

#### **8.4 Effect of implant number**

A reduction of the number of supporting implants to four implants in full arch mandibular prostheses and two implants in three unit FPDs in partial edentulous jaws resulted in the same clinical outcome as when more implants are used. (Eliasson 2008)

In the present study the use of two implants instead of three implants to support a three unit bridge resulted in a stress increase from 10% to 40% depending on the studied configuration and can be a viable option to increase the distribution of the forces occurring in the bone-implant interface, particularly with longer crown and high lateral load.

This observation is in agreement with other previous finite element studies. (Guyen 2015, Klineberg 2012, Ogawa 2010)

#### **8.5 Clinical relevance**

The use of short implants was introduced as an alternative to surgical bone augmentation procedures.

In the mandible the bone augmenting procedures proposed were vertical bone

graft (Nisand 2015), inlay bone grafting (Felice 2014), inferior alveolar nerve transposition (Bovi 2010) or guided bone regeneration (Clementini 2012).

The success rate of those techniques was comparable to the one of short length implants but the costs, timing and complication rate were much higher, and their success depend on the operators' surgical ability.

The use of dental implants up to 6 mm length was validated by recent literature (Lee 2014, Atieh 2012) with similar survival rates than standard length implants in short and medium term.

However the patients and sites conditions have to be considered. Usually short implants have to be placed in highly resorbed position resulting in higher crowns and lower CI ratio.

The clinically more relevant comparison in the present study are therefore among the configurations with standard length implants and the ones with short implants and longer crowns.

Under tilted loading the stress pattern observed stood among physiologic boundaries in all the conditions but in the SL2 configuration was conspicuously higher and potentially dangerous if the patient's loading conditions were worse than the ones considered in this study.

It was observed a similar tension stress between LS2 and SS3 configuration, while in the SL2 configuration was found to be the 60% higher, the suggesting that the use of a third short implant may be a feasible option to dissipate the load.

## **8.6 Limits of the study**

One of the limit of the study is the use of embedded elements, which may generate some numerical artifacts at the implant-bone interface creating a marked

difference between extreme stress and quartiles values. Firstly, the material defined for the host elements (the bone) is not replaced by the material defined for the embedded elements (the implant) at the same location of the integration point. Secondly, embedded elements eliminates the degree of freedom of embedded nodes and constraints them to the degrees of freedom of the host elements; this assumption causes numerical artifacts in the embedded region, due to the implant external surface shape and to the different mesh dimension.

Another limit is that the material properties were assumed to be linear, isotropic, and homogeneous and are subjected to a static occlusal loading.. However, the implants showed a small margin of simplification, approaching the real clinical situation, as in previous studies (de Faria Almeida 2014; Santiago Junior 2013; de Moraes 2013).

Despite these limitations that are common to most all finite element analysis studies, the present investigation may still be a useful tool to identify potential dangerous situations.



# Chapter 9

## CONCLUSIONS

---

This research was performed to better understand the stress entity and distribution for an implant supported three-unit bridge in the posterior mandible with different implant length and crown height.

Under axial loading the values of Von Mises stress, Maximum and Minimum principal stresses were lower than under tilted loading.

Crown height, implant number and implant length seem to be all influencing factors on implant bone stress, however the augmentation of crown height seems to have a greater effect than a reduction of implant length.

Even if the stress observed in all configurations was within a physiological range, a three-unit bridge with 13 mm long crowns supported by two implants may be biomechanically hazardous in the presence of horizontal forces, and the addition of another short implant or increase of bone volume may be suggested to dissipate the stress at bone-implant interface.

In conclusion the use of short dental implants to support a three unit bridge in the posterior mandible can be considered a potential alternative to standard length implants, but crown height and lateral forces have to be carefully analyzed in every patient.

# Chapter 10

## REFERENCES

---

### Chapter 1 - Introduction

Adell R, Eriksson B, Lekholm U, Branemark PI, Jemt T. A long-term follow-up study of osseointegrated implants in the treatment of totally edentulous jaws. *Int J Oral Maxillofac Implants* 1990; 5: 347-59.

Al-Sukhun J, Kelleway J, Helenius M: Development of a three-dimensional finite element model of a human mandible containing endosseous dental implants. I. Mathematical validation and experimental verification. *J Biomed Mater Res A* 2007, 80(1):234–246.

Annibali S, Cristalli MP, Dell’Aquila D, Bignozzi I, La Monaca G, Pilloni G. Short dental implants: a systematic review. *J Dent Res* 2012; 91: 25-32.

Bellini CM, Romeo D, Galbusera F, Taschieri S, Raimondi MT, Zampelis A, Francetti L. Comparison of tilted versus nontilted implant-supported prosthetic designs for the restoration of the edentulous mandible: a biomechanical study. *Int J Oral Maxillofac Implants* 2009; 24: 511-517.

Bellini CM, Romeo D, Galbusera F, Agliardi E, Pietrabissa R, Zampelis A, Francetti L. A finite element analysis of tilted versus nontilted implant configurations in the edentulous maxilla. *Int J Prosthodont* 2009.

Bernard JP, Szmukler-Moncler S, Pessotto S, Vazquez L, Belser UC. The anchorage of Brånemark and ITI implants of different lengths. I. An experimental study in the canine mandible. *Clin Oral Implants Res* 14:593-600. 2003

Bonnet AS, Postaire M, Lipinski P: Biomechanical study of mandible bone supporting a four-implant retained bridge: finite element analysis of the influence of bone anisotropy and foodstuff position. *Med Eng Phys* 2009, 31(7):806–815.

Blanes, R. J. To what extent does the crown- implant ratio affect the survival and complications of implant-supported reconstructions? A systematic review. *Clinical Oral Implant Research* 2009, 20, 67–72.

Chang CL, Chen CS, Huang CH, Hsu ML. Finite element analysis of the dental implant using a topology optimization method. *Med Eng Phys*. 2012 Jul 6.

Chiapasco, M., Romeo, E., Casentini, P. & Rimon- dini, L. (2004) Alveolar distraction osteogenesis vs. Vertical guided bone regeneration for the correction of

vertically deficient edentulous ridges: a 1-3-year prospective study on humans. *Clinical Oral Implants Research* 15: 82–95.

Das Neves, F. D., Fones, D., Bernardes, S. R., do Prado, C. J. & Neto, A. J. (2006) Short implants – an analysis of longitudinal studies. *The International Journal of Oral & Maxillofacial Implants* 21, 86–93.

Del Fabbro M, Rosano G, Taschieri S. Implant survival rates after maxillary sinus augmentation. *Eur J Oral Sci* 2008; 116: 497-506.

Del Fabbro M, Corbella S, Weinstein T, Ceresoli V, Taschieri S. Implant survival rates after osteotome-mediated maxillary sinus augmentation: a systematic review. *Clin Implant Dent Relat Res* 2011 Nov 14

Desai SR, Desai MS, Katti G, Karthikeyan I. Evaluation of design parameters of eight dental implant designs: A two-dimensional finite element analysis. *Niger J Clin Pract.* 2012 Apr-Jun;15(2):176-81.

Field C, Li Q, Li W, Swain M: Biomechanical Response in Mandibular Bone due to Mastication Loading on 3-Unit Fixed Partial Dentures. *J Dent Biomech* 2010, 2010:902537.

Fontana, F., Santoro, F., Maiorana, C., Iezzi, G., Piattelli, A. & Simion, M. (2008) Clinical and histologic evaluation of allogenic bone matrix versus autogenous bone chips associated with titanium-reinforced e-ptfe membrane for vertical ridge augmentation: a prospective pilot study. *The International Journal of Oral & Maxillofacial Implants* 23: 1003–1012.

Frisardi G, Barone S, Razionale A, Paoli A, Frisardi F, Tullio A, Lumbau A, Chessa G. Biomechanics of the press-fit phenomenon in dental implantology: an image-based finite element analysis. *Head Face Med.* 2012 May 29;8(1):18.

Furuyama C, Takaba M, Inukai M, Mulligan R, Igarashi Y, Baba K. Oral health-related quality of life in patients treated by implant-supported fixed dentures and removable partial dentures. *Clin Oral Implants Res.* 2012 Aug;23(8):958-62.

Glantz, P. O. & Nilner, K. Biomechanical aspects of prosthetic implant-borne reconstructions. *Periodontology* 2000 1998, 17, 119–124.

Guan H, van Staden R, Loo YC, Johnson N, Ivanovski S, Meredith N. Influence of bone and dental implant parameters on stress distribution in the mandible: a finite element study. *Int J Oral Maxillofac Implants* 2009; 24: 866-76.

Haas, R., Mensdorff-Pouilly, N., Mailath, G. & Watzek, G. Branemark single tooth implants: A preliminary report of 76 implants. *The Journal of Prosthetic Dentistry* 1995 73, 274–279.

Jemt T, Lekholm U. Oral implant treatment in posterior partially edentulous jaws: a 5-year follow-up report. *Int J Oral Maxillofac Implants* 1993; 8: 635-40.

Katranji A, Fotek P, Wang HL. Sinus augmentation complications: etiology and treatment. *Implant Dent* 2008; 17: 339-49.

Lai HC, Si MS, Zhuang LF, Shen H, Liu YL, Wismeijer D. Long-term outcomes of short dental implants supporting single crowns in posterior region: a clinical retrospective study of 5-10 years. *Clin Oral Implants Res*. 2012 Apr 2.

Lee, J. H., Frias, V., Lee, K. W. & Wright, R. F. Effect of implant size and shape on implant success rates: a literature review. *The Journal of Prosthetic Dentistry* 2005 94, 377–381.

Lekholm, U. & Zarb, G. A. Patient selection and preparation. In: Branemark, P. I., Zarb, G. A. & Albrektsson, T. (eds). *Tissue-Integrated Prostheses: Osseointegration in Clinical Dentistry* 1985, 1st edition, pp. 199–209. Chicago: Quintessence Publishing.

Li T, Yang X, Zhang D, Zhou H, Shao J, Ding Y, Kong L. Analysis of the biomechanical feasibility of a wide implant in moderately atrophic maxillary sinus region with finite element method. *Oral Surg Oral Med Oral Pathol Oral Radiol*. 2012 Aug;114(2):e1-8.

Lum LB. A biomechanical rationale for the use of short implants. *J Oral Implantol* 17:126-131. 1991

Mellal A, Wiskott HW, Botsis J, Scherrer SS, Belser UC. Stimulating effect of implant loading on surrounding bone. Comparison of three numerical models and validation by in vivo data. *Clin Oral Implants Res* 2004;15:239-48.

Merli, M., Migani, M. & Esposito, M. (2007) Vertical ridge augmentation with autogenous bone grafts: resorbable barriers supported by osteosynthesis plates versus titanium-reinforced barriers. A preliminary report of a blinded, randomized controlled clinical trial. *The International Journal of Oral & Maxillofacial Implants* 22: 373–382.

Misch CE, Suzuki JB, Misch-Dietsh FM, Bidez MW. A positive correlation between occlusal trauma and peri-implant bone loss: literature support. *Implant Dent* 2005; 14: 208-16.

Muhlberger G, Svejda M, Lottersberger C, Emshoff R, Putz R, Kuhn V: Mineralization density and apparent density in mandibular condyle bone. *Oral Surg Oral Med Oral Pathol Oral Radiol Endod* 2009, 107(4):573–579.

Park JK, Choi JU, Jeon YC, Choi KS, Jeong CM: Effects of abutment screw coating on implant preload. *J Prosthodont* 2010, 19(6):458–464.

Petrie Cs, Williams JL. Comparative evaluation of implant designs: influence of diameter, length, and taper on strains in the alveolar crest. A three-dimensional finite-element analysis. *Clin Oral Implants Res* 2005; 16: 486-94.

Petricovic N, Celebic A, Renner-Sitar K. A 3-year longitudinal study of quality-of-life outcomes of elderly patients with implant- and tooth-supported fixed partial dentures in posterior dental regions. *Gerodontology*. 2012 Jun;29(2):e956-63.

Pieri F, Aldini NN, Fini M, Marchetti C, Corinaldesi G. Preliminary 2-year report on treatment outcomes for 6-mm-long implants in posterior atrophic mandibles. *Int J Prosthodont*. 2012 May-Jun;25(3):279-89.

Pierrisnard L, Renouard F, Renault P, Barquins M. Influence of implant length and bicortical anchorage on implant stress distribution. *Clin Implant Dent Relat Res* 2003; 5: 254-62.

Pjetursson, B.E., Tan, W.C., Zwahlen, M. & Lang, N.P. (2008) A systematic review of the success of sinus floor elevation and survival of implants inserted in combination with sinus floor elevation. Part I: lateral approach. *Journal of Clinical Periodontology* 35(Suppl): 216–240.

Pommer B, Frantal S, Willer J, Posch M, Watzek G, Tepper G. Impact of dental implant length on early failure rates: a meta-analysis of observational studies. *J Clin Periodontol* 2011; 38: 856-63.

Rangert, B. R., Sullivan, R. M. & Jemt, T. M.. Load factor control for implants in the posterior partially edentulous segment. *The International Journal of Oral and Maxillofacial Implants* 1997, 12, 360–370.

Romeo, E., Bivio, A., Mosca, D., Scanferla, M., Ghisolfi, M. & Storelli, S. The use of short dental implants in clinical practice: literature review. *Minerva Stomatologica* 2010 59, 23–31.

Shigemitsu R, Ogawa T, Matsumoto T, Yoda N, Gunji Y, Yamakawa Y, Ikeda K, Sasaki K. Stress distribution in the peri-implant bone with splinted and non-splinted implants by in vivo loading data-based finite element analysis. *Odontology*. 2012 Jun 29.

Sun HL, Huang C, Wu YR, Shi B. Failure rates of short (<=10 mm) dental implants and factors influencing their failure: a systematic review. *Inj J Oral Maxillofac Implants* 2011; 26: 816-25.

Tawil, G. & Younan, R. (2003) Clinical evaluation of short, machined-surface implants followed for 12 to 92 months. *The International Journal of Oral & Maxillofacial Implants* 18, 894–901.

Telleman G, Raghoobar GM, Vissink A, den Hartog L, Huddleston Slater JJ, Meijer HJ. A systematic review of the prognosis of short (<10 mm) dental implants placed in the partially edentulous patient. *J Clin Periodontol*. 2011 Jul;38(7):667-76.

Ulm C, Kneissel M, Schedle A, Solar P, Matejka M, Schneider B, Donath K. Characteristic features of trabecular bone in edentulous maxillae. *Clin Oral Implants Res*. 1999 Dec;10(6):459-67.

Ulm C, Tepper G, Blahout R, Rausch-Fan X, Hienz S, Matejka M. Characteristic features of trabecular bone in edentulous mandibles. *Clin Oral Implants Res*. 2009 Jun;20(6):594-600.

## Chapter 2 - Biomechanics

Abdel-Latif HH, hobkirk JA, Kelleway JP. Functional mandibular deformation in edentulous subjects treated with dental implants, *Int J Prosthodont* 13:513-519, 2000.

Adell R, Lekholm U, RÖckler B et al. A 15 years study of osseointegrated implants in the treatment of edentulous jaw, *Int J Oral Surg* 10:387-416, 1981.

Adell R, Lekholm U, Rockler B et al. Marginal tissue reactions at osseointegrated titanium fixtures (1). A 3-year longitudinal prospective study, *Int J Oral Maxillofac Surg* 15:39-52, 1986.

Aglietta M, Siciliano VI, Zwahlen M, Brägger U, Pjetursson BE, Lang NP, Salvi GE. A systematic review of the survival and complication rates of implant supported fixed dental prostheses with cantilever extensions after an observation period of at least 5 years. *Clin Oral Implants Res*. 2009 May;20(5):441-51.

Albrektsson T, Zarb GA, Worthington P et al. The longterm efficacy of currently used dental implants: a review and proposed criteria of success, *Int J Oral Maxillofac Implants* 1:11.25, 1986.

Alderman MM. Disorders of the temporomandibular joint and related structures. In Burket LW, editor: *Oral medicine*, ed 6, Philadelphia, 1971, JB Lippincott.

Atkinson SR. Balance-the magic word. *Am J Orthod* 1964;50:189-202

Atwood DA, COy WA. Clinical cephalometric and densitometric study of reduction of residual ridges, *J Prosthet Dent* 26:280-295, 1971.

Baragar FA, Osborn JW (1984). A model relating patterns of human jaw movement to biomechanical constraints. *J Biomechan* 17:757-767.

Bidez MW, CE. Force transfer in implant dentistry: basic concepts and principles, *J Oral Implantol* 18:264-274, 1992.

Bidez MW, Misch CE. Issues in bone mechanics related to oral implants, *Implant Dent* 1:289-294, 1992.

Blanes, R.J., Bernard, J.P., Blanes, Z.M. & Belser. A 10-year prospective study of ITI dental implants placed in the posterior region. II: influence of the crown-to-implant ratio and different prosthetic treatment modalities on crestal bone loss. *Clinical Oral Implants Research* 2007 18: 707–714.

Boggan S, Strong Jt, Misch CE et al. Influence of Hex geometry and prosthetic table width on static and fatigue strength of dental implants, *J Prosthet Dent* 82:436-440, 1999.

Braun S, Bantleon HP, Hnat WP et al. A study of bite force. Part I: relationship to various physical characteristics, *Angle Orthod* 65:367-372, 1995.

Brunski JB, Moccia AF Jr., Pollack SR et al. The influence of functional use of endosseous implants on the tissue implant interface. II. Clinical aspects, *J Dent Res*: 58:1970-1980, 1979.

Brunski JB. Biomechanical factors affecting the bone-dental implant interface. *Clin Mater*. 1992;10(3):153-201.

Burger EH, Klein-Nulend J. Mechanotransduction in bone – role of the lacuno-canalicular network, *FASEB J* 13:S101-S112, 1999.

Carr AB, Laney WR. Maximum occlusal forces in patients with osseointegrated oral implant prostheses and patients with complete dentures, *Int J Oral Maxillofac Impl* 2:101-108, 1987.

Chung DM, Oh Tj, Shotwell B et al. Significance of keratinized mucosa in maintenance of dental implants with different surface conditions [master's thesis], Ann Arbor, Mich, 2005, University of Michigan.

Cowin SC, Hegedus DH. Bone remodeling I: theory of adaptative elasticity, *J Elast* 6:313-326, 1976.

Cowin SC, Hegedus DH. Bone remodeling II: small strain adaptive elasticity, *J Elast* 6:337-352, 1976.

Cowin SC, Moss-Salentijn L, Moss ML. Candidates for the mechanosensory system in bone, *J Biomech Eng* 113:191-197, 1991.

Cowin SC, Nachlinger RR. Bone remodeling II: uniqueness and stability in adaptative elasticity theory, *J Elast* 8:285-295, 1978.

Creugers NH, Kayser HF, Van't Hof MA. A meta analysis of durability data on conventional fixed bridges, *Community Dent Oral Epidemiol* 22:448-452, 1994.

Currey JD. Effects of differences in mineralization on the mechanical properties of bone, *Philos Trans R Soc Lond B Biol Sci* 1121:509-518, 1984.

Dawson PE. Differential diagnosis and treatment of occlusal problems, ed 2, St Louis, 1989, Mosby.

De Marco TJ, Paine D. Mandibular dimensional change, *J Prosthet Dent* 31:482-485, 1974.

Dechow PC, Hylander WL. Elastic properties and masticatory bone stress in the macaque mandible, *Am J Phys Anthropol* 112:553-574, 2000.

Duncan RL, Turner CH. Mechanotransduction and the functional response of bone to mechanical strain, *Calcif Tissue Int* 57:344-358, 1995.

Duyck J, Rønold HJ, Van Oosterwyck H, Naert I, Van der Sloten J, Ellingsen JE. The influence of static and dynamic loading on marginal bone reactions around osseointegrated implants: An animal experimental study. *Clin Oral Implants Res* 2001;12: 207–218.

Enlow DH. Principles of bone remodeling: an account of post-natal growth and remodeling processes in long bones and the mandible, Springfield, Ill, 1963, Thomas.

Fischman B. The rotational aspect of mandibular flexure, *J Prosthet Dent* 64:483-485, 1974.

Fontijn-Tekamp FA, MSLageter AP, van't Hof MA et al. Bite forces with mandibular implant-retained overdentures, *J Dent Res* 77:1832-1839, 1998.

Frost HM. Mechanical adaptation, Frost's mechanostat theory. In Martin RB, Burr DB, editors: *Structure, function, and adaptation of compact bone*, New York, 1989, Raven Press.

Frost HM. Skeletal structural adaptations to mechanical usage (SATMU): 1. Redefining Wolff's law: the bone modeling problem. *Anat Rec.* 1990 Apr;226(4):403-13.

Garretto LP, Chen J, Parr JA et al. Remodeling dynamics of bone supporting rigidly fixed titanium implants. A histomorphometric comparison in four species including human, *Implant Dent* 4:235-243, 1995.

Glass EG, McGlynn FD, Glaros AG, Melton K, Romans K. Prevalence of temporomandibular disorder symptoms in a major metropolitan area. *Cranio.* 1993 Jul;11(3):217-20.

Goodacre CJ, Bernal G, Rungcharassaeng K. Clinical complications with implants and implant prostheses, *J Prosthet Dent* 90:121-132, 2003.

Graf H. Bruxism, *Dent Clin North Am* 13:659-665. 1969.

Grant AA. Some aspects of mandibular movement: acceleration and horizontal distortion, *Ann Acad Med Singapore* 15:305-310, 1986.

Gunne J, Jemt T, Linden B. Implant treatment in partially edentulous patients: a report on prostheses after 3 years, *Int J Prosthodont* 7:143-148, 1994.

Hannam AG, Stavness I, Lloyd JE, Fels S. A dynamic model of jaw and hyoid biomechanics during chewing. *J Biomech.* 2008;41(5):1069-76.

Hart RT, Hennebel VV, Thongpreda N, Van Buskirk WC, Anderson RC. Modeling the biomechanics of the mandible: a three-dimensional finite element study. *J Biomech.* 1992 Mar;25(3):261-86.

Heits-Mayfield LJ, Schmid B, Weigel C et al. Does excessive occlusal load affect osseointegration? An experimental study in the dog, *Clin Oral Impl Res* 15:259-268, 2004.

Herring SW. Masticatory muscles and the skull. a comparative perspective. *Arch Oral Biol.* 2007 Apr;52(4):296-9. Epub 2006 Nov 7

Hylander WL. Stress and strain in the mandibular symphysis of primates: a test of competing hypotheses, *Am J Phys Anthropol* 64: 1-46, 1984.

Hylander WL. The human mandible: lever or link?, *Am J Phys Anthropol* 43:227-242, 1975.

Ingebretsen M. Out of this world workouts, *World Traveler* Feb:10-14, 1997.



Isidor F. Histological evaluation of peri-implant bone at implant subjected to occlusal overload or plaque accumulation, *Clin Oral Implant Res* 8:1-9, 1997.

Isidor F. Loss of osseointegration caused by occlusal load of oral implants: a clinical and radiographic study in monkeys, *Clin Oral Implants Res* 7:143-152, 1996.

Jividen G, Misch CE. Reverse torque testing and early loading failures-help or hindrance, *J Oral Implantology* 26:82-90, 2000.

Kallus T, Bessing C. Loose gold screws frequently occur in full-arch fixed prostheses supported by osseointegrated implants after 5 years, *Int J Oral Maxillofac Implants* 9:169-178, 1991.

Karolyi M. Beobachtungen über Pyorrhoea alveolaris, *Osterenorichisch-Ungarische viertel jahresschrift fur Zahnheilkunde* 17:279, 1991.

Kazarian LE, Von Gierke HE. Bone loss as a result of immobilization and chelation: preliminary results in *Macaca mulatta*, *Chin Orthop Relat Res* 65:67-75, 1969.

Kilamura E, Slegaroui R, Nomura S, et al. Biomechanical aspects of marginal bone resorption around osseointegrated implants: consideration based in a three dimensional finite element analysis. *Clin Oral Implant Res*. 2004;15:401-412.

Klemetti E, Vaino P, Lassila V et al. Trabecular bone mineral density and alveolar height in postmenopausal women, *Scand J Dent Res* 101:166-170, 1993.

Koç D, Dogan A, Bek B. Effect of gender, facial dimensions, body mass index and type of functional occlusion on bite force. *J Appl Oral Sci*. 2011 Jun;19(3):274-9.

Koolstra, J.H., 2002. Dynamics of the human masticatory system. *Critical Reviews in Oral Biology and Medicine* 13, 366–376.

Koolstra, J.H., van Eijden, T.M.G.J., 1995. Biomechanical analysis of jaw closing movements. *Journal of Dental Research* 74, 1564–1570.

Kulmann C. *Die graphische statik* 1, Aufl, Zurich, 1888, Meyer and Zeller.

Lang NP, Wilson TG, Corbet EF. Biological complications with dental implants: their prevention, diagnosis and treatment, *Clin Oral Implants Res* 11(Suppl):146-155, 2000.

Lavelle CLB. Biomechanical considerations of prosthodontic therapy: the urgency of research into alveolar bone responses, *Int J Oral Maxillofac Implants* 8:179-184, 1993.

Lavigne GJ, Montplaisir JY. Restless legs syndrome and sleep bruxism. prevalence and association among Canadians. *Sleep*. 1994 Dec;17(8):739-43.

Lekholm U, Adell R, Lindhe J et al. Marginal tissue reactions at osseointegrated titanium fixtures. II. A cross sectional retrospective study, *Int J Oral Maxillofac Surg* 15:53-61, 1986.

MacMillan HA,. Stuctural characteristic of the alveolar process, *Int J Ortho* 12:711-730, 1926.

Mansour RM, Reynik RJ, Larson PC. In vivo occlusal forces and moments: forces measured in terminal hinge position and associated moments, *J Dent Res* 56:114-120, 1975.

McAlarney ME, Stavropoulos DN. Determination of cantilever length-anterior-posterior spread ratio assuming failure criteria to be the compromise of the prosthesis retaining screw-prosthesis joint. *Int J Oral Maxillofac Implants*. 1996 May-Jun;11(3):331-9.

Meier GH. Die architektur der spongiosa, *Arch Anat Physiol Wess Med* 34:615-628, 1887.

Mercier P, Inoue S. Bone density and serum minerals in cases of residual alveolar ridge atrophy, *J Prosthet Dent* 46:250-255, 1981.

Minaire MC, Neunier P, Edouard C et al. Quantitative histological data on disuse osteoporosis: comparison with biological data, *Calcif Tissue Res* 17:57-73, 1974.

Misch CE, Palattella A. Bruxism and its effect on treatment plans, *Int Mag Oral Implant* 2:6-18, 2002.

Misch CE, Suzuki JB, Misch-Dietsh FM, Bidez MW. A positive correlation between occlusal trauma and peri-implant bone loss: literature support. *Implant Dent*. 2005 Jun;14(2):108-16.

Misch CE. Cantilever length and its relationship to biomechanical stress, In *Misch Implant Institute Manual*, Misch International Implant Institute, Mich, 1990, Dearborn.

Misch CE. Clenching and its effects on implant treatment plans, *Oral Health* 92:11-24, 2002.

Misch CE. Early crestal bone loss etiology and its effect on treatment planning for implants *Dental Learning System Co, Inc, Postgrad Dent* 2.3-17, 1995.

Miyamoto Y, Fujisawa K, Takechi M et al. Effect of the additional installation of implants in the posterior region on the prognosis of treatment in the edentulous mandibular jaw, *Clin Oral Implants Res* 14:727-733, 2003.

Mori S, Burr DB. Increased intracortical remodeling following fatigue damage, *Bone* 14:103-109, 1993.

Morneburg TR, Proschel PA. Measurement of masticatory forces and implant loads: a methodologic clinical study, *Int J Prosthodont* 15:20-27, 2002.

Murry PDF. *Bones: a study of development and structure of the vertebral skeleton*, Cambridge, 1936, Cambridge University Press.

Natali AN, Pavan PG, Ruggero AL. Analysis of bone-implant interaction phenomena by using a numerical approach. *Clin Oral Implants Res* 2006;17:67-74.

National Institutes of Health Consensus Development Conference Statement on Dental Implants, *J Dent Educ* 52:824-827, 13-15., June 1988

Oganov VS. Modern analyses of bone loss mechanisms in microgravity, *J Gravit Physiol* 11:143-146, 2004.

Oh T-J, Yoon J, Misch CE et al. The cause of early implant bone loss: myth or science?, *J Periodontol* 73:322-333, 2002.

Orban B. *Oral histology and embryology*, ed 3, St Louis, 1953, Mosby.

Parfitt AM. Investigation of the normal variations in the alveolar bone trabeculation, *Oral Surg Oral Med Pathol* 15: 1453-1463, 1962.

Peterson J, Wang Q, Dechow PC. Material properties of the dentate maxilla, *Anat Rec A Discov Mol Cell Evol Biol* 288:962-972, 2006.

Picton DC, Johns RB, Wills DJ et al. The relationship between the mechanisms of tooth and implant support, *Oral Sci Rev* 5:3-22, 1971.

Picton DC. The effect of external forces on the periodontium. In Melcher AH, Bowen WH, editors: *Biology of the periodontium*, London, 1969, Academic Press.

Proffit WR. The facial musculature in its relation to the dental occlusion. In Carlson DS, McNamara JA, editors: *Muscle adaptation in the craniofacial region. Proceedings of symposium, Craniofacial Growth Series, Monograph 8*, Ann Arbor, Mich, 1978, University of Michigan.

Raadsheer MC, van Eijden TM, van Ginkel FC et al. Contribution of jaw muscle size and craniofacial morphology to human bite force magnitude, *J Dent Res* 87:31-42, 1999.

Reilly DT, Burstein AH. The elastic and ultimate properties of compact bone tissue, *J Biomech* 8:393, 1975.

Rhineland FW. The normal circulation of bone and its response to surgical intervention, *J Biomed Mater Res* 8:87-90, 1974.

Roberts EW, Turley PK, Brezniak N et al. Bone physiology and metabolism, *J Calif Dent Assoc* 15:54-61, 1987.

Roberts WE, Smith RK, Ziberman Y et al. Osseous adaptation to continuous loading of rigid endosseous implants, *Am J Orthod*, 86:96-111, 1984.

Rodriguez AM, Aquilino SA, Lund PS. Cantilever and implant biomechanics: a review of the literature. Part 1. *J Prosthodont* 1994; 3(1): 41-6.

Rodriguez AM, Aquilino SA, Lund PS. Cantilever and implant biomechanics: a review of the literature, Part 2. *J Prosthodont* 1994; 3(2): 114-8.

Rosenberg ES, Torosian JP, Slots J. Microbial differences in 2 clinically distinct types of failures of osseointegrated implants, *Clin Oral Implants Res* 2:135-144, 1991.

Schwartz-Dabney CL, Dechow PC. Variations in cortical material properties throughout the human dentate mandible, *Am J Phys Anthropol* 120:252-277, 2003.

Scott J, Ash MM Jr. A six-channel intra-oral transmitter for measuring occlusal forces, *J Prosthet Dent* 16:56, 1966.

Simmons DJ, Russell JE, Winter F. Space flight and the non-weight bearing bones of the rat skeleton, *Trans Orthop Res Soc* 4:65, 1981.

Snauwaert K, Duyck J, van Steenberghe D et al. Time dependent failure rate and marginal bone loss of implant supported prostheses: a 15-year follow up study, *Clin Oral Invest* 4:13-20, 2000.

Tonetti MS, Schmid J. Pathogenesis of implant failures, *Periodontology* 2000 4:127-138, 1994.

Turner CH, Pavalko FM. Mechanotransduction and the functional response of the skeleton to physical stress: the mechanism and mechanics of bone adaptation, *J Orthop Sci* 3:346-355, 1988.

Turner CH. Three rules for bone adaptation to mechanical stimuli, *Bone* 23:399-407, 1998.

Uthoff HK, Jaworski ZF. Bone loss in response to longterm immobilization, *J Bone Joint Surg Br* 60-B:420-429, 1978.

Ulm C, Kneissel M, Schedle A, Solar P, Matejka M, Schneider B, Donath K. Characteristic features of trabecular bone in edentulous maxillae. *Clin Oral Implants Res.* 1999 Dec;10(6):459-67.

Ulm C, Tepper G, Blahout R, Rausch-Fan X, Hienz S, Matejka M. Characteristic features of trabecular bone in edentulous mandibles. *Clin Oral Implants Res.* 2009 Jun;20(6):594-600.

Van Steenberghe D, Tricio J, Van den Eynde E et al. Soft and hard tissue reactions towards implant design and surface characteristics and the influence of plaque and/or occlusal loads. In Davidovitch Z (ed.) *The biological mechanism of tooth eruption, resorption and replacement by implants*, Boston, 1994, Harvard Society for the advancement of Orthodontics.

Vezeridis PS, Semeins CM, Chen Q et al. Osteocytes subjected to pulsating fluid flow regulate osteoblast proliferation and differentiation, *Biochem Biophys Res Commun* 348:1082-1088, 2006.

Westbroek I, Ajubi NE, Alblas MJ et al. differential stimulation of prostaglandin G/H synthase-2 in osteocytes and other osteogenic cells by pulsating fluid flow, *Biochem Biophys Res Commun* 268:414-419, 2000.

Wolf J. *Das Gesetz der Transformation der Knochen*, Berlin, 1892, A Hirshwald.

Zarone F, Apicell A, Nicolais L et al. Mandibular flexure and stress build up in mandibular full-arch fixed prostheses supported by osseointegrated implants, *Clin Oral Implants Res* 14:103-114, 2003.

Zurdo J, Romão C, Wennström JL. Survival and complication rates of implant-supported fixed partial dentures with cantilevers: a systematic review. *Clin Oral Implants Res.* 2009 Sep;20 Suppl 4:59-66.



## Chapter 3 - Finite element analysis

Alper Gultekin, Pinar Gultekin and Serdar Yalcin. Application of Finite Element Analysis in Implant Dentistry. Intech.24-54

Arisan V, Karabuda ZC, Avsever H, Özdemir T. Conventional multi-slice computed tomography (CT) and cone-beam CT (CBCT) for computer-assisted implant placement. Part I: relationship of radiographic gray density and implant stability. Clin Implant Dent Relat Res. 2013 Dec;15(6):893-906.

Assunção WG, Barão VA, Tabata LF, Gomes EA, Delben JA, dos Santos PH. Biomechanics studies in dentistry: bioengineering applied in oral implantology. J Craniofac Surg. 2009 Jul;20(4):1173-7.

Bayraktar M, Gultekin BA, Yalcin S, Mijiritsky E. Effect of crown to implant ratio and implant dimensions on periimplant stress of splinted implant-supported crowns: a finite element analysis. Implant Dent. 2013 Aug;22(4):406-13.

Bellini CM, Romeo D, Galbusera F, Taschieri S, Raimondi MT, Zampelis A, Francetti L. Comparison of tilted versus nontilted implant-supported prosthetic designs for the restoration of the edentulous mandible: a biomechanical study. Int J Oral Maxillofac Implants 2009; 24: 511-517

Cahoon P, Hannam AG. Interactive modeling environment for craniofacial reconstruction. Visual data exploration and analysis. SPIE Proc. 1994; 2178:206-15.

Cehreli M, Duyck J, De Cooman M, Puers R, Naert I. Implant design and interface force transfer. A photoelastic and strain-gauge analysis. Clin Oral Implants Res. 2004 Apr;15(2):249-57.

Choi AH, Conway RC, Ben-Nissan B. Finite-element modeling and analysis in nanomedicine and dentistry. Nanomedicine (Lond). 2014 Aug;9(11):1681-95.

Doblare M, Garcia JM, Gomez MJ. Modelling bone tissue fracture and healing: a review. Eng Fract Mech. 2004;71:1809e1840.

Francetti L, Cavalli N, Villa T, La Barbera L, Taschieri S, Corbella S, Del Fabbro M. Biomechanical in vitro evaluation of two full-arch rehabilitations supported by four or five implants. Int J Oral Maxillofac Implants. 2015 Mar-Apr;30(2):419-26.

Galli C, Guizzardi S, Passeri G, Martini D, Tinti A, Mauro G, Macaluso GM.

Comparison of human mandibular osteoblasts grown on two commercially available titanium implant surfaces. *J Periodontol.* 2005 Mar;76(3):364-72.

Geng JP, Tan KB, Liu GR. Application of finite element analysis in implant dentistry: a review of the literature. *J Prosthet Dent.* 2001 Jun;85(6):585-98

Geng JP, Ma QS, Xu W, Tan KB, Liu GR. Finite element analysis of four thread-form configurations in a stepped screw implant. *J Oral Rehabil.* 2004 Mar;31(3):233-9.

Haraldson T. A photoelastic study of some biomechanical factors affecting the anchorage of osseointegrated implants in the jaw. *Scand J Plast Reconstr Surg.* 1980;14(3):209-14.

Lee WH, Kim TS. Methods for high-resolution anisotropic finite element modeling of the human head: automatic MR white matter anisotropy-adaptive mesh generation. *Med Eng Phys.* 2012 Jan;34(1):85-98.

Meriç G, Erkmen E, Kurt A, Eser A, Ozden AU. Biomechanical comparison of two different collar structured implants supporting 3-unit fixed partial denture: a 3-D FEM study. *Acta Odontol Scand.* 2012 Jan;70(1):61-71.

Moeen F , Nisar S, Nimra D A step by step guide to finite element analysis in dental implantology. *Pakistan Oral & Dental Journal.* 2014; 34 (1): 164-169

Pellizzer EP, de Mello CC, Santiago Junior JF, de Souza Batista VE, de Faria Almeida DA, Verri FR. Analysis of the biomechanical behavior of short implants: The photo-elasticity method. *Mater Sci Eng C Mater Biol Appl.* 2015 Oct 1;55:187-92.

Pesqueira AA, Goiato MC, Filho HG, Monteiro DR, Santos DM, Haddad MF, Pellizzer EP. Use of stress analysis methods to evaluate the biomechanics of oral rehabilitation with implants. *J Oral Implantol.* 2014 Apr;40(2):217-28.

Romeed SA, Fok SL, Wilson NH. A comparison of 2D and 3D finite element analysis of a restored tooth. *J Oral Rehabil.* 2006 Mar;33(3):209-15.

Sagat G, Yalcin S, Gultekin BA, Mijiritsky E. Influence of arch shape and implant position on stress distribution around implants supporting fixed full-arch prosthesis in edentulous maxilla. *Implant Dent.* 2010 Dec;19(6):498-508.

Sevimay M, Turhan F, Kiliçarslan MA, Eskitascioglu G. Three-dimensional finite element analysis of the effect of different bone quality on stress distribution in an implant-supported crown. *J Prosthet Dent.* 2005 Mar;93(3):227-34.

Suedam V, Souza EA, Moura MS, Jacques LB, Rubo JH. Effect of abutment's height and framework alloy on the load distribution of mandibular cantilevered implant supported prosthesis. *Clin Oral implant Res* 2009;20:196-200.

Trivedi S. Finite element analysis: A boon to dentistry. *J Oral Biol Craniofac Res.* 2014 Sep-Dec;4(3):200-3.

Turkyilmaz I, Ozan O, Yilmaz B, Ersoy AE. Determination of bone quality of 372 implant recipient sites using Hounsfield unit from computerized tomography: a clinical study. *Clin Implant Dent Relat Res.* 2008 Dec;10(4):238-44.

Weinstein AM, Klawitter JJ, Anand SC, Schuessler R. Stress analysis of porous rooted dental implants. *J Dent Res*. 1976 Sep-Oct;55(5):772-7.

Wennerberg A, Albrektsson T, Andersson B. Bone tissue response to commercially pure titanium implants blasted with fine and coarse particles of aluminum oxide. *Int J Oral Maxillofac Implants*. 1996 Jan-Feb;11(1):38-45.



## Chapter 4 - Short implants

Al-Marshood MM, Junker R, Al-Rasheed A, Al Farraj Aldosari A, Jansen JA, Anil S. Study of the osseointegration of dental implants placed with an adapted surgical technique. *Clin Oral Implants Res.* 2011 Jul;22(7):753-9.

Ante IH. The fundamental principles of abutments. *Michigan State Dental Society Bulletin* 1926;8:14-23

Atieh MA, Zadeh H, Stanford CM, Cooper LF. Survival of short dental implants for treatment of posterior partial edentulism: a systematic review. *Int J Oral Maxillofac Implants.* 2012 Nov-Dec;27(6):1323-31.

Attard NJ, Zarb GA. Implant prosthodontic management of partially edentulous patients missing posterior teeth: the Toronto experience. *J Prosthet Dent.* 2003 Apr;89(4):352-9.

Baggi L, Cappelloni I, Di Girolamo M, Maceri F, Vairo G. The influence of implant diameter and length on stress distribution of osseointegrated implants related to crestal bone geometry: a three-dimensional finite element analysis. *J Prosthet Dent.* 2008 Dec;100(6):422-31.

Bahat O. Brånemark system implants in the posterior maxilla: clinical study of 660 implants followed for 5 to 12 years. *Int J Oral Maxillofac Implants.* 2000 Sep-Oct;15(5):646-53.

Balshe AA, Assad DA, Eckert SE, Koka S, Weaver AL. A retrospective study of the survival of smooth- and rough-surface dental implants. *Int J Oral Maxillofac Implants.* 2009 Nov-Dec;24(6):1113-8.

Barone and Bianchi, *Manuale di Chirurgia Orale*, 724-726. 2013, Elsevier Ed

Blanes, R. J. To what extent does the crown- implant ratio affect the survival and complications of implant-supported reconstructions? A systematic review. *Clinical Oral Implant Research* 2009, 20, 67–72.

Cawood JI, Howell RA. A classification of the edentulous jaws. *Int J Oral Maxillofac Surg.* 1988 Aug;17(4):232-6.

Deporter D. Short dental implants: what works and what doesn't? A literature interpretation. *Int J Periodontics Restorative Dent.* 2013 Jul-Aug;33(4):457-64.

Friberg B, Jemt T, Lekholm U. Early failures in 4,641 consecutively placed Brånemark dental implants: a study from stage 1 surgery to the connection of completed prostheses. *Int J Oral Maxillofac Implants.* 1991 Summer;6(2):142-6.

Fugazzotto PA, Beagle JR, Ganeles J, Jaffin R, Vlassis J, Kumar A. Success and

failure rates of 9 mm or shorter implants in the replacement of missing maxillary molars when restored with individual crowns: preliminary results 0 to 84 months in function. A retrospective study. *J Periodontol.* 2004 Feb;75(2):327-32.

Hassani A, Saadat S, Moshiri R, Shahmirzad S, Hassani A. Nerve Retraction During Inferior Alveolar Nerve Repositioning Procedure: A New Simple Method and Review of the Literature. *J Oral Implantol.* 2015 Jul;41 Spec No:391-4.

Himmlová L, Dostálová T, Káčovský A, Konvicková S. Influence of implant length and diameter on stress distribution: a finite element analysis. *J Prosthet Dent.* 2004 Jan;91(1):20-5.

Lulic M, Brägger U, Lang NP, Zwahlen M, Salvi GE. Ante's (1926) law revisited: a systematic review on survival rates and complications of fixed dental prostheses (FDPs) on severely reduced periodontal tissue support. *Clin Oral Implants Res.* 2007 Jun;18 Suppl 3:63-72.

Lum LB. A biomechanical rationale for the use of short implants. *J Oral Implantol* 17:126-131. 1991

Milinkovic I, Cordaro L. Are there specific indications for the different alveolar bone augmentation procedures for implant placement? A systematic review. *Int J Oral Maxillofac Surg.* 2014 May;43(5):606-25.

Moreno Vazquez JC, Gonzalez de Rivera AS, Gil HS, Mifsut RS. Complication rate in 200 consecutive sinus lift procedures: guidelines for prevention and treatment. *J Oral Maxillofac Surg.* 2014 May;72(5):892-901.

Nisand D, Renouard F. Short implant in limited bone volume. *Periodontol* 2000. 2014 Oct;66(1):72-96.

Pommer B, Frantal S, Willer J, Posch M, Watzek G, Tepper G. Impact of dental implant length on early failure rates: a meta-analysis of observational studies. *J Clin Periodontol* 2011; 38: 856-63.

Renouard F, Nisand D. Impact of implant length and diameter on survival rates. *Clin Oral Implants Res.* 2006 Oct;17 Suppl 2:35-51.

Shalabi MM, Gortemaker A, Van't Hof MA, Jansen JA, Creugers NH. Implant surface roughness and bone healing: a systematic review. *J Dent Res.* 2006 Jun;85(6):496-500. Review.

Smith DE, Zarb GA. Criteria for success of osseointegrated endosseous implants. *J Prosthet Dent.* 1989 Nov;62(5):567-72.

Srinivasan M, Vazquez L, Rieder P, Moraguez O, Bernard JP, Belser UC. Survival rates of short (6 mm) micro-rough surface implants: a review of literature and meta-analysis. *Clin Oral Implants Res.* 2014 May;25(5):539-45.

Tawil, G. & Younan, R. (2003) Clinical evaluation of short, machined-surface implants followed for 12 to 92 months. *The International Journal of Oral & Maxillofacial Implants* 18, 894–901.

Telleman G, Raghoobar GM, Vissink A, den Hartog L, Huddleston Slater JJ, Meijer HJ. A systematic review of the prognosis of short (<10 mm) dental implants placed in the partially edentulous patient. *J Clin Periodontol*. 2011 Jul;38(7):667-76.

Urdaneta RA, Rodriguez S, McNeil DC, Weed M, Chuang SK. The effect of increased crown-to-implant ratio on single-tooth locking-taper implants. *Int J Oral Maxillofac Implants*. 2010 Jul-Aug;25(4):729-43.

Weng D, Jacobson Z, Tarnow D, Hürzeler MB, Faehn O, Sanavi F, Barkvoll P, Stach RM. A prospective multicenter clinical trial of 3i machined-surface implants: results after 6 years of follow-up. *Int J Oral Maxillofac Implants*. 2003 May-Jun;18(3):417-23.

Wennerberg A, Albrektsson T. Effects of titanium surface topography on bone integration: a systematic review. *Clin Oral Implants Res*. 2009 Sep;20 Suppl 4:172-84.

Wyatt CC, Zarb GA. Treatment outcomes of patients with implant-supported fixed partial prostheses. *Int J Oral Maxillofac Implants*. 1998 Mar-Apr;13(2):204-11.

## Chapter 6 - Materials and methods

Moeen F , Nisar S, Nimra D A step by step guide to finite element analysis in dental implantology. *Pakistan Oral & Dental Journal*. 2014; 34 (1): 164-169

P. Xin, P. Nie, B. Jiang, S. Deng, G. Hu, S.G. Shen. Material assignment in finite element modeling: heterogeneous properties of the mandibular bone. *The Journal of cranial surgery*, 24(2): 405-410, 2013.

## Chapter 8 - Discussion

Atieh MA, Zadeh H, Stanford CM, Cooper LF. Survival of short dental implants for treatment of posterior partial edentulism: a systematic review. *Int J Oral Maxillofac Implants*. 2012 Nov-Dec;27(6):1323-31.

Baggi L, Cappelloni I, Di Girolamo M, Maceri F, Vairo G. The influence of implant diameter and length on stress distribution of osseointegrated implants related to crestal bone geometry: a three-dimensional finite element analysis. *J Prosthet Dent*. 2008 Dec;100(6):422-31.

Blanes, R. J. To what extent does the crown- implant ratio affect the survival and complications of implant-supported reconstructions? A systematic review. *Clinical Oral Implant Research* 2009, 20, 67–72.

Bovi M, Manni A, Mavriqi L, Bianco G, Celletti R. The use of piezosurgery to mobilize the mandibular alveolar nerve followed immediately by implant insertion: a case series evaluating neurosensory disturbance. *Int J Periodontics Restorative Dent*. 2010 Feb;30(1):73-81.

Bulaqi HA, Mousavi Mashhadi M, Safari H, Samandari MM, Geramipanah F. Effect of increased crown height on stress distribution in short dental implant components and their surrounding bone: A finite element analysis. *J Prosthet Dent*. 2015 Jun;113(6):548-57.

Chang SH, Lin CL, Hsue SS, Lin YS, Huang SR. Biomechanical analysis of the effects of implant diameter and bone quality in short implants placed in the atrophic posterior maxilla. *Med Eng Phys*. 2012 Mar;34(2):153-60.

Chun HJ, Cheong SY, Han JH, Heo SJ, Chung JP, Rhyu IC, Choi YC, Baik HK, Ku Y, Kim MH. Evaluation of design parameters of osseointegrated dental implants using finite element analysis. *J Oral Rehabil*. 2002 Jun;29(6):565-74.

Clementini M, Morlupi A, Canullo L, Agrestini C, Barlattani A. Success rate of dental implants inserted in horizontal and vertical guided bone regenerated areas: a systematic review. *Int J Oral Maxillofac Surg*. 2012 Jul;41(7):847-52.

de Faria Almeida DA, Pellizzer EP, Verri FR, Santiago JF Jr, de Carvalho PS. Influence of tapered and external hexagon connections on bone stresses around tilted dental implants: three-dimensional finite element method with statistical analysis. *J Periodontol*. 2014 Feb;85(2):261-9.

de Moraes SL, Verri FR, Santiago JF Jr, Almeida DA, de Mello CC, Pellizzer EP. A 3-D finite element study of the influence of crown-implant ratio on stress distribution. *Braz Dent J*. 2013 Nov-Dec;24(6):635-41.

Desai SR, Karthikeyan I, Singh R. Evaluation of Micromovements and Stresses around Single Wide-Diameter and Double Implants for Replacing Mandibular Molar: A Three-Dimensional FEA. *ISRN Dent*. 2012;2012:680587.

Eliasson A. On the role of number of fixtures, surgical technique and timing of loading. *Swed Dent J Suppl*. 2008;(197):3-95.

Esposito M, Cannizarro G, Soardi E, Pellegrino G, Pistilli R, Felice P. A 3-year post-loading report of a randomised controlled trial on the rehabilitation of posterior atrophic mandibles: short implants or longer implants in vertically augmented bone? *Eur J Oral Implantol*. 2011 Winter;4(4):301-11.

Felice P, Barausse C, Pistilli R, Spinato S, Bernardello F. Guided "sandwich" technique: a novel surgical approach for safe osteotomies in the treatment of vertical bone defects in the posterior atrophic mandible: a case report. *Implant Dent*. 2014 Dec;23(6):738-44.

Frost HM. A 2003 update of bone physiology and Wolff's Law for clinicians. *Angle Orthod*. 2004 Feb;74(1):3-15.

Fugazzotto PA. Shorter implants in clinical practice: rationale and treatment results. *Int J Oral Maxillofac Implants*. 2008 May-Jun;23(3):487-96.

Guven S, Beydemir K, Dundar S, Eratilla V. Evaluation of stress distributions in peri-implant and periodontal bone tissues in 3- and 5-unit tooth and implant-supported fixed zirconia restorations by finite elements analysis. *Eur J Dent*. 2015 Jul-Sep;9(3):329-39.

Himmlová L, Dostálová T, Káčovský A, Konvicková S. Influence of implant length and diameter on stress distribution: a finite element analysis. *J Prosthet Dent*. 2004 Jan;91(1):20-5.

Klineberg IJ, Trulsson M, Murray GM. Occlusion on implants - is there a problem? *J Oral Rehabil*. 2012 Jul;39(7):522-37.

Lee SA, Lee CT, Fu MM, Elmisalati W, Chuang SK. Systematic review and meta-analysis of randomized controlled trials for the management of limited vertical height in the posterior region: short implants (5 to 8 mm) vs longer implants (> 8 mm) in vertically augmented sites. *Int J Oral Maxillofac Implants*. 2014 Sep-Oct;29(5):1085-97.

Li T, Yang X, Zhang D, Zhou H, Shao J, Ding Y, Kong L. Analysis of the biomechanical feasibility of a wide implant in moderately atrophic maxillary sinus region with finite element method. *Oral Surg Oral Med Oral Pathol Oral Radiol*. 2012 Aug;114(2):e1-8.

Lum LB. A biomechanical rationale for the use of short implants. *J Oral Implantol* 17:126-131. 1991

Moeen F , Nisar S, Nimra D A step by step guide to finite element analysis in dental implantology. *Pakistan Oral & Dental Journal*. 2014; 34 (1): 164-169

Nisand D, Picard N, Rocchietta I. Short implants compared to implants in vertically augmented bone: a systematic review. *Clin Oral Implants Res*. 2015 Sep;26 Suppl 11:170-9.

Ogawa T, Dhaliwal S, Naert I, Mine A, Kronstrom M, Sasaki K, Impact of implant number, distribution and prosthesis material on loading on implants supporting xed prostheses. *J Oral Rehabil* 2010;37:525-31.

Papavasiliou G, Kamposiora P, Bayne SC, Felton DA. Three-dimensional finite element analysis of stress-distribution around single tooth implants as a function of bony support, prosthesis type, and loading during function. *J Prosthet Dent*. 1996 Dec;76(6):633-40.

Rossi F, Ricci E, Marchetti C, Lang NP, Botticelli D. Early loading of single crowns supported by 6-mm-long implants with a moderately rough surface: a prospective 2-year follow-up cohort study. *Clin Oral Implants Res*. 2010 Sep;21(9):937-43.

Santiago Junior JF, Pellizzer EP, Verri FR, de Carvalho PS. Stress analysis in bone tissue around single implants with different diameters and veneering materials: a 3-D finite element study. *Mater Sci Eng C Mater Biol Appl*. 2013 Dec 1;33(8):4700-14.

Shigemitsu R, Ogawa T, Matsumoto T, Yoda N, Gunji Y, Yamakawa Y, Ikeda K, Sasaki K. Stress distribution in the peri-implant bone with splinted and non-splinted implants by in vivo loading data-based finite element analysis. *Odontology*. 2013 Jul;101(2):222-6.

Srinivasan M, Vazquez L, Rieder P, Moraguez O, Bernard JP, Belser UC. Efficacy and predictability of short dental implants (<8 mm): a critical appraisal of the recent literature. *Int J Oral Maxillofac Implants*. 2012 Nov-Dec;27(6):1429-37.

Verri FR, Batista VE, Santiago JF Jr, Almeida DA, Pellizzer EP. Effect of crown-to-implant ratio on peri-implant stress: a finite element analysis. *Mater Sci Eng C Mater Biol Appl*. 2014 Dec;45:234-40.

Wolf J. *Das Gesetz der Transformation der Knochen*, Berlin, 1892, A Hirshwald.